THE ROLE OF FIRE IN THE CARBON DYNAMICS OF THE BOREAL FOREST

A

THESIS

Presented to the Faculty

of the University of Alaska Fairbanks

in Partial Fulfillment of the Requirements

for the Degree of

DOCTOR OF PHILOSOPHY

By

Michael S. Balshi, A.A.S., B.S., M.Phil.

Fairbanks, Alaska

December 2007

THE ROLE OF FIRE IN THE CARBON DYNAMICS OF THE BOREAL FOREST

By

Michael S. Balshi

RECOMMENDED:

Advisory Committee Chair

Chair, Department of Biology & Wildlife

APPROVED:

Dean, College of Natural Science and Mathematics

Dean of the Graduate School

Aug 28, 2007

Date

Abstract

The boreal forest contains large reserves of carbon, and across this region wildfire is a common occurrence. To improve the understanding of how wildfire influences the carbon dynamics of this region, methods were developed to incorporate the spatial and temporal effects of fire into the Terrestrial Ecosystem Model (TEM). The historical role of fire on carbon dynamics of the boreal region was evaluated within the context of ecosystem responses to changing atmospheric CO_2 and climate. These results show that the role of historical fire on boreal carbon dynamics resulted in a net carbon sink; however, fire plays a major role in the interannual and decadal scale variation of source/sink relationships. To estimate the effects of future fire on boreal carbon dynamics, spatially and temporally explicit empirical relationships between climate and fire were quantified. Fuel moisture, monthly severity rating, and air temperature explained a significant proportion of observed variability in annual area burned. These relationships were used to estimate annual area burned for future scenarios of climate change and were coupled to TEM to evaluate the role of future fire on the carbon dynamics of the North American boreal region for the 21st Century. Simulations with TEM indicate that boreal North America is a carbon sink in response to CO_2 fertilization, climate variability, and fire, but an increase in fire leads to a decrease in the sink strength. While this study highlights the importance of fire on carbon dynamics in the boreal region, there are uncertainties in the effects of fire in TEM simulations. These uncertainties are associated with sparse fire data for northern Eurasia, uncertainty in

estimating carbon consumption, and difficulty in verifying assumptions about the representation of fires that occurred prior to the start of the historical fire record. Future studies should incorporate the role of dynamic vegetation to more accurately represent post-fire successional processes, incorporate fire severity parameters that change in time and space, and integrate the role of other disturbances and their interactions with future fire regimes.

Table of Contents

PAGE

PAGE

PAGE

PAGE

List of Figures

PAGE

PAGE

PAGE

PAGE

List of Tables

PAGE

Acknowledgements

Funding for this study was provided by grants from the National Science Foundation Biocomplexity Program (ATM-0120468) and Office of Polar Programs (OPP-0531047, OPP-0328282, and OPP-0327664); the National Aeronautics and Space Administration Land Cover Land Use Change Program (NAF-11142) and North America Carbon Program (NNG05GD25G); the Bonanza Creek LTER (Long-Term Ecological Research) Program (funded jointly by NSF grant DEB-0423442 and USDA Forest Service, Pacific Northwest Research Station grant PNW01-JV11261952-231); and the U.S. Geological Survey. This study was also supported in part by a grant of high performance computing resources from the Arctic Region Supercomputing Center at the University of Alaska Fairbanks as part of the Department of Defense High Performance Computing Modernization Program.

In addition to the numerous organizations and individuals that provided financial and professional support I acknowledge the following people. I express my deepest gratitude to my advisor, Dr. A. David McGuire, for his excellent advice and guidance over the past five years. Thank you for believing in me and for your encouragement to do well in my scientific career. I could not ask for a better doctoral committee and thank Dr. F. Stuart Chapin, III, Dr. T. Scott Rupp, and Dr. David Verbyla for their helpful comments and advice throughout my entire project. Thank you to all of my co-authors on published manuscripts or those in review: Qianlai Zhuang, Jerry Melillo, Dave Kicklighter, Eric Kasischke, Christian Wirth, Mike Flannigan, Jennifer Harden, Jeff McAllister, Werner Kurz, Mike Apps, Anatoly Shvidenko, Paul Duffy, and John Walsh.

I also wish to acknowledge and thank members of the Spatial Ecology Lab, in particular, Joy Clein and Todd Burnside for their help on various projects, advice, and help with manuscript reviews. Finally I thank Falk Heuttmann, Shawn Houston, Dan Cardin, Jock Irons, the Department of Biology and Wildlife, the Institute of Arctic Biology, the USGS Alaska Cooperative Fish and Wildlife Research Unit, and the Bonanza Creek Long Term Ecological Research program.

I thank my family and friends (here and abroad) for their love and support over the past five years. In particular I thank my parents, brother, sister-in-law, niece, grandparents, Dr. Leslie Kanat, Louis Miklos, and Drs. Frank and Kathleen Kucer. Finally I thank R. Stockton Taylor, Jr., to whom I dedicate this dissertation. I am grateful for everything you have done for me and extremely fortunate to have you in my life.

Introduction

The boreal forest is one of the largest biomes on earth, covering an area of 13.7 million km^2 (Chapin et al., 2002) and contains approximately 40% of the world's soil reactive carbon, an amount similar to that held in the atmosphere (McGuire et al., 1995). Observational evidence suggests that the northern high latitudes have experienced significant warming in the recent past (Chapman and Walsh, 1993; Serreze et al., 2000; Serreze and Francis, 2006; McGuire et al., 2006) that is largely associated with increases in greenhouse gas concentrations (Intergovernmental Panel on Climate Change, IPCC, 2001). Additionally, projections of future climate change by global climate models (GCMs) show significant warming in air temperature over the next century, particularly across high latitude regions (IPCC, 2001). Across the boreal region, fire is a common disturbance and is a major influence on ecosystem structure and function across multiple time scales. Changes in climate are having pronounced effects on fire regime (Gillett et al., 2004; Kasischke and Turetsky, 2006) that have consequences for the carbon dynamics of this region (Kasischke et al., 1995; Stocks et al., 1998; Flannigan et al., 2005; McGuire et al., 2006). These changes may be accelerated under future climate regimes (Bachelet et al., 2005; Zhuang et al., 2006).

At the time of fire, carbon is directly released into the atmosphere through the combustion of aboveground and ground-layer fuels. The amount of carbon emitted depends on the depth of burn, or fire severity, which can vary significantly from region to region. Understanding the effects of fire on carbon storage with respect to the depth of burn is important because the ground layer contains a substantial portion of the carbon

stored in the boreal forest. Over the short term, increases in future fire will result in an overall decrease in the ground layer carbon stocks due to the combination of both fire and decomposition following fire. The potential for an increase in carbon release to the atmosphere, both directly and indirectly, may have major implications for the climate system.

Fire strongly influences secondary successional processes and therefore controls long-term patterns of carbon storage across the landscape. The combined legacy of multiple fires is an important consideration in determining the carbon balance of the boreal forest. The net ecosystem carbon balance (NECB) in terrestrial ecosystems is used as a measure of the net rate of accumulation (or loss) of carbon in ecosystems. NECB depends on the difference between net primary production (NPP), heterotrophic respiration (R_h), and total carbon losses at the time of fire. NECB can be either positive, indicating a carbon sink, or negative indicating a carbon source to the atmosphere. The carbon dynamics immediately following fire disturbance are different than the carbon dynamics as stands become older. NPP is low immediately following fire disturbance due to the low vegetation biomass while R_h often increases due to both more favorable conditions for decomposition (from increased soil temperature) and more dead organic matter (from vegetation killed by fire). As a result, R_h results in carbon losses to the atmosphere in the early stages of secondary succession. In early- to mid-successional stages, NPP begins to outpace the carbon losses resulting from R_h and results in a net gain of carbon by vegetation. To properly estimate NECB, the state of the landscape

prior to a fire event must be considered (McGuire et al., 2004) as it is a major factor that influences carbon dynamics (Kurz and Apps, 1999; Chen et al., 2002, 2003).

The fire return interval, or the length of time required to burn an area equal in size to a specified area, directly affects the stand age distribution across the landscape and can vary depending on the vegetation and type of fire that dominates a given region. The North American boreal forest is characterized by a lower-frequency, high-intensity crown-fire regime in comparison to much of boreal Eurasia where the fire regime is characterized by a high-frequency, lower intensity surface fire regime. Stand-replacing (crown-fire) regimes are characterized by complete mortality of trees in the stand. In contrast, surface fire regimes burn the upper organic layer and include a size-selective mortality regime (i.e., younger trees are subject to mortality while older trees survive). More frequent surface fires, as are dominant in Siberia, keep surface fuels low thus reduce the potential for crowning. The potential for more frequent, large fires in response to climate change, and the influence this will have on secondary successional processes, can have major implications for the future carbon balance of this region as well as feedbacks to the climate system.

Pronounced warming in high latitudes, which has been occurring for the past several decades (Chapman and Walsh, 1993; Serreze et al., 2000; Serreze and Francis, 2006; McGuire et al., 2006), is altering the fire regime of the region (Gillett et al., 2004; Kasischke and Turetsky, 2006) and has consequences for carbon storage of northern ecosystems (Kasischke et al., 1995; Stocks et al., 1998; Flannigan et al., 2005). Changes in the carbon emitted due to wildfire in response to changes in climate may act as a

potentially strong positive feedback to atmospheric CO_2 concentrations (Kasischke et al., 1995) and either a positive or negative feedback to surface energy exchange (Chapin et al., 2000; Chambers and Chapin, 2003; Randerson et al., 2006). It is therefore important to understand how future climate change will influence fire regime and thus the short- and long-term carbon dynamics across this region. Increases in area burned may result in greater amounts of carbon emitted over the short term, but can also potentially change carbon storage over the long term by altering the proportion of early- to mid-successional stands across the landscape. However, the ability to make projections of future changes in carbon dynamics of the boreal region is limited by our understanding of how the temporal and spatial aspects of fire influence historical carbon dynamics. The first chapter of this work (Balshi et al., 2007, *Journal of Geophysical Research*) seeks to understand the historical role of fire in the carbon dynamics of the boreal region. In this chapter I developed spatially and temporally explicit methods for incorporating the role of historical fire in the carbon dynamics of the pan-boreal region in the context of ecosystem responses to changes in climate and atmospheric CO_2 concentrations. Understanding the response of carbon dynamics to fire and other environmental factors in a retrospective sense is essential prior to understanding how future fire regimes will affect the carbon dynamics of the boreal region in a changing climate.

The frequency and size of fires has a close association with climate (Clark, 1990; Flannigan and Van Wagner, 1991; Johnson and Wowchuk, 1993; Skinner et al., 1999, 2002; Duffy et al., 2005) and future changes in climate are likely to have pronounced effects on fire regime (Wotton and Flannigan, 1993; Flannigan et al., 2000, 2005;

Carcaillet et al., 2001). The second chapter of this work (submitted to *Global Change Biology*) seeks to develop an empirical approach that accurately simulates area burned that can be easily coupled to current GCMs for predicting future fire regime. However, developing empirical relationships often depends on the spatial and temporal coverage of model development data sets. While the historical fire data sets for Eurasia are limited, the availability of historical data sets for the North American boreal forest makes it possible to develop more accurate relationships between climate and fire. Spatially and temporally explicit empirical models are developed that relate historical area burned to air temperature and fuel moisture components of the Canadian Fire Weather Index System. A unique aspect of the models is that they take into account the temporal and spatial variation in the model input variables and their relationship to historical area burned in an attempt to capture differences in regional fire regimes. The models are then applied across boreal North America using the output of GCM climate scenarios to estimate future area burned for the 21st Century.

The large reserves of carbon in the boreal forest have major implications for the carbon dynamics and feedbacks to the climate system in the future as fire regime changes. Larger fires in response to a changing climate can result in greater amounts of carbon emitted to the atmosphere at the time of fire as well as increased post-fire soil carbon efflux due to enhanced microbial respiration. Warmer temperatures have the potential to increase the length of the fire season due to more favorable conditions to ignition and burning and can also result in deeper thaw depths of the active layer that can in turn result in deeper burning. Conversely, increases in atmospheric CO_2 and climate

have potential to result in an increase in carbon storage due to more favorable conditions for growth and therefore outweigh the effects of fire. The final chapter of this work (in preparation for *Global Change Biology*) combines the methods developed in the first and second chapters to evaluate the role of future fire on the carbon dynamics of the North American boreal region in the context of future climate change and future atmospheric CO_2 concentrations.

References

Bachelet, D., J. Lenihan, R. Neilson, R. Drapek, and T. Kittel (2005), Simulating the response of natural ecosystems and their fire regimes to climatic variability in Alaska, *Can. J. For. Res.*, *35*, 2244-2257.

Balshi, M. S., A. D. McGuire, Q. Zhuang, J. Melillo, D. W. Kicklighter, E. Kasischke, C. Wirth, M. Flannigan, J. Harden, J. S. Clein, T. J. Burnside, J. McAllister, W. A. Kurz, M. Apps, and A. Shvidenko (2007), The role of historical fire disturbance in the carbon dynamics of the pan-boreal region: a process-based analysis, *J. Geophys. Res.*, *112*, G02029, doi:10.1029/2006JG000380.

Carcaillet, C., Y. Bergeron, P. J. H. Richard, B. Fréchette, S. Gauthier, and Y. T. Prairie (2001), Change of fire frequency in the eastern Canadian boreal forests during the Holocene: does vegetation composition or climate trigger the fire regime?, *Journal of Ecology*, *89*, 930-946.

Chambers, S. D. and F.S. Chapin III (2003), Fire effects on surface-atmosphere exchange in Alaskan black spruce ecosystems: implications for feedbacks to regional climate, *J. Geophys. Res.*, *108(D1)*, doi: 10.1029/2001JD000530.

Chapin, F. S., III, A. D. McGuire, J. Randerson, R. Pielke Sr., D. Baldocchi, S. E. Hobbie, N. Roulet, W. Eugster, E. Kasischke, E. B. Rastetter, S. A. Zimov, and S. W. Running (2000), Arctic and boreal ecosystems of western North America as components of the climate system, *Global Change Biology*, *6(Suppl. 1)*, 211-223.

Chapin, F. S. III, H. A. Mooney, M. C. Chapin, and P. M. Matson (2002), *Principles of Terrestrial Ecosystem Ecology*, Springer, 472 pp.

Chapman, W. L. and J. E. Walsh (1993), Recent variations of sea ice and air temperatures in high latitudes. *Bull. Amer. Meteor. Soc.*, *74*, 33-47.

Chen, W., J. M. Chen, D. T. Price, and J. Cihlar (2002), Effects of stand age on net primary productivity of boreal black spruce forests in Ontario, Canada, *Can. J. For. Res.*, *32*, 833-842.

Chen, J. M., W. Ju, J. Cihlar, D. Price, J. Liu, W. Chen, J. Pan, A. Black, and A. Barr (2003), Spatial distribution of carbon sources and sinks in Canada's forests. *Tellus*, *55B*, 622-641.

Clark, J. S. (1990), Effect on climate change on fire regimes in northwestern Minnesota, *Nature*, *334*, 233-235.

Duffy, P. A., J. E. Walsh, J. M. Graham, D. H. Mann, and T. S. Rupp (2005), Impacts of large-scale atmospheric-ocean variability on Alaskan fire season severity, *Ecol. Appl.*, *15(4)*, 1317-1330.

Flannigan, M. D. and C. E. Van Wagner (1991), Climate change and wildfire in Canada, *Can. J. For. Res.*, *21*, 66-72.

Flannigan, M. D., B. J. Stocks, and B. M. Wotton (2000), Climate change and forest fires, *The Science of the Total Environment*, *262*, 221-229.

Flannigan, M. D., K. A. Logan, B. D. Amiro, W. R. Skinner, and B. J. Stocks (2005), Future area burned in Canada, *Climatic Change*, *72*, 1-16.

Gillett, N. P., A. J. Weaver, F. W. Zwiers, and M. D. Flannigan (2004), Detecting the effect of climate change on Canadian forest fires, *Geophys. Res. Lett.*, *31*, L18211, doi:10.1029/2004GL020876

IPCC (2001), *Climate Change 2001: The Scientific Basis. Contribution of Working Group I to the Third Assessment Report of the Intergovernmental Panel on Climate Change*., J.T. Houghton, Y. Ding, D. J. Griggs, M. Noguer, P. J. van der Linden, X. Dai, K. Maskell, and C. A. Johnson (eds), Intergovernmental Panel on Climate Change, Cambridge University Press, 572pp.

Johnson, E. A. and D. R. Wowchuk (1993), Wildfires in the southern Canadian Rocky Mountains and their relationship to mid-tropospheric anomalies, *Can. J. For. Res.*, *23*, 1213-1222.

Kasischke E., N. L. Christensen Jr., and B. J. Stocks (1995), Fire, global warming, and the carbon balance of boreal forests. *Ecol. Appl.*, *5*, 437-451.

Kasischke, E. S. and M. R. Turetsky (2006), Recent changes in the fire regime across the North American boreal region – spatial and temporal patterns of burning across Canada and Alaska, *Geophysical Res. Lett.*, *33*, L09703, doi:10.1029/2006GL025677.

Kurz, W. A. and M. J. Apps (1999), A 70-year retrospective analysis of carbon fluxes in the Canadian forest sector, *Ecol. Appl.*, *9(2)*, 526-547.

McGuire, A. D., J. M. Mellilo, D. W. Kicklighter, and L. A. Joyce (1995), Equilibrium responses of soil carbon to climate change: empirical and process-based estimates. *Journal of Biogeography*, *22*, 785-796.

McGuire, A. D., M. Apps, F. S. Chapin III, R. Dargaville, M. D. Flannigan, E. S. Kasischke, D. Kicklighter, J. Kimball, W. Kurz, D. J. McRae, K. McDonald, J. Melillo, R. Myneni, B. J. Stocks, D. L. Verbyla, and Q. Zhuang (2004), Land cover disturbances and feedbacks to the climate system in Canada and Alaska, in *Land Change Science: Observing, Monitoring, and Understanding Trajectories of Change on the Earth's Surface*, edited by G. Gutman et al., pp. 139-161, Kluwer Academic Publishers, Dordrecht, Netherlands.

McGuire, A. D., F. S. Chapin III, J. E. Walsh, and C. Wirth (2006), Integrated regional changes in arctic climate feedbacks: Implications for the global climate system, *Annual Review of Environment and Resources*, *31,* 61-91.

Randerson, J. T., H. Liu, M. G. Flanner, S. D. Chambers, Y. Jin, P. G. Hess, G. Pfister, M. C. Mack, K. K. Treseder, L. R. Welp, F. S. Chapin, J. W. Harden, M. L. Goulden, E. Lyons, J. C. Neff, E. A. G. Schuur, and C. S. Zender (2006), The impact of boreal forest fire on climate warming, *Science*, *314(5802)*, 1130-1132.

Serreze, M. C., J. E. Walsh, F. S. Chapin III, T. Osterkamp, M. Dyurgerov, V. Romanovsky, W. C. Oechel, J. Morison, T. Zhang, and R. G. Barry (2000), Observational evidence of recent change in the northern high-latitude environment, *Climatic Change*, *46*, 159-207.

Serreze, M.C. and J. A. Francis (2006), The Arctic amplification debate, *Climatic Change, 76,* 241-264.

Skinner, W. R., B. J. Stocks, D. L. Martell, B. Bonsal, and A. Shabbar (1999), The association between circulation anomalies in the mid-troposphere and area burned by wildland fire in Canada, *Theoretical and Applied Climatology*, *63*, 89-105.

Skinner, W. R., M. D. Flannigan, B. J. Stocks, D. L. Martell, B. M. Wotton, J. B. Todd, J. A. Mason, K. A. Logan, and E. M. Bosch (2002), A 500 hPa synoptic wildland fire climatology for large Canadian forest fires, 1959-1996, *Theoretical and Applied Climatology*, *71*, 157-169.

Stocks, B. J., M. A. Fosberg, T. J. Lynham, L. Mearns, B. M. Wotton, Q. Yang, J-Z. Jin, K. Lawrence, G. R. Hartley, J. A. Mason, and D. W. McKenney (1998), Climate change and forest fire potential in Russian and Canadian boreal forests, *Climatic Change*, *38*, 1-13.

Wotton, B. M. and M. D. Flannigan (1993), Length of the fire season in a changing climate, *Forestry Chronicle*, *69*, 187-192.

Zhuang, Q., J. M. Melillo, B. S. Felzer, D. W. Kicklighter, A. D. McGuire, M. C. Sarofim, A. Sokolov, R. G. Prinn, P. A. Steudler, and S. Hu (2006), CO_2 and CH_4 exchanges between land ecosystems and the atmosphere in northern high latitudes over the 21st century, *Geophys. Res. Lett.*, *33*, L17403, doi:10.1029/2006GL026972.

CHAPTER 1

THE ROLE OF HISTORICAL FIRE DISTURBANCE IN THE CARBON DYNAMICS OF THE PAN-BOREAL REGION: A PROCESS-BASED ANALYSIS[1]

1.1 Abstract

Wildfire is a common occurrence in ecosystems of northern high latitudes, and changes in the fire regime of this region have consequences for carbon feedbacks to the climate system. To improve our understanding of how wildfire influences carbon dynamics of this region, we used the process-based Terrestrial Ecosystem Model to simulate fire emissions and changes in carbon storage north of 45° N from the start of spatially explicit historically recorded fire records in the 20th Century through 2002, and evaluated the role of fire in the carbon dynamics of the region within the context of ecosystem responses to changes in atmospheric CO_2 concentration and climate. Our analysis indicates that fire plays an important role in inter-annual and decadal scale variation of source/sink relationships of northern terrestrial ecosystems and also suggests that atmospheric CO_2 may be important to consider in addition to changes in climate and fire disturbance. There are substantial uncertainties in the effects of fire on carbon storage in

[1] M. S. Balshi, A. D. McGuire, Q. Zhuang, J. Melillo, D. W. Kicklighter, E. Kasischke, C. Wirth, M. Flannigan, J. Harden, J. S. Clein, T. J. Burnside, J. McAllister, W. A. Kurz, M. Apps, and A. Shvidenko, 2007. The role of historical fire disturbance in the carbon dynamics of the pan-boreal region: A process-based analysis, *Journal of Geophysical Research*, 112, G02029, doi:10.1029/2006JG000380, 2007.

our simulations. These uncertainties are associated with sparse fire data for northern Eurasia, uncertainty in estimating carbon consumption, and difficulty in verifying assumptions about the representation of fires that occurred prior to the start of the historical fire record. To improve the ability to better predict how fire will influence carbon storage of this region in the future, new analyses of the retrospective role of fire in the carbon dynamics of northern high latitudes should address these uncertainties.

1.2 Introduction

Terrestrial ecosystems in high latitudes contain large reserves of carbon (McGuire et al., 2002, 2006). Wildfire is a common disturbance that affects the structure and function of ecosystems in the region (McGuire et al., 2006). Pronounced warming in high latitudes, which has been occurring for the past several decades (Chapman and Walsh, 1993; Serreze et al., 2000; Serreze and Francis, 2006; McGuire et al., 2006), is altering the fire regime of the region (Gillett et al., 2004; Kasischke and Turetsky, 2006) and has consequences for carbon storage of northern ecosystems (Kasischke et al., 1995; Stocks et al., 1998, Flannigan et al., 2005). While many studies have focused on using fire observation data to estimate fire emissions in northern high latitudes (Conard and Ivanova, 1997; French et al., 2000; Shvidenko and Nilsson, 2000; Kajii et al., 2002; Conard et al., 2002; Kasischke and Bruhwiler, 2003; Potter et al., 2003a; Soja et al., 2004; Yurganov et al., 2004; Kasischke et al., 2005), understanding the role of fire on carbon dynamics in this region requires consideration of several additional factors.

The state of the landscape, or stand age distribution across the landscape before a fire event occurs is one of the factors that influences carbon dynamics (Kurz and Apps, 1999; Chen et al., 2002, 2003). Stand age distributions in fire-prone systems are directly affected by the historical patterns of fire across the landscape. Although data sets exist that provide an historical picture of fires across the landscape, estimating the effects of fire on carbon dynamics requires that fires are accounted for prior to the start of the historical record (McGuire et al., 2004). While several studies have used fire cycle

information to account for recurring fires, they generally do not explicitly consider the history of fire across the landscape (e.g., Thonicke et al., 2001, Venevsky et al., 2002).

Another important factor to consider when estimating the effects of fire on carbon dynamics is influence of burn severity, which can be defined as the fractional amount of carbon consumed during a fire from both aboveground and ground layer biomass (Kasischke et al., 2005). Burn severity is highly variable in northern ecosystems, and depends on the time of the year in which the fire occurs (Kasischke et al., 1995, 2000), amount of fuel (Furyaev, 1996), spatial heterogeneity of vegetation and topography across the landscape (Turner and Romme, 1994), and weather conditions at the time of fire (Johnson, 1992). As a result, representing burn severity across large spatial scales has proven to be difficult and is typically associated with a particular vegetation type or ecoregion (French et al., 2002). Furthermore, the amount of carbon consumed on a per-fire basis can differ with respect to the type of fire regime, which is defined by the intensity, frequency, seasonality, size, and type of fire (Weber and Flannigan, 1997). In the North American boreal forest fires are predominantly stand-replacing and characterized by a high-intensity crown fire regime (Johnson, 1992). Fires that occur across boreal Eurasia range from low-intensity surface fires (e.g., Siberian Scots pine stands) to high-intensity crown fires that dominate boreal needle-leaf, larch (deciduous conifer), and pine stands (evergreen conifer) (Conard and Ivanova, 1997; Wirth et al., 2002a).

To understand the role of fire in the carbon dynamics of northern ecosystems, it is also important to evaluate changes in fire disturbance in the context of other

environmental changes. While several studies have been conducted that incorporate the influence of fire on carbon dynamics in the context of forest inventory data (Kurz and Apps, 1999; Shvidenko and Nilsson, 2002, 2003; see also Myneni et al., 2001), these studies do not explicitly consider the effects of other environmental factors such as changes in atmospheric CO_2 and climate. Process-based models are designed to evaluate how changes in climate and environmental chemistry influence carbon dynamics, and simulations can be conducted to quantify the effect of individual factors (McGuire et al., 2001). Process-based models also complement estimates of regional carbon storage made by atmospheric inversion models (Schimel et al., 2001; Dargaville et al., 2002, 2006; Gurney et al., 2004), which collectively can identify uncertainties in the net exchange between the earth's surface and the atmosphere, but are not able to evaluate the mechanisms responsible for the exchanges.

Several process-based studies have been conducted that incorporate the influence of disturbance on carbon dynamics but focus primarily on its response to land-use change (McGuire et al., 2001) or regional fire regimes (Peng and Apps, 1999; Amiro et al., 2000; Venevsky et al., 2002; Chen et al., 2000, 2003). Other process-based studies have used the satellite record to infer disturbance, but have not explicitly considered the role of fire dynamics prior to the start of the satellite record (e.g., Potter et al., 2003a, 2003b, 2005). Mouillot et al. (2006) used a process-based model to estimate fire emissions, but do not estimate the overall effect of fire on the carbon budget. To our knowledge, a study conducted by Zhuang et al. (2006) is the only analysis that uses a process-based approach to simulate the effects of fire on northern ecosystems using historical fire records.

However, Zhuang et al. (2006) did not consider how carbon dynamics are influenced by spatial variability in burn severity and spatial variability in fire frequency prior to the start of the historical record. The observed changes in climate (Chapman and Walsh, 1993; Serreze et al., 2000) and the potential for a changing climate to alter future fire regimes of northern high latitudes (Wotton and Flannigan, 1993; Flannigan et al., 1998; Kasischke et al., 1995; Stocks et al., 1998; Wotton et al., 2003; Flannigan et al., 2005; McCoy and Burn, 2005) suggest that it is important to project how future changes in carbon dynamics respond to changes in the fire regime. Our ability to make projections of future changes in carbon dynamics of northern ecosystems is limited by our understanding of how the temporal and spatial aspects of fire influence historical carbon dynamics.

The focus of this study is to improve our understanding of the role of historically recorded fire on carbon dynamics in ecosystems of northern high latitudes north of 45° N (referred to hereafter as the "pan-boreal region"). In particular, our objectives are to estimate fire emissions and changes in carbon storage in the pan-boreal region, to evaluate the role of historically recorded fire in carbon dynamics of the region in the context of ecosystem responses to changes in atmospheric CO_2 concentrations and climate, and to identify sources of uncertainty that should be reduced in retrospective analyses of the role of fire in the carbon dynamics of the pan-boreal region. In comparison to a previous study by Zhuang et al. (2006), our analysis considers how carbon dynamics are influenced by spatial variability in burn severity and by spatial variability in fire frequency prior to the start of the historical record of fire in terrestrial ecosystems of northern high latitudes. We also identify key sources of uncertainty that

should be reduced in order to better understand the role of fire in the carbon dynamics of the pan-boreal region.

1.3 Methods

1.3.1 Overview

In this study we evaluate how changes in atmospheric CO_2 concentration, climate, and fire influence carbon dynamics for North America and Eurasia north of 45° N using the process-based Terrestrial Ecosystem Model (TEM). The advantage of using a process-based model for simulating carbon dynamics is that individual processes that affect carbon storage can be isolated. To initialize our simulations we first ran the model to equilibrium (annual net primary production = annual heterotrophic respiration) in year 1000 for each terrestrial 0.5° (latitude by longitude) grid cell north of 45° N using the mean monthly climate from 1901-1930. We then conducted a 900 year spinup (from year 1001-1900) to dynamically equilibrate the model to the fire regime and to multi-decadal variability in the climate. During the spinup period, climate for the period 1901-1930 was repeated. A backcasting approach (see Section 1.3.4) was used to account for the influence of fire on carbon dynamics (including the spinup period) before 1959 for North America and before 1996 for Eurasia. The model was then run from year 1901-2002 using gridded monthly climate based on observations (see Section 1.3.3). In this study, we conducted two sets of simulations. In the first set of simulations, photosynthesis was sensitive to increasing atmospheric CO_2 concentrations (a CO_2 fertilization effect), while in the second set photosynthesis was not sensitive to increasing

atmospheric CO_2 concentrations. For the set considering the effect of atmospheric CO_2 fertilization we conducted three simulations. In simulation one (S1), atmospheric CO_2 concentration was allowed to vary, but a mean monthly climate from 1901-1930 was used to represent climate for each year (i.e. "constant climate") and no fire disturbances are assumed to occur. In simulation two (S2), both atmospheric CO_2 concentration and climate are allowed to vary, but again, no fire disturbances are assumed to occur. In simulation three (S3), atmospheric CO_2 concentration and climate were allowed to vary and fire disturbances were assumed to occur. For the second set of simulations we conducted the same three simulations as described in the first set, but with atmospheric CO_2 fixed at 296 ppm, which is the mole fraction used to initialize each simulation. We then analyzed our simulation results for the periods of historically recorded fire disturbance, which are 1959-2002 in boreal North America and 1996-2002 in the pan-boreal region. The effect of CO_2 fertilization on carbon storage was determined by the results of the S1 simulation. The effect of climate on carbon storage was determined as the difference in results between the S2 and S1 simulations. Similarly, the effect of fire on carbon storage was determined as the difference in results between the S3 and S2 simulations.

1.3.2 The Terrestrial Ecosystem Model (TEM)

The TEM is a large-scale, process-based biogeochemical model that estimates monthly pools and fluxes of carbon and nitrogen for land-based areas. The model is coupled to a soil thermal model and can be applied on both permafrost and non-

permafrost soils (Zhuang et al., 2003). The TEM is driven by a series of spatially explicit data sets that include climate, elevation, soil texture, and vegetation. The equations and parameters of TEM have been documented in previous studies (Raich et al., 1991; McGuire et al., 1992; Tian et al., 1999; Zhuang et al., 2003; Euskirchen et al., 2006). The model has been applied previously to various regions across the globe including northern ecosystems (e.g., McGuire et al., 2000a, 2000b, 2001, 2002, 2004; Clein et al., 2000, 2002; Zhuang et al., 2001, 2002, 2003; Euskirchen et al., 2006). Our application of TEM to this study is based on version 5.1 of the model (see Euskirchen et al., 2006), which has been modified in this study to incorporate the effects of fire (Figure 1.1). Several of the parameters within TEM are defined based on values obtained from the peer-reviewed literature. However, the rate limiting parameters are defined by calibrating the model to pools and fluxes of field sites representative of particular ecosystems (e.g., tundra and boreal forest). To estimate changes in carbon storage, we calculated the Net Ecosystem Carbon Balance (NECB; see Chapin et al., in 2006) for outputs generated by the model as:

$$NECB = NPP - R_h - TCE \quad (1.1)$$

where NPP is net primary production, R_h is heterotrophic respiration, and TCE is total carbon emitted due to fire. It is important to note that our analysis does not consider the effects of other disturbances that affect carbon storage in the pan-boreal region, for example, insect disturbance, forest harvest, or land-use change, in the calculation of NECB.

1.3.3 Input datasets

To extrapolate TEM across North America and the pan-boreal region, we used driving datasets that had (1) temporal variability, but no spatial variability (atmospheric CO_2 concentration), (2) spatial variability but no temporal variability (elevation, soil texture, and vegetation), and both temporal and spatial variability (air temperature, precipitation, cloudiness, and fire disturbance). Below, we describe these datasets in more detail.

1.3.3.1 Atmospheric CO_2, elevation, soil texture, and vegetation datasets

In this study atmospheric CO_2 data were obtained from the Mauna Loa station (Keeling et al., 2005). TerrainBase v1.1 elevation data were obtained from the National Geophysical Data Center, Boulder, CO (NGDC, 1994) and aggregated to a 0.5° latitude x 0.5° longitude spatial resolution. Soil texture, represented as percent silt plus percent clay in TEM, was based on the Global Gridded Surfaces of Selected Soil Characteristics data set (Global Soil Data Task Group/ IGBP-DIS, 2000) and gridded at a 0.5° latitude x 0.5° longitude spatial resolution. The input vegetation dataset, gridded at the 0.5° resolution, is represented by a potential natural vegetation map described by Melillo et al. (1993).

1.3.3.2 Temperature, precipitation, and cloudiness datasets

Monthly air temperature (°C), precipitation (mm), and cloudiness (%) data derived from observations for the period 1901-2002 gridded at 0.5° resolution were

obtained from the Climate Research Unit, University of East Anglia (Mitchell and Jones, 2005).

1.3.3.3 Historical fire datasets

A database of fire point location data and 1-km resolution fire scar data sets were acquired for Alaska, Canada, and Eurasia and then assembled into a 0.5° grid. For Alaska, we used the Alaska fire scar location database initially developed by Kasischke et al. (2002) and maintained by the Bureau of Land Management, Alaska Fire Service (2005). The database contains point and boundary location information for fires in Alaska from 1950-2002. Fires greater than 1000 acres (~404 ha) are included from 1950-1987, inclusive, and fires greater than 100 acres (~40.4 ha) are included from 1988-2002, inclusive. Although our analysis is focused on the region north of 45° N, fires in the northern conterminous United States are not considered.

For Canada we used a combination of point location data from the Canadian Large Fire Database (LFDB) and provincial polygon data, with a preference for using the provincial polygon data when available. The LFDB is a compilation of provincial and territorial wildfire data that represents all fires greater than 200 ha that occurred from 1959-1999. For the point location datasets for Canada (Flannigan and Little, 2002), we used the longitudinal and latitudinal point locations to calculate a radius for each location based on the area of the historical fire. Circular fire boundaries were then created for each point by buffering each point by a distance equal to the calculated radius. The provincial polygon data represent fires in all provinces from 1980-2002 (provided by M.

Flannigan; unpublished data, 2006). Also, historical fire data for Saskatchewan (Naelapea and Nickeson, 1998) and Alberta (Government of Alberta, 2005) were also available as polygon coverages for the periods 1945-1979 and 1931-1979, respectively. There was no redundancy between the use of point location data of the Canadian LFDB and the provincial polygon data in our assembly of the historical data set of fire in Canada for use in our simulations.

For Russia, we used Advanced Very High Resolution Radiometer (AVHRR) satellite-derived fire scars data from 1996-2002 produced at the Sukachev Institute of Forestry in Krasnoyarsk (Sukhinin, 2004).

Our examination of the spatially explicit fire scar data indicated that there were a number of spatial units within each 0.5° grid cell that had unique fire histories over the length of the fire scar record. These unique fire histories result in stands of different age that have different legacies of fire disturbance on carbon storage within a 0.5° grid cell. To properly represent this legacy of disturbance within a 0.5° grid cell, we labeled each spatial unit within a 0.5° grid cell that has a unique fire history based on the fire scar record as a "cohort". The number of cohorts per grid cell depended on both the historical fire record and fires that we inserted prior to the start of the historical fire record as part of backcasting algorithm (see section 1.3.4). To estimate carbon storage changes for a 0.5° grid cell, we conducted simulations for each cohort within the grid cell and aggregated the simulated carbon storage estimates across all of the cohorts of the grid cell.

1.3.4 Fire return intervals and backcasting

To take into account fires prior to the start of the historical fire record, we developed a backcasting algorithm which requires information on the fire return interval (FRI). We defined FRI as the time required to burn an area equal to the entire 0.5° grid cell. Each cohort within a given 0.5° grid cell has the same FRI regardless of when the cohort burned historically. For North America, we calculated FRI based on the historical fire record from 1950-2002 in Alaska and 1959–2002 in Canada. This was accomplished by taking into account the proportion of a grid cell burned each year by first calculating a fire rate (F_R) given by:

$$F_R = (A_B/A_T)/N_Y \quad (1.2)$$

in which A_B is the area burned within a 0.5° grid cell, A_T is the total area of the 0.5° grid cell, and N_Y is the number of years representing the historical fire record. Since FRI is the time required to burn an area equal to the entire 0.5° grid cell, it is calculated as the inverse of the fire rate:

$$FRI = 1/F_R \quad (1.3)$$

The FRI map as calculated above was then smoothed using a nearest-neighbor method in order to be more spatially representative of fire regime by reducing pixilation (Figure 1.2a).

A different approach was used for estimating FRI for Eurasia (Figure 1.2b) because of the short length of the historical fire record as well as the lack of large-scale FRI data. FRIs were estimated based on available data using ordinary cokriging methods in the ESRI ArcMap v9.0 Geostatistical Analyst Extension Package. The available FRI

data for Eurasia were obtained in the form of non-temporally explicit points provided by C. Wirth (unpublished data, 2006) and transects. Transect data were based on the IGBP high-latitude transect study of McGuire et al. (2002). Vegetation data at 1-km resolution (Euskirchen et al., 2007) were used as a second predictor variable to help improve the interpolated surface. Because the fire scar record for boreal Eurasia was so short, we then adjusted the initial Eurasia FRI estimates based on the assumption that the ratio of mean annual area burned from 1996-2002 to long-term mean annual area burned was similar over the long-term in boreal Eurasia and Canada. To implement this assumption, the interpolated surface of the initial FRI (IFRI) estimates was standardized relative to a factor δ calculated from historical burn area for 1996-2002 and interpolated FRIs in Eurasia and Canada as:

$$FRI_{Eurasia} = \delta \, IFRI_{Eurasia} \tag{1.4}$$

in which δ is calculated as:

$$\delta = \varphi_E/\varphi_C \tag{1.5}$$

in which

$$\varphi_C = \mu_C / \mu_{FRICanada} \tag{1.6}$$

and

$$\varphi_E = \mu_E / \mu_{IFRIEurasia} \tag{1.7}$$

where φ_C and φ_E are the respective burn ratios for Canada or Eurasia, μ_C and μ_E are the respective mean annual areas burned from 1996-2002 for Canada and Eurasia, and $\mu_{FRICanada}$ and $\mu_{IFRIEurasia}$ are the respective mean annual areas burned based on

interpolated fire return intervals for the boreal forest area of Canada and on the initial interpolated fire return intervals for the boreal forest area of Eurasia.

Throughout the pan-boreal region, the interpolated FRIs were then used by the backcasting algorithm to insert fires prior to the start of the historical period based on the fire record of each cohort within a 0.5° grid cell and the FRI of that grid cell. Fires were inserted by one of two ways. If a given cohort burned over the length of the historical period, previous fire(s) events were calculated by the difference between the first historical burn year and the FRI. If the cohort did not burn during the historical fire record, fires were inserted stochastically based on the FRI of the grid cell prior to the historical fire record. Backcasting fires only occurred if the grid cell FRI was less than or equal to 500 years (i.e., each cohort would burn at least two times during a 900 year spin-up period), allowing a dynamic equilibrium to be reached prior to the start of the realistic transient climate period (1901-2002). Fires were not inserted for Europe (defined as west of 22° E and north of 45° N in this study) because we assumed that human activities have effectively suppressed wildfire in this region; the historical fire record we used for Russia did not contain any fires west of 22° E and north of 45° N.

1.3.5 Burn severity implementation

Our approach to modeling emissions was based on calculating the total carbon emitted during a fire event from aboveground and ground layer carbon consumption estimates. Literature estimates (Table 1.1) of aboveground and ground layer carbon fraction consumed during a fire for boreal North America (French et al., 2000) and boreal

Eurasia (FIRESCAN science team, 1996; Kajii et al., 2002; Wirth et al., 2002b) were used to address the issue of burn severity. Total annual carbon emissions were then calculated using these parameters by calculating fluxes for both vegetation and soil carbon pools during a fire by:

$$TCE = (ß_a * V_c) + (ß_g * S_c) \quad (1.8)$$

where TCE is the total carbon emitted, $ß_a$ is the aboveground C fraction consumed, $ß_g$ is the ground layer carbon fraction consumed during a fire, V_c is vegetation carbon, and S_c is soil carbon. Dead wood following a fire event entered the soil carbon pool. Based on Harden et al. (2004) and Wirth et al. (2002a), we assumed that 85% of soil and vegetation nitrogen was retained at the time of fire. The nitrogen lost from the ecosystem as a result of fire was reintroduced into the system annually in equal increments obtained by dividing the total net nitrogen lost to the atmosphere during the most recent fire event by FRI.

We also differentiated between crown and surface fires in our simulations. For boreal North America we assumed a fire regime that was predominantly stand replacing and specified that one percent of live plant biomass would be available for regeneration following a fire. For Eurasia, we assumed a stand-replacing fire regime for larch forests across eastern Siberia and grassland/steppe at the southern boundary of our study region. Areas east of 22° E not dominated by larch forests or grassland were classified as being driven by a surface fire regime, and we assumed that 60% of aboveground vegetation remains following fire events (Wirth, 2005).

1.4 Results

We first present our estimates of fire emissions across North America and the pan-boreal region. We then examine the relative importance of these fire emissions to other environmental factors in the carbon dynamics of terrestrial ecosystems in North America and the pan-boreal region. North America is highlighted because we had a longer period of historical fire data for this region (1959-2002) than for the entire pan-boreal region (1996-2002).

1.4.1 Fire emissions

Fire emissions calculated by TEM are presented as total carbon lost to the atmosphere at the time of a fire event. We calculated decadal averages to examine the long-term trends in simulated fire emissions for boreal North America. The results of our simulations indicate that the decadal average annual fire emissions for Alaska, Canada, and North America (Alaska and Canada combined) approximately doubled from the 1960s to the 1980s and that CO_2 fertilization had little effect on the estimated emissions (Figure 1.3a). Although a slight decrease in average fire emissions from the 1980s to 1990s was simulated for Canada (and boreal North America), simulated fire emissions for Alaska nearly doubled.

In our pan-boreal simulations from 1996-2002, boreal Eurasia accounted for approximately 80% of estimated emissions, and CO_2 fertilization had little effect on emissions estimates. Across the pan-boreal region the estimated mean annual emissions of total carbon from 1996-2002 as a result of wildfire were 262.5 Tg C yr^{-1} and 254.5 Tg

C yr^{-1} for the simulations that considered and excluded the effect of atmospheric CO_2 fertilization, respectively (Figure 1.3b). For Eurasia mean annual emissions of total carbon were 215.7 Tg C yr^{-1} and 208.8 Tg C yr^{-1} for the simulations that considered and excluded atmospheric CO_2 fertilization, respectively. The mean annual emissions of total carbon for the simulations that considered and excluded CO_2 fertilization for North America were 46.8 Tg C yr^{-1} and 45.7 Tg C yr^{-1}, respectively. For the North American sub-regions of Alaska and Canada, mean annual total carbon emissions for the simulation that considered CO_2 fertilization were estimated to be 13.9 Tg C yr^{-1} and 32.9 Tg C yr^{-1}, respectively, while the simulation that excluded CO_2 fertilization estimated emissions to be 13.7 Tg C yr^{-1} and 32.2 Tg C yr^{-1}.

To understand the spatial variability of emissions among subregions with different burn severity parameters (Table 1.1), we calculated the mean annual area burned, mean total annual carbon emissions, and mean annual total carbon emissions per square meter of burned area for subregions of North America and Eurasia for the periods 1959-2002 and 1996-2002, respectively (Table 1.1). Across North America, the mean emissions per unit area burned was greatest across the Boreal Cordillera, Boreal Plain, West Boreal Shield, and the Alaska Boreal Interior subregions (Table 1.1). In our simulations, the three highest values for ground layer fraction consumed were in the Boreal Cordillera, the Alaska Boreal Interior, and the Boreal Plain subregions, while the highest value of aboveground fraction consumed was in the West Boreal Shield (Table 1.1). Among the three subregions in Eurasia, the stand-replacing regime of the larch forest subregion, which has the highest value of ground layer fraction consumed in Eurasia (Table 1.1),

was responsible for the highest carbon emissions per square meter of burned area (Table 1.1).

1.4.2 North American carbon dynamics 1959-2002

Our simulations that considered atmospheric CO_2 fertilization revealed that boreal North America was a carbon sink of 81.7 Tg C yr^{-1} (7.5 g C m^{-2} yr^{-1}) from 1959-2002 (Table 1.2a), while the simulations that excluded CO_2 fertilization estimate a sink of 18.7 Tg C yr^{-1} (1.5 g C m^{-2} yr^{-1}) over the same period (Table 1.2b). For the case of CO_2 fertilization, climate variability and CO_2 fertilization were about equally responsible for sequestering carbon at a rate of 46.9 Tg C yr^{-1} (3.7 g C m^{-2} yr^{-1}) and 50.4 Tg C yr^{-1} (4.0 g C m^{-2} yr^{-1}), respectively, whereas fire was responsible for carbon release to the atmosphere at a rate of 15.6 Tg C yr^{-1} (1.2 g C m^{-2} yr^{-1}). The effect of CO_2 on carbon storage (Figure 1.4a) is generally positive across North America while the effect of climate on carbon storage shows both uptake from and release to the atmosphere (Figure 1.4b); release of carbon is most evident in the Canadian Archipelago, with greater release of carbon from the simulations that excluded CO_2 fertilization. In regions where fires are concentrated over the period 1959-2002 (interior Alaska extending southeast from the Yukon Territory through central Canada to portions of eastern Quebec), carbon losses are observed in response to fire, with greater losses observed for the simulations that excluded CO_2 fertilization, while areas not burned during this period generally responded as a carbon sink (Figure 1.4c). Overall, North America acts as a carbon sink in response to the combined effects of CO_2, climate, and fire (Figure 1.4d), except for regions where

fires occurred and in the Canadian Archipelago which lost carbon in response to climatic variability.

We further analyzed the effects of CO_2, climate, and fire for North America in order to understand how each effect influences decadal-scale carbon dynamics (Figure 1.5). Our analysis indicates that increasing CO_2 concentrations enhanced carbon storage per decade from the 1960s through the 1990s (Figure 1.5a). Similarly, carbon storage increased in response to increasing mean annual air temperature from the 1960s to the 1990s for both sets of simulations (Figure 1.5b). The effect of fire on carbon storage shows that the 1960s and 1970s were periods of sink activity, but that the sink weakened in the 1970s as area burned increased (Figure 1.5c). In the 1980s and 1990s, the effect of fire acted to release carbon to the atmosphere, with the effect being larger in the 1990s even though fire emissions were higher in the 1980s (Figure 1.3a). It is important to recognize that the effect of fire during a particular decade in Figure 1.5c is not simply correlated with fire emissions as it integrates the legacy of how fire history influences the balance between NPP and R_h on regrowing stands during the decade in addition to fire emissions during the decade. Thus, from the 1970s through the 1990s, our simulations indicate that the increase in mean annual area burned promoted decreases in carbon storage. The combined effects of CO_2, climate, and fire in our simulations indicate, however, that North America acted as a carbon sink in each decade from the 1960s to 1990s (Figure 1.5d). The simulated sink activity generally increased over time with a slight dip in the 1980s and was greatest in the 1990s. The combined effects of climate and fire for the simulations that excluded CO_2 fertilization show sink activity from the

1970s through 1990s, with an increase in sink activity from the 1960s to 1970s followed by a decrease from the 1970s to the 1980s and 1990s due to an increase in the area burned between the two decades.

1.4.3 Pan-boreal carbon dynamics 1996-2002

For the period from 1996 through 2002, we estimate that carbon storage of the pan-boreal region north of 45° N increased by 405.6 Tg C yr^{-1} (10.6 g C m^{-2} yr^{-1}) in response to CO_2, climate, and fire (Table 1.2a). We estimate that about twice as much carbon has been sequestered in Eurasia than in North America. For the pan-boreal region, our simulations that considered CO_2 fertilization indicated that CO_2 fertilization sequestered over twice as much carbon (284.6 Tg C yr^{-1} or 7.5 g C m^{-2} yr^{-1}) as climate variability (136.9 Tg C yr^{-1} or 3.6 g C m^{-2} yr^{-1}), and that fire is responsible for releasing 15.9 Tg C yr^{-1} (0.4 g C m^{-2} yr^{-1}) to the atmosphere. For both North America and Eurasia, the simulated effects of atmospheric CO_2 and climate variation are responsible for sequestering carbon while fire acted to release carbon to the atmosphere. Similar to our longer-term analysis for boreal North America, the effects of CO_2 and climate are similar in promoting carbon storage in boreal North America from 1996-2002. In contrast, the effects of increasing CO_2 are about four times larger than the effects of climate in promoting carbon storage in Eurasia. Our simulations indicate that the effects of fire in North America are about four times larger than in Eurasia in promoting carbon release between 1996 and 2002.

The simulations that excluded CO_2 fertilization estimate that the combined effects of climate and fire were responsible for a release of 4.9 Tg C yr^{-1} (0.1 g C m^{-2} yr^{-1}) to the atmosphere over the period 1996-2002 (Table 1.2b). Of these effects, climate was responsible for sequestering 36.9 Tg C yr^{-1} (1.0 g C m^{-2} yr^{-1}) while fire was responsible for releasing 41.6 Tg C yr^{-1} (1.1 g C m^{-2} yr^{-1}) to the atmosphere.

To better understand how CO_2 fertilization, climate and fire may have influenced carbon storage in the pan-boreal region, we first analyzed the patterns of interannual variability in terrestrial carbon storage or loss. Increasing atmospheric CO_2 concentration increased carbon storage from 1996–2002 (Figure 1.6a). Our analysis of the effect of climate on carbon storage did not identify a relationship with mean annual air temperature from 1996-2002 (Figure 1.6b). In comparison to the simulations that considered CO_2 fertilization, the effect of climate on carbon storage in the simulations that excluded CO_2 fertilization was to generally act as either a smaller sink or a greater source (Figure 1.6b). We evaluated relationships between the climate effect on carbon storage and associated air temperature and precipitation for each subregion (boreal Eurasia and North America) and for each vegetation type within a subregion, but at these scales we could not explain how climate variability influenced inter-annual variation in carbon storage with simple empirical relationships. The effect of fire on carbon storage shows that as total area burned increases, carbon storage decreases (Figure 1.6c). For both sets of simulations, larger fire years promoted less carbon storage than more moderate fire years. Overall, our simulations of the combined effects of CO_2, climate, and fire indicate that the pan-boreal region acted as a carbon sink from 1996-2002 except

for an estimated release of carbon in 2002 (Figure 1.6d). In contrast, the combined effects of climate and fire for simulations excluding CO_2 indicate that the pan-boreal region acts as a carbon source in larger fire years.

We further explored how the influence of these environmental factors on carbon storage varied spatially (Figure 1.7). Across the pan-boreal region increasing atmospheric CO_2 promoted carbon storage (Figure 1.7a), while climate variability promoted both source and sink activity (Figure 1.7b). Across Eurasia, losses associated with climate are observed south of Scandinavia, the Kazakh Uplands, and the Mongolian Plateau, while in North America losses are observed in the Queen Elizabeth Islands and portions of Alberta and Saskatchewan. In Eurasia, carbon losses appear to be greater south of the Scandinavian region for the simulations without CO_2 fertilization. Carbon gains associated with climate occur across Eurasia from western Europe to the Russian Far East and across North America from Alaska to Labrador. The effect of fire generally promoted losses of carbon to the atmosphere in areas identified as burned in the historical fire records that we used to drive our simulations (Figure 1.7c). The combined effects of CO_2, climate, and fire generally promoted carbon storage across the pan-boreal region except for carbon losses in areas where fire occurred between 1996 and 2002 (Figure 1.7d). The combined effects of climate and fire also show a similar pattern for the simulations without CO_2 fertilization; however regions across Eurasia (south of Scandinavia to the Russian Far East) and North America (Canadian Archipelago) show greater carbon losses.

1.5 Discussion

The results presented here attempt to evaluate the historical effects of fire disturbance on carbon dynamics across the entire pan-boreal region in the context of changes in atmospheric CO_2 and climate. We also discuss uncertainties with respect to the role of atmospheric CO_2 fertilization in calculating the overall carbon budget. Given the spatial and temporal scales of our analysis, it is difficult to directly validate our results. We are able, however, to compare our results with the existing regional estimates of fire emissions and carbon balance to evaluate inter-annual and decadal variation in our simulations.

1.5.1 Comparison of fire emission estimates

Our estimates of fire emissions for each set of simulations do not appear to be greatly influenced by the effects of CO_2 fertilization on photosynthesis. The simulations that included atmospheric CO_2 fertilization are between 1-14 Tg C higher than those that excluded the effect of CO_2 fertilization. A number of studies have been conducted that use long-term historical fire data sets to estimate fire emissions within our study region (Table 1.3). For boreal North America, our estimates are 15-31% higher than the decadal scale estimates of Conard and Ivanova (1997) and French et al. (2000). It is important to recognize that the burn severity parameters for boreal North America in our simulations are based on burn severity parameters from French et al. (2000). Amiro et al. (2001) used the Canadian Forest Fire Behaviour Prediction System (FBP) System model (Forestry Canada, 1992) to estimate both the surface and crown fuel consumed during a

fire, and to calculate carbon emissions for Canada. Although inter-annual variability in our emissions between 1959 and 1995 are highly correlated with those of Amiro et al. from 1959-1995 (Figure 1.8; $R^2 = 0.92$), they are higher by about 50%. The discrepancy between our estimates and Amiro et al. (2001) appears to be associated with the higher level of soil organic matter consumed associated with our use of the French et al. (2000) carbon consumption estimates (see also Kasischke and Bruhwiler, 2003).

Across the pan-boreal region from 1996-2002, our estimates of emissions are higher than the range of emissions estimated by Yurganov et al. (2004), Kasischke et al. (2005), Mouillot et al. (2006), and Zhuang et al. (2006) (Table 1.3). Note that the range of emissions estimated by Kasischke et al. (2005) does not overlap with the range of Yurganov et al. (2004). Our estimates of fire emissions for boreal Russia (Table 1.3) are also higher than those of Conard and Ivanova (1997) for 1971-1991 and those of Shvidenko and Nilsson (2000) for 1988-1992, which are time periods that correspond to the backcasting portion of our simulations for Eurasia. Our estimates are also higher than those estimated by van der Werf et al. (2006) for the period 1997-2000 and by Mouillot et al. (2006) for the 1990s. In contrast, our estimate of fire emissions for boreal Siberia from 1998-2002 are within the range reported by Soja et al. (2004; Table 1.3), but it should be noted that the range is quite large.

Because 1998 was a high fire year in Eurasia, a number of studies have conducted analyses of fire emissions for that year. Our estimate of 1998 emissions at the pan-boreal scale (Table 1.3) is within the range reported by Kasischke and Bruhwiler (2003), but is substantially higher than the range reported by Conard et al. (2002). Similarly, our

estimates at the boreal Russia/Siberia scale (Table 1.3) are substantially higher than Conard et al. (2002) and Kajii et al. (2002).

The comparison of fire emissions between our study and those of other studies identify that there is substantial uncertainty in estimates of fire emissions in the pan-boreal region. Our estimates of fire emissions tend to be higher than many of the previously published estimates because of the burn severity parameters used. Thus, the uncertainty among studies appears to be largely associated with how burn severity is implemented among the approaches, an issue which we discuss in more detail below.

1.5.2 Comparison of carbon balance estimates

Inverse modeling studies have estimated exchange of CO_2 between the pan-boreal region and the atmosphere based on variability in the concentration of CO_2 that has been measured at various sites throughout the globe (e.g., Dargaville et al., 2006). The results of our simulations for the combined responses to changes in atmospheric CO_2, climate, and fire are within the range of uncertainty reported by Gurney et al. (2004) for boreal Asia and boreal North America from 1992-1996 (Table 1.4). However, it is important to note that the range of uncertainty from inversion-based modeling studies is quite large. We further compare our results to inventory- and process-based modeling studies to gain additional insight. In interpreting these comparisons it is also important to recognize that our simulations only considered one disturbance factor (fire), and that other disturbance factors in the pan-boreal region (e.g., insect disturbance, forest harvest, and land-use change) have the potential to influence regional carbon dynamics. For example, the

analysis of Kurz and Apps (1999) indicates that insect disturbance was responsible for more loss of carbon than fire from Canadian forests in the late 20th Century.

Inventory-based modeling studies capture a wide range of impacts on carbon dynamics from human to natural disturbance. These studies generally focus on particular transects or regions in the boreal forest, and are useful because they incorporate natural and anthropogenic disturbance regimes. In contrast, the estimates from our simulation consider the influence of fire disturbance in addition to CO_2 fertilization and climate variability. In comparison to previous inventory studies for Russia, the increase in vegetation carbon storage estimated by our simulations is substantially lower than the increases estimated by Shvidenko and Nilsson (2002, 2003), which considered a broader array of disturbances (Table 1.4). Myneni et al. (2001) conducted a study that relied on regression relationships between satellite-derived reflectance and forest inventory information to estimate changes in carbon storage for terrestrial areas north of 30° N from 1995-1999. In comparison to estimates of Myneni et al. (2001), the estimates of changes in carbon storage from our simulations that incorporated atmospheric CO_2 fertilization are slightly higher for Canada and substantially lower for Eurasia. Kurz and Apps (1999) conducted an inventory-based modeling study across Canada that analyzed variability across multiple decades. Over the period 1970-1989, they report a change in carbon storage similar to the estimate from our simulations that incorporate atmospheric CO_2 fertilization (Table 1.4). They also reported that Canadian forests acted as a sink from 1920-1979, then switched to a source from 1980-1989 as a result of changes to the disturbance regime (increased insect outbreaks and fires in the 1970s). Our results are

consistent with these findings, but it is likely that our estimates of carbon storage in Canada in the late 20th Century would be lower if we considered insect disturbance in addition to fire. However, carbon storage in our simulations would likely be higher if we considered the effects of nitrogen deposition in fertilizing ecosystems in eastern Canada. In general, our simulations with an atmospheric CO_2 fertilization effect appear to be more consistent with estimates of changes in carbon estimated by inventory-based modeling studies than the simulations that excluded CO_2 fertilization. Thus, our study suggests that ecosystem responses to changes in atmospheric CO_2 may be important to consider in addition to changes in climate and disturbance regimes.

The influence of fire has been incorporated into several process-based models and studies have focused primarily on modeling the regional or global area burned (Venevsky et al., 2002, Thonicke et al., 2001) or investigating carbon fluxes in response to fire for specific regions (Chen et al., 2000, 2003; Hicke et al., 2003; Amiro et al., 2000; Peng and Apps, 1999). While several process-based models have been applied at large spatial scales (Potter et al., 2003b, 2005; McGuire et al., 2001), they do not coincide well with our study region or have not explicitly considered the effects of historical fire. Zhuang et al. (2006) simulated the effects of fire on carbon dynamics for high-latitude ecosystems north of 50° N from 1860-2100 and reported an overall net CO_2 source of 240 Tg C yr^{-1} for the 1990s. The approach of Zhuang et al. (2006) differed from the approach of this study in several ways, but the key methodological difference responsible for the differences in results of the two studies is the assumption by Zhuang et al. (2006) of a fixed fire return interval (150 years) to account for fires prior to the start of the historical

record. This highlights the sensitivity of simulated carbon dynamics to factors affecting the stand age distribution of forests in the simulations. Another process-based modeling study that has considered historical fire is that by Chen et al. (2000), who used the Integrated Terrestrial Ecosystem Carbon-budget model (InTEC) to simulate the annual carbon balance of Canada's forests from 1896-1996 in response to CO_2, climate, nitrogen deposition, and disturbance (insects, logging, and fire). The analysis of Chen et al. (2000) estimated that Canada (as one spatial unit) was a sink for carbon from 1980-1996. Our simulations driven by changes in CO_2, climate, and fire are within the range of variability reported by Chen et al. (2000) but are substantially lower than the simulations that excluded the effect of atmospheric CO_2 fertilization (Table 1.4). While our analysis is not exactly comparable to Chen et al. (2000), as it did not consider the effects of forest harvest, insect disturbance, or nitrogen deposition, both studies highlight the potential importance of responses of ecosystems to variability in atmospheric CO_2 and climate in addition to changes in disturbance regimes.

1.5.3 Relative roles of CO_2, climate, and fire

The advantage of using process-based models for simulating carbon dynamics is that individual processes that affect carbon storage can be isolated. This helps to provide a better picture of the roles of different environmental factors on carbon storage that cannot be addressed through atmospheric inversion and inventory-based modeling studies. Our analysis identifies that CO_2, climate, and fire each have substantial influences on simulated carbon dynamics across the pan-boreal region. For the factors

included in this analysis, if we group the effects into non-disturbance factors (CO_2 fertilization and climate variability) and disturbance factors (fire), our analysis indicates that the non-disturbance factors are primarily responsible for the estimated carbon sink for the period 1996-2002. A similar conclusion was found across Canada for the 1980s and 1990s, which is also consistent with other findings for that region (Chen et al., 2003). As stated earlier, it is important to recognize that our simulations do not incorporate other disturbance factors including insect disturbance, forest harvest, and land-use change.

Although the response of TEM to increases in atmospheric CO_2 is highly constrained by the representation of the nitrogen cycle in the model (McGuire et al., 1993, 1997, 2001; Kicklighter et al., 1999), the model does have the capacity for a response to increasing atmospheric CO_2 as the ratio of vegetation carbon to nitrogen widens (McGuire et al., 1997). For the pan-boreal region, the CO_2 fertilization effect in our simulations is 7.5 g C m^{-2} yr^{-1} from 1996-2002. There is still substantial debate about whether or not CO_2 fertilization is occurring in the terrestrial biosphere (Caspersen et al., 2000; Hungate et al., 2003; Luo et al., 2004; DeLucia et al., 2005; Norby et al., 2005), and the resolution of this issue remains an important challenge as many process-based models indicate that this factor is responsible for substantial sink activity in the terrestrial biosphere in recent decades (e.g., McGuire et al., 2001). The comparison of our simulations with and without atmospheric CO_2 fertilization highlight this uncertainty. In general, the results of our simulations that incorporate an atmospheric CO_2 fertilization effect appear to be more consistent with previous analyses of carbon dynamics in the pan-boreal region.

The positive response of carbon storage to a warming climate in our simulations is largely associated with the increase of soil nitrogen availability to vegetation, as increased decomposition in response to soil warming enhances nitrogen mineralization. This response of TEM is well-documented (e.g., McGuire et al., 1992; Melillo et al., 1993; Xiao et al., 1997; Tian et al., 1999), but there is much inter-annual and spatial variability in the response because it depends on soil moisture status (McGuire et al., 2000a; Thompson et al., 2006). Over decadal time scales the response to a warming climate in the simulation results reported in this study was in general characterized by a faster increase in net primary production (NPP) than in decomposition, a pattern that resulted in a carbon sink of 3.6 g C m^{-2} yr^{-1} associated with climate variability between 1996 and 2002 at the pan-boreal scale. The increase in NPP in our simulations is consistent with a number of studies that have suggested that NPP in the pan-boreal region has been increasing in recent decades in response to warming (Nemani et al., 2003; Euskirchen et al., 2006; Kimball et al., 2006, 2007; but see Goetz et al., 2005). Our study is also consistent with a recent study indicating that boreal ecosystems sequester more carbon in warmer years (Chen et al., 2006).

Although the effects of non-disturbance factors generally outweigh the effects of fire, we show that it is important to incorporate the role of fire when calculating the overall carbon budget for the pan-boreal region. Incorporating fire in our analysis shows that it reduces carbon storage across the pan-boreal region and, in large fire years (or averaged over decades), can switch from acting as a carbon sink to a carbon source to the atmosphere. Thus, fire plays an important role in the interannual variation in source/sink

relationships. Although we find that the effects of fire are less than the effects of CO_2 and climate, increases in fire frequency and burn severity in a changing climate may enhance the effect of fire on carbon dynamics across the pan-boreal region.

1.5.4 Limitations, uncertainties, and future challenges

We encountered several issues when attempting to evaluate the role of historical fire on high latitude carbon dynamics. We identify four main challenges that are important in influencing fire emissions estimates as well as the overall carbon budget: (1) the length of historical fire records, (2) the methods used for calculating stand age distribution prior to the start of the historical record, (3) accurately representing the influence of burn severity on carbon and nitrogen consumption, and (4) the role of peatland fires in estimating fire emissions.

The lack of long-term spatially explicit fire data for Eurasia continues to be a problem for attempting to evaluate the role of fire in carbon dynamics of this region. This limitation also creates a great challenge with respect to accurately representing the state of the fire-driven landscape through the inclusion of fires prior to the short historical record using coarsely interpolated fire return intervals. Our results rely on a seven year historical period in terms of inserting pre-historical fires, and therefore the frequency and size of fires in the short period is most likely not representative of the long term dynamic of fires across Eurasia. Extending the existing satellite derived fire record prior to 1996 would help to reduce uncertainties. The extensive historical fire record for North America gives us a better understanding of the role of fire on carbon dynamics over the

longer term and can be used to help reduce uncertainties associated with the short record for Eurasia for interpolating fire return intervals (e.g., standardizing Eurasian FRIs relative to North American FRIs).

Another challenge closely related to the issue of data limitation on historical fires is the need to accurately represent the age distribution of forests prior to the start of using historical fire records in simulations. McGuire et al. (2004) documented that assumptions about historical fire prior to the start of the historical record have a large effect on simulations of carbon storage in Alaska. In boreal North America, we relied on using FRI based on the fire records from 1950-2002 for Alaska and 1959-2002 for Canada. The implementation of this approach essentially makes the assumption that the fire effect is neutral over these time periods in Alaska and Canada. However, our simulations estimated a fire effect of 15.6 to 17.4 Tg C, depending on CO_2 fertilization (Table 1.2), from terrestrial ecosystems of boreal North America to the atmosphere. Thus, the fire effect we report for boreal North America may largely be an artifact of how fires were inserted prior to the start of the historical record. For Eurasia we relied on using FRI from sparse literature estimates, which may result in FRI estimates that are not entirely representative of a given region or a particular vegetation type. The limitations imposed by available data for this region further compound the problem in that the pre-historical fires are inserted based on a seven year burn record for Russia. The comparison between the results of Zhuang et al. (2006) and this study highlight the need for spatially explicit data sets on stand-age distribution in order to evaluate methodologies that estimate stand-age distributions prior to the start of historical fire data. It should be recognized that if

stand age has been the result of multiple disturbances in a region, then the reconstruction of stand age distributions will need to consider the relevant set of disturbances in the region.

A third challenge to incorporating fire into carbon balance estimates is related to the aboveground and ground layer carbon fraction consumed during a fire. Currently the definition of aboveground and ground layer carbon consumption and fire regime differentiation is limited to our understanding of what is presented in the literature. Therefore it can only be taken as a coarse estimate of what might actually be occurring in a given region. Also, the consumption parameters that we implemented in this study are fixed in time and do not take into account the seasonal variation in depth of burn. The importance of accounting for depth of burn is highlighted by Kasischke et al. (2005) and Kasischke and Turetsky (2006); however accounting for these seasonal differences in depth of burn will require that relationships among burn severity, seasonality of fire, and other factors be developed.

An issue related to burn severity is the amount of nitrogen combusted from soil and vegetation nitrogen pools at the time of fire. Our assumption of 15 % nitrogen loss from soil and vegetation at the time of fire is based on the assumption that nitrogen loss is highly variable across the boreal forest and in some cases can be reintroduced to the system by canopy ash (Harden et al., 2004). We conducted a sensitivity analysis that evaluated this uncertainty by assuming no retention of soil and vegetation nitrogen at the time of fire (see Wang et al., 2001). We found that the effect of fire on carbon storage across the pan-boreal region from 1996-2002 increased (i.e., became more of a source) by

a factor of 50%, and decreased the overall carbon sink in response to all factors by 7%. Thus, in addition to better information on how burn severity influences carbon release, information on how burn severity influences nitrogen release would help improve the ability to represent interactions between how carbon and nitrogen affect carbon storage.

The fourth challenge to incorporating fire into carbon balance estimates of the pan-boreal region is the role of peatland fires. Several studies have highlighted the importance of peatland fires in calculating current and future fire emissions (Turetsky et al., 2002, 2006; Kasischke and Turetsky, 2006). With projections that some high-latitude regions will become drier in addition to warmer, it is possible that the fire regime will shift to later in the growing season, which may result in greater peatland fuel consumption with deeper thaw depths and therefore higher fire emissions. Therefore, it is important to accurately represent peatland burning in future studies to reduce uncertainties associated with estimating fire emissions.

1.6 Conclusion

Our analysis suggests that CO_2, climate, and fire each are important in the carbon dynamics of the pan-boreal region at inter-annual, decadal, and multi-decadal time scales. It also shows that it is important to incorporate fire in a temporally and spatially explicit manner when simulating the effects of fire on carbon dynamics for the boreal forest. While our analysis does not consider the full suite of disturbances in the pan-boreal region, our estimates are generally within the uncertainty of those presented in previous inversion-, inventory-, and process-based modeling studies within this region.

Our analysis indicates that fire plays an important role in the inter-annual and decadal scale variability of source/sink relationships of the pan-boreal region. Other analyses indicate that changes in fire regime have the potential to substantially influence carbon source/sink relationships of northern terrestrial ecosystems at multi-decadal to century time scales (McGuire et al., 2004; Zhuang et al., 2006). While we found that the pan-boreal region acted as a carbon sink for the period 1996-2002 in response to CO_2, climate, and fire (Eurasia accounting for more than half of this reported sink activity), fire tended to decrease the strength of the sink. Although we report that the pan-boreal region is currently a net carbon sink when considering changes in atmospheric CO_2, climate and fire, there are substantial uncertainties in our estimates. These uncertainties are due to several factors, which include sparse fire data across the Eurasian continent, uncertainty in estimating carbon consumption, and the difficulty in verifying assumptions about the representation of fires prior to the start of the historical fire record. The reduction of these uncertainties can be accomplished through the retrospective extension of the satellite-derived burn record in Eurasia back to the early 1980s using existing methods, better information on the spatial and temporal variability of above- and below-ground carbon fraction consumed, and the spatially explicit representation of stand age distribution throughout the pan-boreal region.

Projecting the combined effects of increasing atmospheric CO_2, a changing climate, and a changing fire regime on net carbon storage across boreal North America and Eurasia is currently difficult. If the proportion of large, severe fires increases as a result of a warmer climate, then the sink strength of northern terrestrial ecosystems may

be weakened and potentially change the ecosystem to becoming a net carbon source to the atmosphere. Our ability to project future temporal and spatial changes in carbon dynamics at large spatial scales is limited by our understanding of how the temporal and spatial aspects of fire influence historical carbon dynamics. Further analyses of the retrospective role of fire in the pan-boreal region should include (1) improved data sets of fire area for Eurasia, (2) improved estimates of how carbon consumed by fire varies spatially and temporally, and (3) integration of fire with other important disturbances so that reconstructions of stand age based on assumptions about historical disturbance can be verified with data on current stand-age distributions.

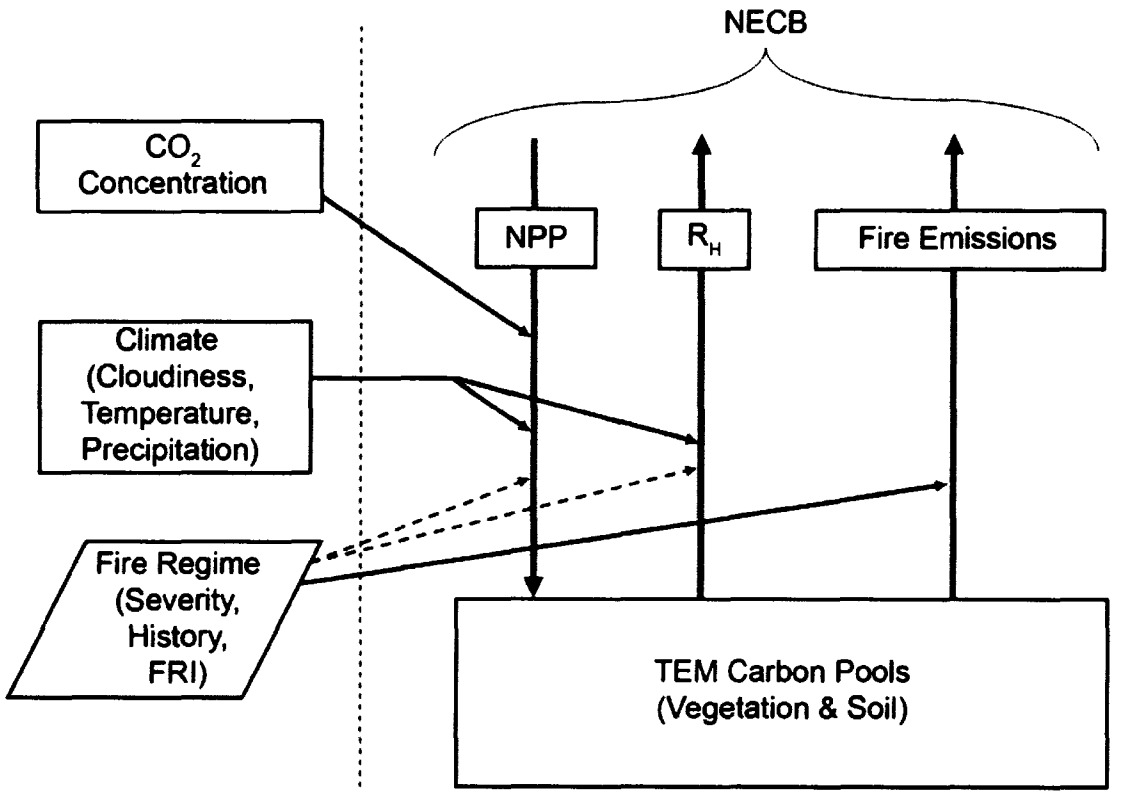

Figure 1.1 The simulation framework of this study in which the Terrestrial Ecosystem Model (TEM) was used to simulate the effects of fire on carbon dynamics. Input data sets include CO_2 concentration, cloudiness, air temperature, precipitation, and spatially explicit information on fire history (area burned), burn severity (carbon fraction consumed during a fire event), and fire return interval (FRI, used for inserting fires prior to the historical record). Burn severity parameters, fire history, and FRI are used to calculate fire emissions from TEM carbon pools (vegetation and soil carbon). Fire regime also has indirect effects on net primary production (NPP) and heterotrophic respiration (RH) through the influence on soil and vegetation carbon pools. Model outputs are NPP, RH, and fire emissions, which are used to calculate the net ecosystem carbon balance (NECB).

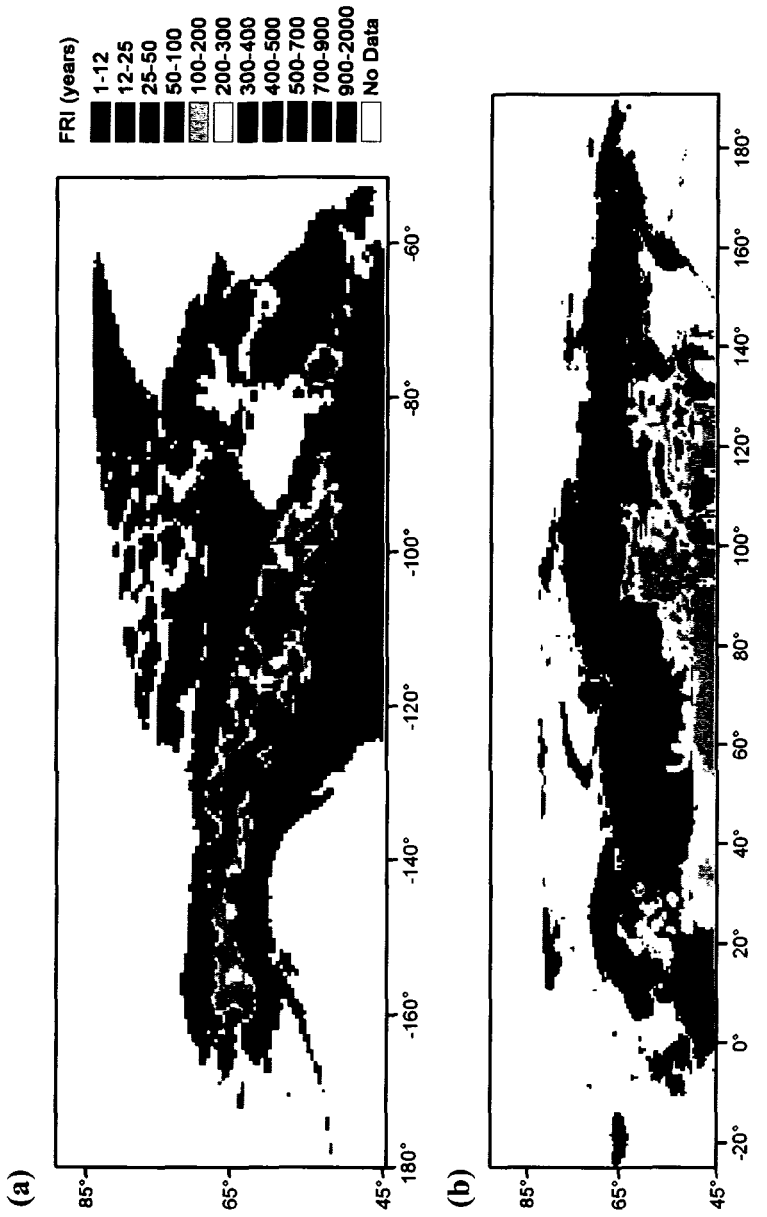

Figure 1.2 Fire return interval (FRI) maps for (a) North America and (b) Eurasia. North American FRIs were based on the proportion of a 0.5 degree cell burned over the historical fire record (1950-2002 for Alaska; 1959-2002 for Canada). Eurasian FRIs were interpolated using ordinary cokriging methods based on non-temporally explicit literature estimates.

(a)

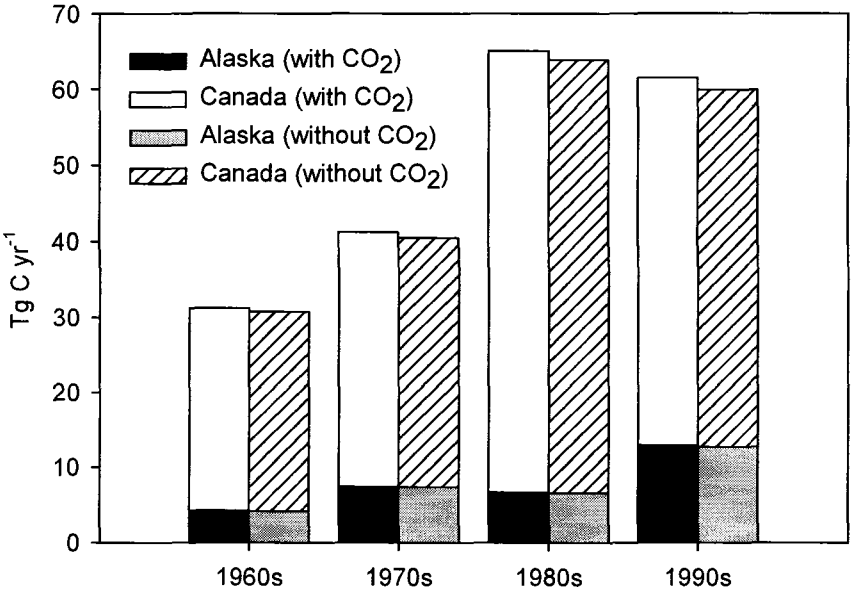

(b)

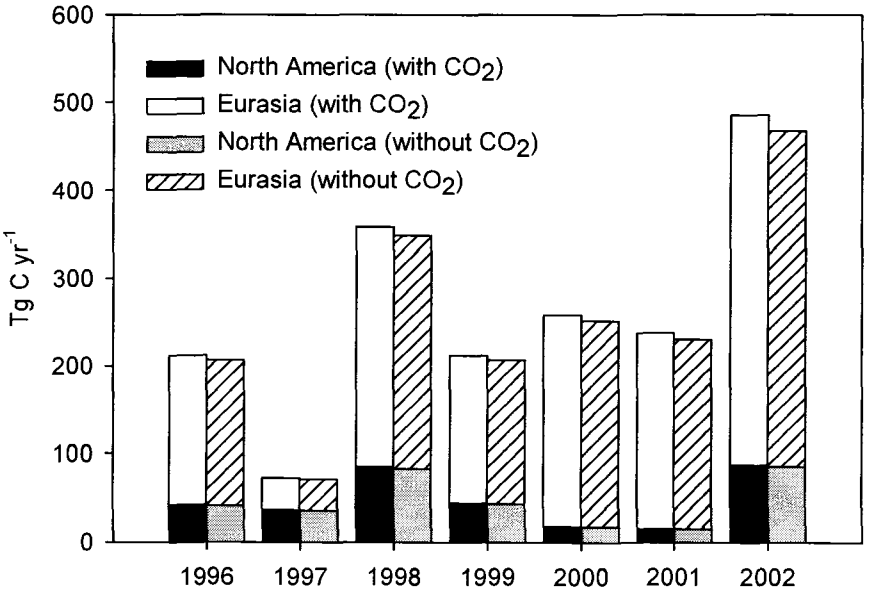

Figure 1.3 Fire emissions of total carbon: (a) average decadal emissions for Alaska and Canada; and (b) annual emissions for Eurasia and North America. Units are Tg C yr^{-1}.

Figure 1.4 Simulated mean annual net ecosystem carbon balance (NECB) of North America from 1959-2002 in response to (a) CO_2 fertilization (b) climate, (c) fire, and (d) CO_2, climate, and fire. Results are presented for simulations conducted with and without a CO_2 fertilization effect on photosynthesis. A control corresponding to panel (a) for the simulations without CO_2 fertilization is not presented because NECB would be zero throughout the region. Units are in g C m^{-2} yr^{-1}. Positive values represent carbon sequestered by terrestrial ecosystems while negative values represent release of carbon to the atmosphere.

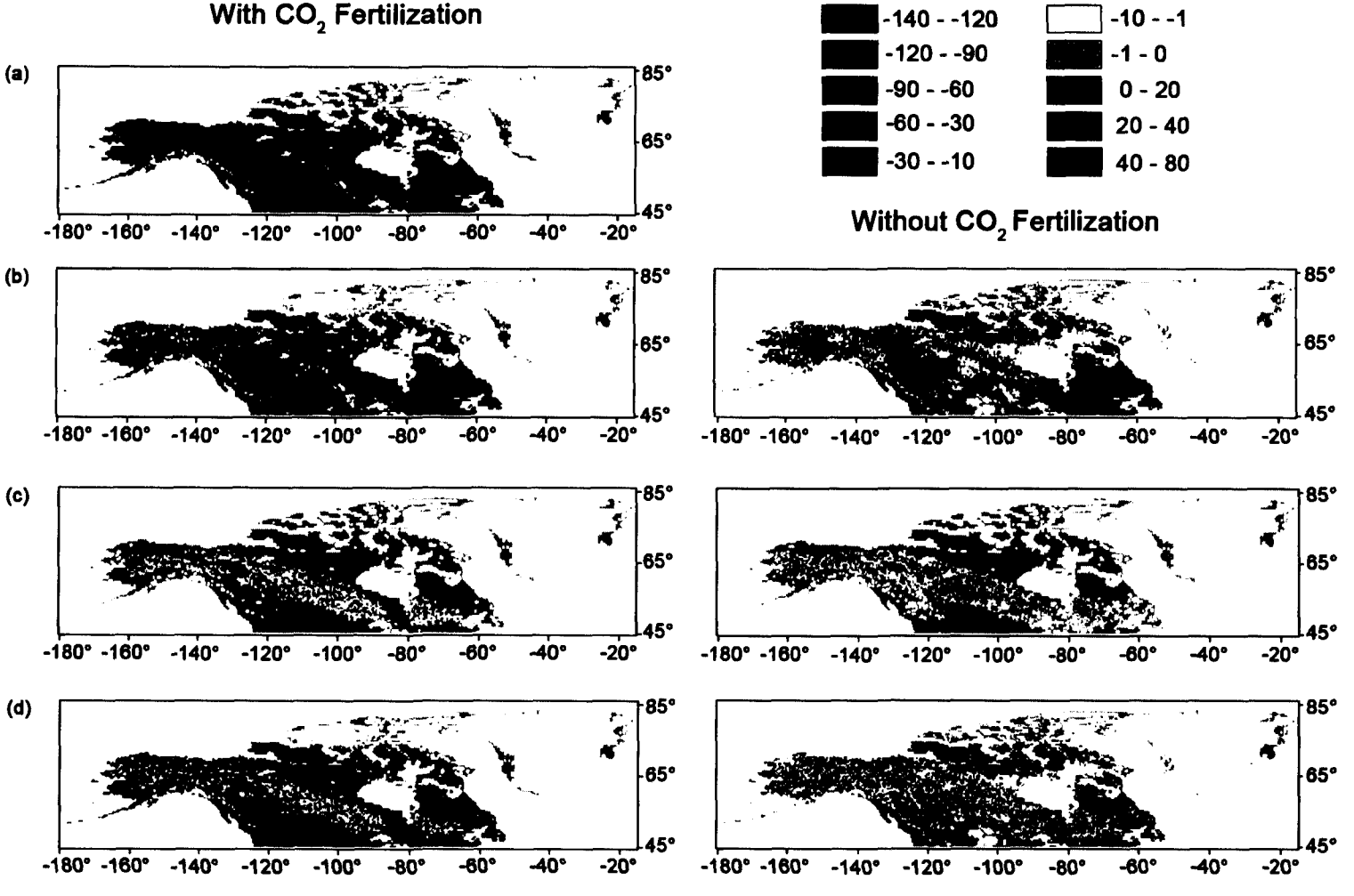

Figure 1.5 Decadal effects of (a) CO_2, (b) climate, (c) fire, and (d) the combination of CO_2, climate and fire on simulated net ecosystem carbon balance for North America from the 1960s through the 1990s. Effects are compared to model driving data of mean decadal CO_2, air temperature, and area burned. Positive values represent carbon sequestered by terrestrial ecosystems while negative values represent release of carbon to the atmosphere.

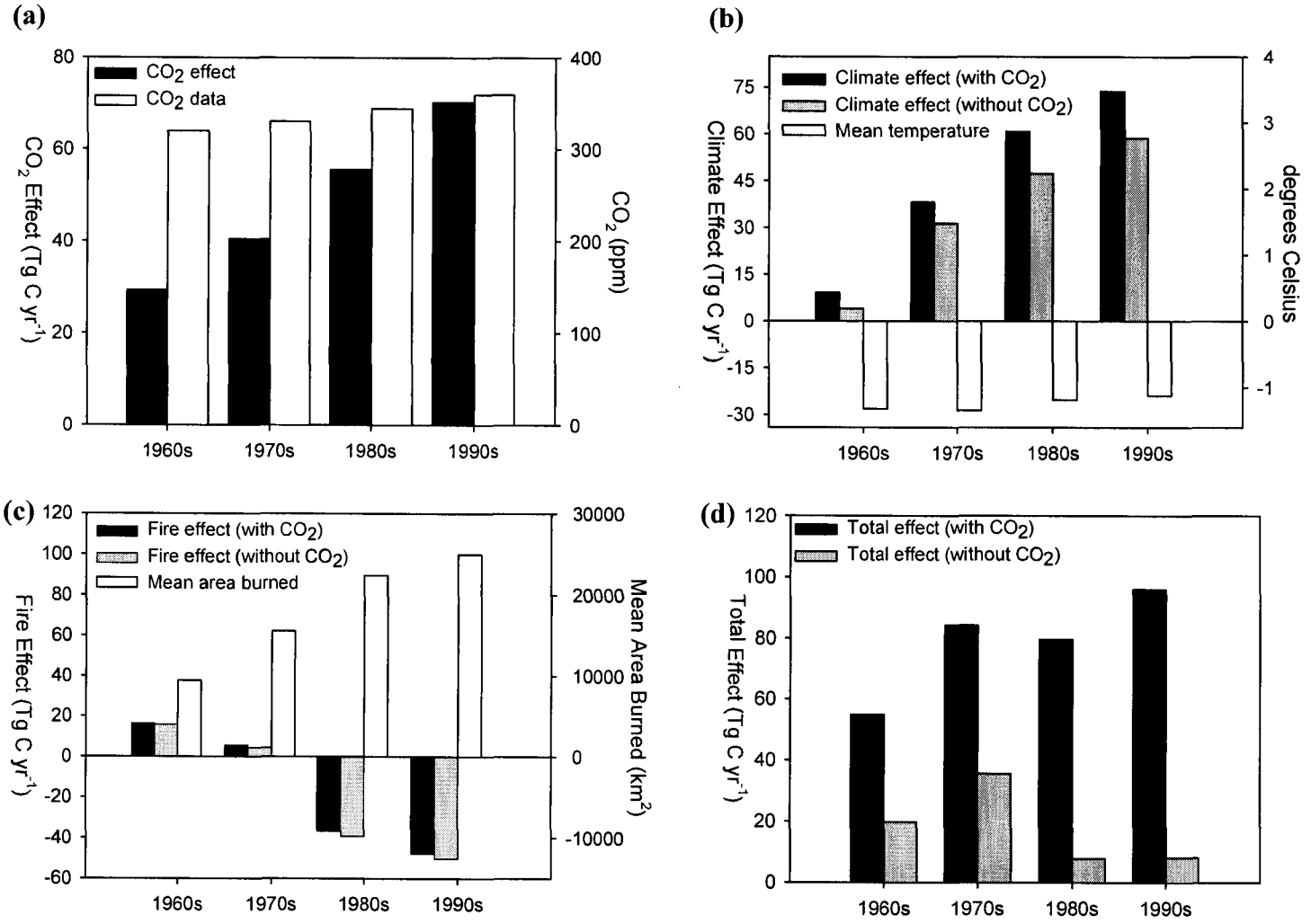

Figure 1.6 Effects of (a) CO_2, (b) climate, (c) fire, and (d) the combination of CO_2, climate and fire on simulated annual net ecosystem carbon balance for the pan-boreal region from 1996-2002. Effects are compared to model driving variables of annual CO_2, air temperature, and total area burned. Positive values represent carbon sequestered by terrestrial ecosystems while negative values represent release of carbon to the atmosphere.

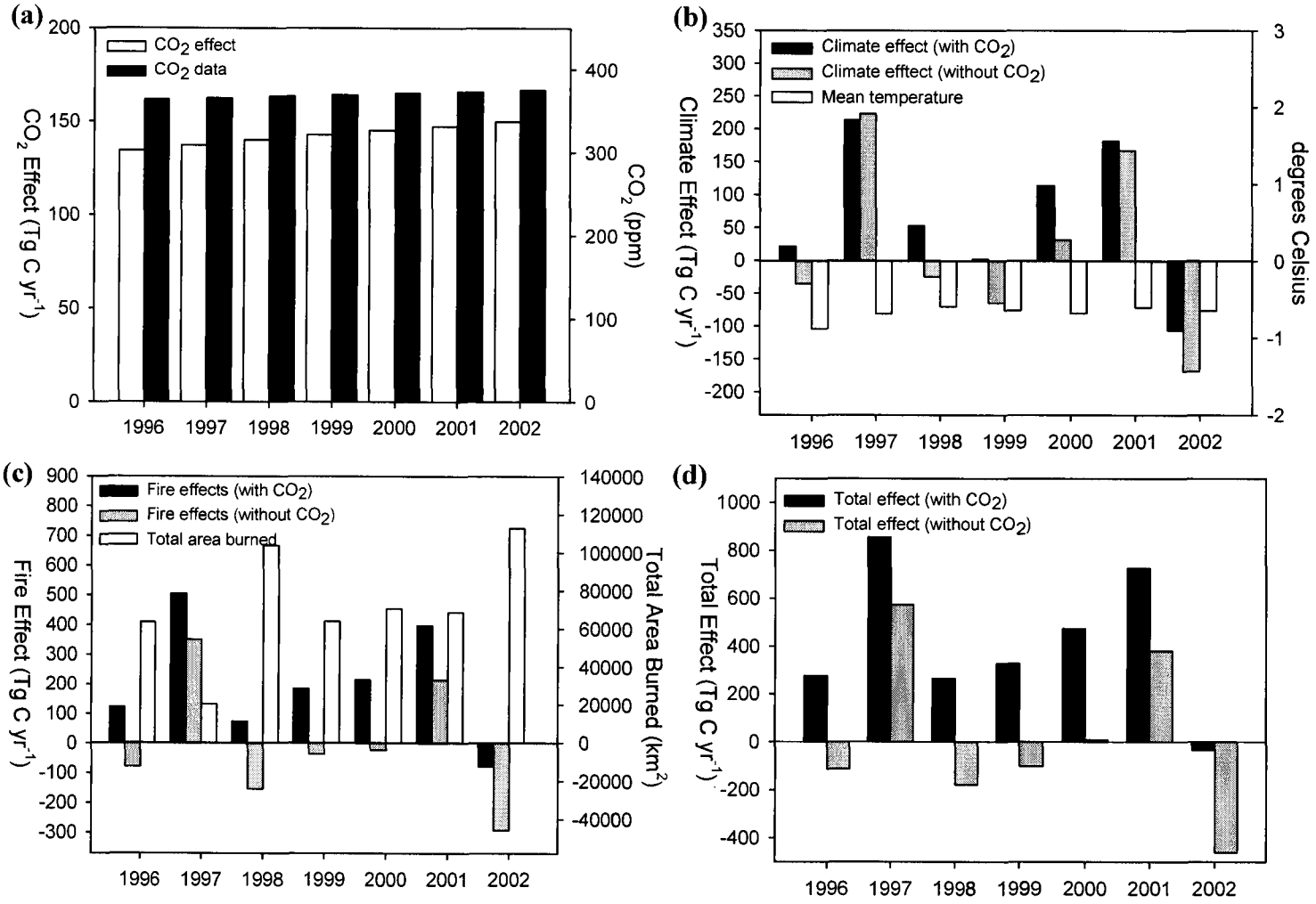

Figure 1.7 Simulated mean net ecosystem carbon balance (NECB) of the pan-boreal region from 1996-2002 in response to (a) CO_2 fertilization (b) climate, (c) fire, and (d) the combination of CO_2, climate, and fire. Results are presented for simulations conducted with and without a CO_2 fertilization effect on photosynthesis. A control corresponding to panel (a) for the simulations without CO_2 fertilization is not presented because NECB would be zero throughout the region. Units are in g C m^{-2} yr^{-1}. Positive values represent carbon sequestered by terrestrial ecosystems while negative values represent release of carbon to the atmosphere.

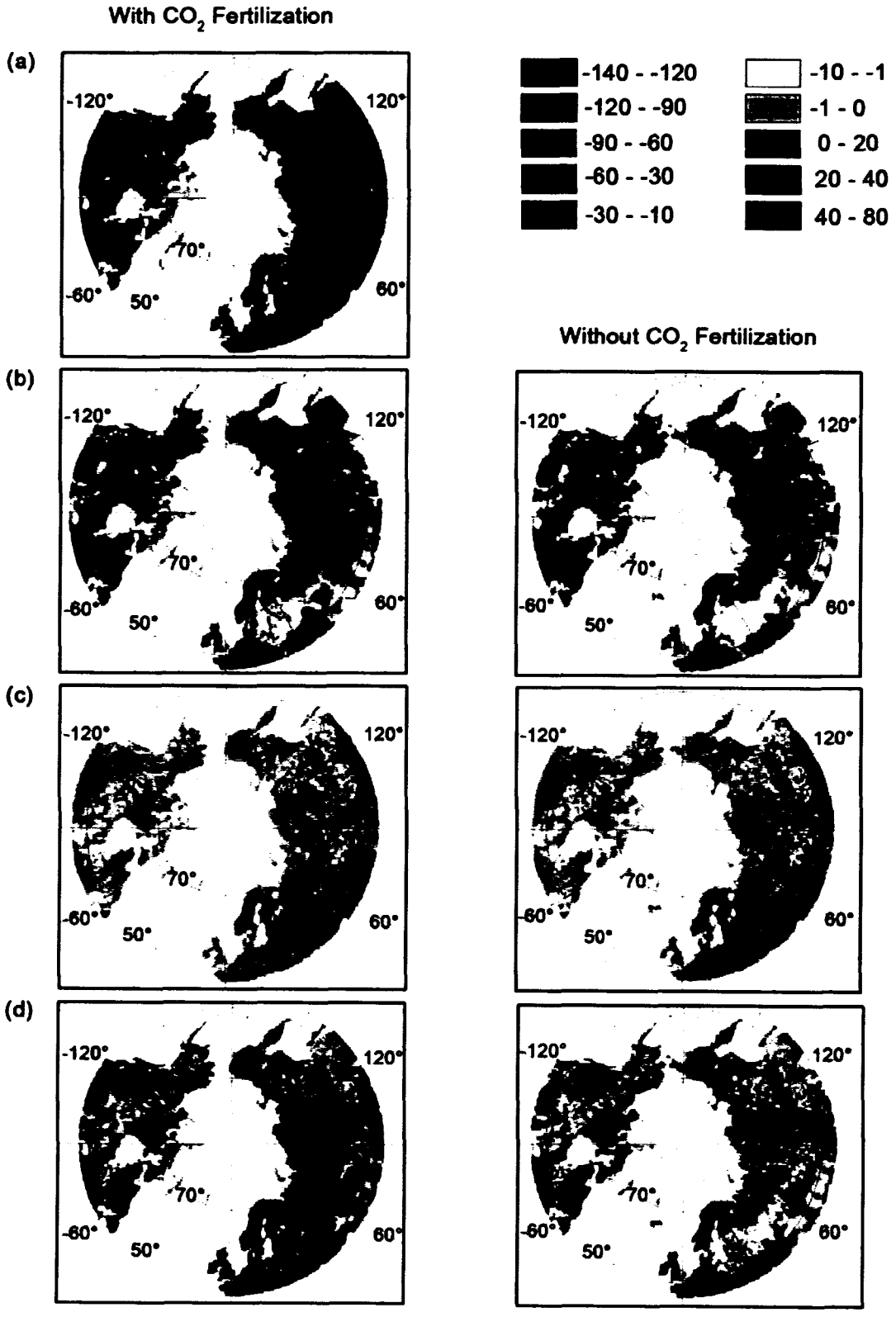

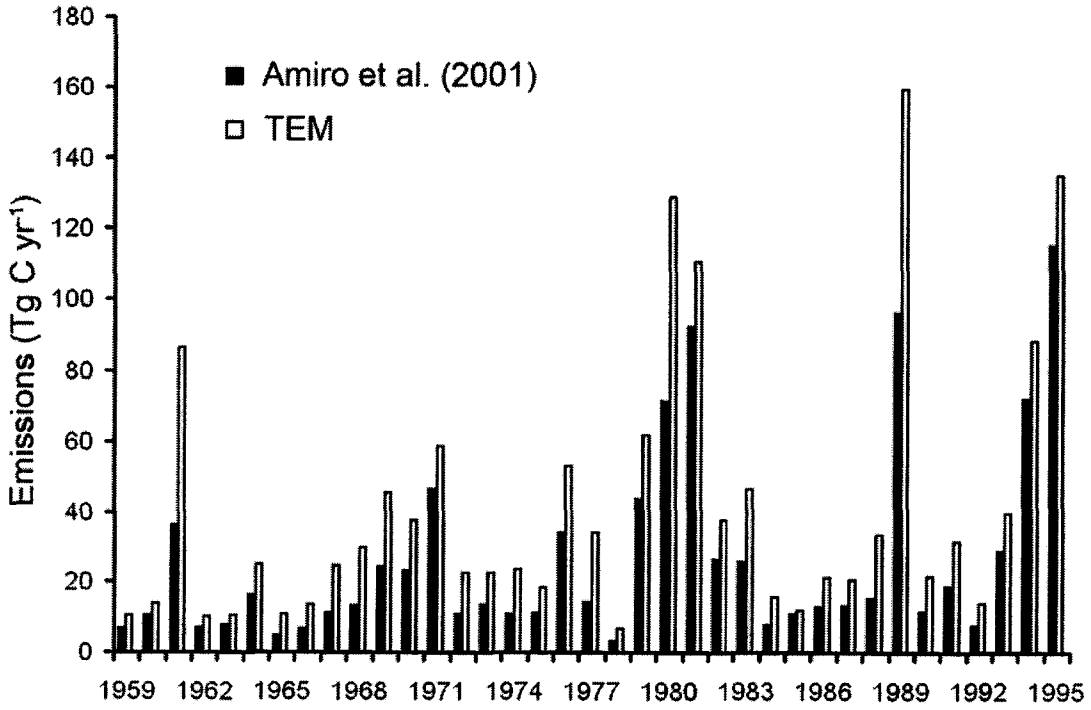

Figure 1.8 Comparison of TEM emission estimates for Canada with estimates from Amiro et al. (2001).

Table 1.1 Literature estimates of average aboveground ($ß_a$) and ground layer ($ß_b$) carbon fraction consumed used for emissions estimates during a fire event for North America (French et al., 2000) and Eurasia (FIRESCAN science team, 1996; Kajii et al., 2002; Wirth et al., 2002a). Also shown are mean annual area burned, mean annual total carbon emission, and mean annual total carbon emission per square meter of burned area from model simulations for North America (1959-2002) and Eurasia (1996-2002).

Ecozone	Aboveground ($ß_a$) C fraction consumed	Ground Layer ($ß_b$) C fraction consumed	Average area burned (ha)	Average emission (Tg C yr^{-1})	Average emission per m^2 of burned area (g C m^2 yr^{-1})
North America					
Alaska Boreal Interior	0.23	0.36	289000	7.2	2470
Boreal Cordillera	0.13	0.38	159000	5.7	3580
Taiga Plain	0.25	0.06	362000	6.0	1650
West Taiga Shield	0.25	0.05	369000	3.3	896
East Taiga Shield	0.25	0.05	141000	2.1	1490
West Boreal Shield	0.26	0.06	531000	15.2	2860
East Boreal Shield	0.22	0.06	95000	0.2	256
Boreal Plain	0.24	0.11	227000	7.8	3420
Hudson Plain	0.24	0.05	56300	0.8	1430
Eurasia					
Larch Forests	0.15	0.28	2090000	106.8	5110
Ground fire regime	0.15	0.15	2540000	73.3	2880
Grassland/Steppe	0.85	0.01	753000	35.6	4720

Table 1.2 Mean annual changes in carbon storage simulated for North America from 1959– 2002 and for the pan-boreal region from 1996 - 2002. Units are given in Tg C yr^{-1}. Positive values represent carbon sequestered by terrestrial ecosystems while negative values represent release of carbon.

(a) With CO_2 fertilization

			Effects		
Period	Region	CO_2	Climate	Fire	Total
1959-2002	North America	50.4	46.9	-15.6	81.7
1996-2002	Pan-boreal	284.6	136.9	-15.9	405.6
	Eurasia	207.7	50.9	21.5	280.2
	North America	76.9	86.0	-37.5	125.4

(b) Without CO_2 fertilization

			Effects		
Period	Region	CO_2	Climate	Fire	Total
1959-2002	North America	-0.3	36.4	-17.4	18.7
1996-2002	Pan-boreal	-0.2	36.9	-41.6	-4.9
	Eurasia	0.1	-29.4	-0.1	-29.4
	North America	-0.3	66.3	-41.5	24.5

Table 1.3 Comparison of emissions estimates (total carbon emitted, Tg C yr^{-1}) from previous studies with estimates developed in this study

				This Study	
Region	Study	Years	Emissions	With CO_2	Without CO_2
Canada	Amiro et al. [2001]	1959-1995	26	41	40
	Mouillot et al. [2006]	1990-1999	43	49	47
Boreal North America	Conard and Ivanova [1997]	1971-1991 mean	42	55	53
	French et al. [2000]	1980-1994 mean	53	61	60
	Conard et al. [2002]	1998	52-55	85	83
	van der Werf et al. [2006]	1997-2002 mean	35	48	46
Pan-boreal	Conard et al. [2002]	1998	187-245	358	349
	Kasischke and Bruhwiler [2003]	1998	290-383	358	349
	Kasischke et al. [2005]	Range of mean emissions for 1996-2002[a]	110-211	262	255
	Yurganov et al. [2004]	1996-2001 mean	6-63	225	219
	Zhuang et al. [2006]	1990-1999 mean	58	256	245
	Mouillot et al. [2006]	1990-1999 mean	209	256	245
Boreal Russia/Siberia	Conard and Ivanova [1997]	1971-1991 mean	194	204	197
	Conard et al. [2002]	1998	135-190	273	266
	Shvidenko and Nilsson [2000]	1988-1992 mean	58	244	230
	Kajii et al. [2002]	1998	176	273	266
	Soja et al. [2004]	1998-2002 mean	116-520	261	252
	van der Werf et al. [2006]	1997-2002 mean	185	223	216
	Mouillot et al. [2006]	1990-1999 mean	166	194	185

[a] Range is based on average emissions from low and high burn severity scenarios for this period.

Table 1.4 Comparison of previous carbon balance estimates (Tg C yr^{-1}) with estimates from this study.

				This Study	
Study type	**Years**	**Region**	**Literature Estimates**	**With CO_2**	**Without CO_2**
Atmospheric Inversion					
Gurney et al. [2004]	1992-1996	Boreal North America	-200 ± 280	91	12
		Boreal Asia	360 ± 510	227	-52
Inventory-based					
Shvidenko and Nilsson [2002][a]	1961-1998 mean	Russia	210 ± 30	159	70
Shvidenko and Nilsson [2003][b]	1961-1998 mean	Russia	322	220	68
Myneni et al. [2001]	1995-1999 mean	Canada	73	80	0.4
		Eurasia	470	314	-4
Kurz and Apps [1999][c]	1970-1989 mean	Canada	52	58	12
Process-based					
Chen et al. [2000][c]	1980-1996	Canada	53 ± 27	57	-1

[a] average net carbon storage in vegetation only
[b] average net carbon storage in vegetation and soil while also taking into account fluxes generated by disturbances
[c] Results include disturbances due to fire, insects, and logging

1.7 Acknowledgements

Funding for this study was provided by grants from the National Science Foundation Biocomplexity Program (ATM-0120468) and Office of Polar Programs (OPP-0531047 and OPP-0327664); the National Aeronautics and Space Administration Land Cover Land Use Change Program (NAF-11142) and North America Carbon Program (NNG05GD25G); the Bonanza Creek LTER (Long-Term Ecological Research) Program (funded jointly by NSF grant DEB-0423442 and USDA Forest Service, Pacific Northwest Research Station grant PNW01-JV11261952-231); and the U.S. Geological Survey. This study was also supported in part by a grant of HPC resources from the Arctic Region Supercomputing Center at the University of Alaska Fairbanks as part of the Department of Defense High Performance Computing Modernization Program.

1.8 References

Amiro, B. D., J. M. Chen, and J. Liu (2000), Net primary productivity following forest fire for Canadian ecoregions, *Can. J. For. Res.*, *30*, 939-947.

Amiro, B. D., J. B. Todd, B. M. Wotton, K. A. Logan, M. D. Flannigan, B. J. Stocks, J. A. Mason, D. L. Martell, and K. G. Hirsch (2001), Direct carbon emissions from Canadian fires, *Can. J. For. Res.*, *31*, 512-525.

Bureau of Land Management, Alaska Fire Service (2005), Alaska Fire History, 1950-2004, Vector Digital Data: http://agdc.usgs.gov/data/blm/fire/index.html

Caspersen, J. P., S. W. Pacala, J. C. Jenkins, G. C. Hurtt, and P. R. Moorcroft (2000), Contributions of land-use history to carbon accumulation in U.S. forests, *Science*, *290(5494)*, 1148-1151.

Chapin, F.S., III, G.M. Woodwell, J.T. Randerson, G.M. Lovett, E.B. Rastetter, G.M. Lovett, D.D. Baldocchi, D.A. Clark, M.E. Harmon, D.S. Schimel, R. Valentini, C. Wirth, J.D. Aber, J.J. Cole, M.L. Goulden, J.W. Harden, M. Heimann, R.W. Howarth, P.A. Matson, A.D. McGuire, J.M. Melillo, H.A. Mooney, J.C. Neff, R.A. Houghton, M.L. Pace, M.G. Ryan, S.W. Running, O.E. Sala, W.H. Schlesinger, and E.-D. Schulze (2006), Reconciling carbon-cycle concepts, terminology, and methods. *Ecosystems*, *9*, 1041-1050.

Chapman, W. L. and J. E. Walsh (1993), Recent variations of sea ice and air temperatures in high latitudes. *Bull. Amer. Meteor. Soc.*, *74*, 33-47.

Chen J., W. Chen, J. Liu, J. Cihlar, and S. Gray (2000), Annual carbon balance of Canada's forests during 1895-1996, *Global Biogeochem. Cycles*, *14(3)*, 839-849.

Chen, W., J. M. Chen, D. T. Price, and J. Cihlar (2002), Effects of stand age on net primary productivity of boreal black spruce forests in Ontario, Canada. *Can. J. For. Res.*, *32*, 833-842.

Chen, J. M., W. Ju, J. Cihlar, D. Price, J. Liu, W. Chen, J. Pan, A. Black, and A. Barr (2003), Spatial distribution of carbon sources and sinks in Canada's forests. *Tellus*, *55B*, 622-641.

Chen, J. M., B. Chen, K. Higuchi, J. Liu, D. Chan, D. Worthy, P. Tans, and A. Black. (2006), Boreal ecosystems sequestered more carbon in warmer years. *Geophys. Res. Lett.*, *33*, L10803, doi:10.1029/2006GL025919.

Clein J. S., B. Kwiatkowski, A. D. McGuire, J. E. Hobbie, E. B. Rastetter, J. M. Melillo, and D. W. Kicklighter (2000), Modeling carbon responses of tundra ecosystems to historical and projected climate: A comparison of a plot- and a global-scale ecosystem model to identify process-based uncertainties, *Global Change Biology*, *6*, S127-S140.

Clein, J. S., A. D. McGuire, X. Zhang, D. W. Kicklighter, J. M. Melillo, S. C. Wofsy, P. G. Jarvis, and J. M. Massheder (2002), Historical and projected carbon balances of mature black spruce ecosystems across North America: The role of carbon-nitrogen interactions, *Plant and Soil*, *242*, 15-32.

Conard S. G., and G. A. Ivanova (1997), Wildfire in Russian boreal forests – potential impacts of fire regime characteristics on emissions and global carbon balance estimates, *Environmental Pollution*, *98(3)*, 305-313.

Conard, S. G., A. I. Sukhinin, B. J. Stocks, D. R. Cahoon, E. P. Davidenko, and G. A. Ivanova (2002), Determining effects of area burned and fire severity on carbon cycling and emissions in Siberia, *Climatic Change*, *55*, 197-211.

Dargaville, R., A. D. McGuire, and P. Rayner (2002), Estimates of large-scale fluxes in high latitudes from terrestrial biosphere models and an inversion of atmospheric CO_2 measurements, *Climatic Change*, *55*, 273-285.

Dargaville, R., D. Baker, C. Rödenbeck, P. Rayner, and P. Ciais (2006), Estimating high latitude carbon fluxes with inversions of atmospheric CO_2, *Mitigation and Adaptation Strategies for Global Change*, *11,* doi:10.1007/s11027-005-9018-1.

DeLucia, E. H., D. J. Moore, and R. J. Norby (2005), Contrasting responses of forest ecosystems to rising atmospheric CO_2: implications for the global C cycle, *Global Biogeochem. Cycles*, *19*, GB3006, doi:10.1029/2004GB002346.

Euskirchen, S. E., A. D. McGuire, D. W. Kicklighter, Q. Zhuang, J. S. Clein, R. J. Dargaville, D. G. Dye, J. S. Kimball, K. C. McDonald, J. M. Melillo, V. E. Romanovsky, and N. V. Smith (2006), Importance of recent shifts in soil thermal dynamics on growing season length, productivity, and carbon sequestration in terrestrial high-latitude ecosystems, *Global Change Biology*, *12*, doi: 10.1111/j.1365-2486.2006.01113.x.

Euskirchen, E. S., A. D. McGuire, and F. S. Chapin III (2007), Energy feedbacks to the climate system associated with snow cover dynamics in northern high latitudes during warming periods of the 20th Century, Submitted to *Global Change Biology*.

FIRESCAN Science Team (1996), Fire in ecosystems of boreal Eurasia: The Bor Forest Island Fire Experiment, Fire Research Campaign Asia-North (FIRESCAN), in *Biomass Burning and Global Change*, vol. 2, edited by J. S. Levine, pp. 848-873, The MIT Press, Cambridge, M. A.

Flannigan, M. D. and J. Little (2002), Canadian Large Fire Database, 1959-1999 point dataset, Canadian Forest Service http://www.nofc.forestry.ca/fire/research/climate_change/lfdb/lfdb_download_e.htm

Flannigan, M. D., Bergeron, Y., Engelmark, O. and B. M. Wotton (1998), Future wildfire in circumboreal forests in relation to global warming, *J. Veg. Sci.*, *9*, 469-476.

Flannigan, M. D., K. A. Logan, B. D. Amiro, W. R. Skinner, and B. J. Stocks (2005), Future area burned in Canada, *Climatic Change*, *72*, 1-16.

French, N. H. F., E. S. Kasischke, B. J. Stocks, J. P. Mudd, D. L. Martell, and B. S. Lee (2000), Carbon release from fires in the North American boreal forest, in *Fire, Climate Change, and Carbon Cycling in the Boreal Forest*, Ecological Studies vol. 138, edited by E. S. Kasischke and B. J. Stocks, pp. 377-388, Springer-Verlag, New York.

French, N. H. F., E. S. Kasischke, and D. G. Williams (2002), Variability in the emission of carbon-based trace gases from wildfire in the Alaskan boreal forest, *J. Geophys. Res.*, *108*, 8151, doi:10.1029/2001JD000480.

Forestry Canada (1992), Development and structure of the Canadian forest fire behavior prediction system. Can. For. Serv. Inf. Rep. ST-X-3.

Furyaev, V. V. (1996), Role of fires in forest forming process, Nauka, Novosibirsk, Russia [in Russian].

Gillett, N. P., Weaver, A. J., Zwiers, F. W. and M. D. Flannigan (2004), Detecting the effect of climate change on Canadian forest fires, *Geophys. Res. Lett.*, *31(18)*, L18211, doi:10.1029/2004GL020876.

Global Soil Data Task Group (2000), Global Gridded Surfaces of Selected Soil Characteristics (International Geosphere-Biosphere Programme - Data and Information System), Oak Ridge National Laboratory Distributed Active Archive Center, Oak Ridge, Tennessee.

Goetz, S. J., A. G. Bunn, G. J. Fiske, and R. A. Houghton (2005), Satellite observed photosynthetic trends across boreal North America associated with climate and fire disturbance, *PNAS*, *103(38)*, 13521-13525.

Government of Alberta (2005), Historical Wildfires: 1931-1979, PFFC.GIS@gov.ab.ca, Wildfire Resource Information Section, Forest Protection Division, Sustainable Resource Development, Government of Alberta, Edmonton, Alberta.

Gurney, K. R., R. M. Law, A. S. Denning, P. J. Rayner, B. C. Pak, D. Baker, P. Bousquet, L. Bruhwiler, Y. Chen, P. Ciasis, I. Y. Fung, M. Heimann, J. John, T. Maki, S Maksyutov, P. Peylin, M. Prather, and S. Taguchi (2004), Transcom 3 inversion intercomparison: model mean results for the estimation of seasonal carbon sources and sinks, *Global Biogeochem. Cycles*, *18*, GB1010, doi:10.1029/2003GB002111.

Harden, J. W., J. C. Neff, D. V. Sandberg, M. R. Turetsky, R. Ottmar, G. Gleixner, T. L. Fries, and K. L. Manies (2004), Chemistry of burning the forest floor during the FROSTFIRE experimental burn, interior Alaska, 1999, *Global Biogeochem. Cycles*, *18*, GB3014, doi:10.1029/2003GB002194.

Hicke, J. A., G. P. Asner, E. S. Kasischke, N. H. F. French, J. T. Randerson, G. J. Collatz, B. J. Stocks, C. J. Tucker, S. O. Los, and C. B. Field (2003), Postfire response of North American boreal forest net primary productivity analyzed with satellite observations, *Global Change Biology*, *9*, 1145-1157.

Hungate, B. A., J. S. Dukes, M. R. Shaw, Y. Luo, and C. B. Field (2003), Nitrogen and climate change, *Science*, *302(5650)*, 1512-1513.

Johnson, E. A. (1992), *Fire and Vegetation Dynamics: Studies from the North American boreal forest*, 129 pp., Cambridge University Press, Cambridge.

Kajii, Y., S. Kato, D. G. Streets, N. Y. Tsai, A. Shvidenko, S. Nilsson, I. McCallum, N. P. Minko, N. Abushenko, D. Altyntsev, and T. V. Khodzer (2002), Boreal forest fires in Siberia in 1998: Estimation of area burned and emissions of pollutants by advanced very high resolution radiometer satellite data, *J. Geophys. Res.*, *107*, D244745, doi:10.1029/2001JD001078.

Kasischke, E. S., N. L. Christensen, Jr., and B. J. Stocks (1995), Fire, global warming, and the carbon balance of boreal forests, *Ecol. Appl.*, *5(2)*, 437-451.

Kasischke, E. S., K. P. O'Neill, N. H. F. French, and L. L. Bourgeau-Chavez (2000), Controls on patterns of biomass burning in Alaskan boreal forests, in *Fire, Climate Change, and Carbon Cycling in the Boreal Forest*, Ecological Studies vol. 138, edited by E. S. Kasischke and B. J. Stocks, pp. 173-196, Springer-Verlag, New York.

Kasischke, E. S., D. Williams, and D. Barry (2002), Analysis of the patterns of large fires in the boreal forest region of Alaska, *International Journal of Wildland Fire*, *11*, 131-144.

Kasischke, E. S., and L. P. Bruhwiler (2003), Emissions of carbon dioxide, carbon monoxide, and methane from boreal forest fires in 1998, *J. Geophys. Res.*, *108*, D18146, doi:10.1029/2001JD000461.

Kasischke, E. S., E. J. Hyer, P. C. Novelli, L. P. Bruhwiler, N. H. F. French, A. I. Sukhinin, J. H. Hewson, and B. J. Stocks (2005), Influences of boreal fire emissions on Northern Hemisphere atmospheric carbon and carbon monoxide, *Global Biogeochem. Cycles*, *19*, GB1012, doi:10.1029/2004GB002300.

Kasischke, E. S. and M. R. Turetsky (2006), Recent changes in the fire regime across the North American boreal region – spatial and temporal patterns of burning across Canada and Alaska, *Geophysical Res. Lett.*, *33*, L09703, doi:10.1029/2006GL025677.

Keeling, C. D. and T. P. Whorf (2005), Atmospheric CO_2 records from sites in the SIO air sampling network, in *Trends: A Compendium of Data on Global Change*, Carbon Dioxide Information Analysis Center, Oak Ridge National Laboratory, U.S. Department of Energy, Oak Ridge, Tenn., U.S.A.

Kicklighter, D. W., M. Bruno, S. Dönges, G. Esser, M. Heimann, J. Helfrich, F. Ift, F. Joos, J. Kaduk, G. H. Kohlmaier, A. D. McGuire, J. M. Melillo, R. Meyer, B. Moore III, A. Nadler, I. C. Prentice, W. Sauf, A. L. Schloss, S. Sitch, U. Wittenberg, and G. Würth (1999), A first-order analysis of the potential role of CO_2 fertilization to affect the global carbon budget: a comparison of four terrestrial biosphere models, *Tellus*, *51B*, 343-366.

Kimball, J. S., K. C. McDonald, and M. Zhao (2006), Spring thaw and its effect on terrestrial vegetation productivity in the western Arctic observed from satellite microwave and optical remote sensing, *Earth Interactions, 10*, [available online at http://earthinteractions.org].

Kimball, J. S., M. Zhao, A. D. McGuire, F. A. Heinsch, J. Clein, M. Calef, W. M. Jolly, S. Kang, S. E. Euskirchen, K. C. McDonald, and S. W. Running (2007), Recent climate driven increases in vegetation productivity for the western Arctic: Evidence of an acceleration of the northern terrestrial carbon cycle, *Earth Interactions*, *11*, [available online at http://earthinteractions.org].

Kurz, W. A. and M. J. Apps (1999), A 70-year retrospective analysis of carbon fluxes in the Canadian forest sector, *Ecol. Appl.*, *9(2)*, 526-547.

Luo, Y., B. Su, W. S. Currie, J. S. Dukes, A. Finzi, U. Hartwig, B. Hungate, R. E. McMurtrie, R. Oren, W. J. Parton, D. E. Pataki, M. R. Shaw, D. R. Zak, and C. B. Field (2004), Progressive nitrogen limitation of ecosystem responses to rising atmospheric carbon dioxide, *BioScience*, *54(8)*, 731-739.

McCoy, V. M. and C. R. Burn (2005), Potential alteration by climate change of the forest-fire regime in the boreal forest of Central Yukon Territory, *Arctic*, *58(3)*, 276-285.

McGuire, A. D., J. M. Melillo, L. A. Joyce, D. W. Kicklighter, A. L. Grace, B. Moore III, and C. J. Vorosmarty (1992), Interactions between carbon and nitrogen dynamics in estimating net primary productivity for potential vegetation in North America, *Global Biogeochem. Cycles*, *6*, 101-124.

McGuire, A. D., L. A. Joyce, D. W. Kicklighter, J. M. Melillo, G. Esser, and C. J. Vorosmarty (1993), Productivity response of climax temperate forests to elevated temperature and carbon dioxide: A North American comparison between two global models, *Climatic Change*, *24*, 287-310.

McGuire, A. D., J. M. Melillo, D. W. Kicklighter, Y. Pan, X. Xiao, J. Helfrich, B. Moore III, C. J. Vorosmarty, and A. L. Schloss (1997), Equilibrium responses of global net primary production and carbon storage to doubled atmospheric carbon dioxide: Sensitivity to changes in vegetation nitrogen concentration, *Global Biogeochem. Cycles*, *11*, 173-189.

McGuire, A. D., J. Clein, J. M. Melillo, D. W. Kicklighter, R. A. Meier, C. J. Vorosmarty, and M. C. Serreze (2000a), Modeling carbon responses of tundra ecosystems to historical and projected climate: The sensitivity of pan-arctic carbon storage to temporal and spatial variation in climate, *Global Change Biology*, *6*, S141-S159.

McGuire, A. D., J. M. Melillo, J. T. Randerson, W. J. Parton, M. Heimann, R. A. Meier, J. S. Clein, D. W. Kicklighter, and W. Sauf (2000b), Modeling the effects of snowpack on heterotrophic respiration across northern temperate and high latitude regions: Comparison with measurements of atmospheric carbon dioxide in high latitudes, *Biogeochemistry*, *48*, 91-114.

McGuire, A. D., S. Sitch, J. S. Clein, R. Dargaville, G. Esser, J. Foley, M. Heimann, F. Joos, J. Kaplan, D. W. Kicklighter, R. A. Meier, J. M. Melillo, B. Moore III, I. C. Prentice, N. Ramankutty, T. Reichenau, A. Schloss, H. Tian, L. J. Williams, and U. Wittenberg (2001), Carbon balance of the terrestrial biosphere in the twentieth century: Analyses of CO_2, climate and land use effects with four process-based ecosystem models, *Global Biogeochem. Cycles*, *15(1)*, 183-206.

McGuire, A. D., C. Wirth, M. Apps, J. Beringer, J. Clein, H. Epstein, D. W. Kicklighter, J. Bhatti, F. S. Chapin, III, B. de Groot, D. Efremov, W. Eugster, M. Fukuda, T. Gower, L. Hinzman, B. Huntley, G. J. Jia, E. Kasischke, J. Melillo, V. Romanovsky, A. Shvidenko, E. Vaganov, and D. Walker (2002), Environmental variation, vegetation distribution, carbon dynamics and water/energy exchange at high latitudes, *J. Veg. Sci.*, *13*, 301-314.

McGuire, A. D., M. Apps, F. S. Chapin III, R. Dargaville, M. D. Flannigan, E. S. Kasischke, D. Kicklighter, J. Kimball, W. Kurz, D. J. McRae, K. McDonald, J. Melillo, R. Myneni, B. J. Stocks, D. L. Verbyla, and Q. Zhuang (2004), Land cover disturbances and feedbacks to the climate system in Canada and Alaska, in *Land Change Science: Observing, Monitoring, and Understanding Trajectories of Change on the Earth's Surface*, edited by G. Gutman et al., pp. 139-161, Kluwer Academic Publishers, Dordrecht, Netherlands.

McGuire, A. D., F. S. Chapin III, J. E. Walsh, and C. Wirth (2006), Integrated regional changes in arctic climate feedbacks: Implications for the global climate system, *Annual Review of Environment and Resources*, *31,* 61-91.

Melillo, J. M., A. D. McGuire, D. W. Kicklighter, B. Moore III, C. J. Vorosmarty, and A. L. Schloss (1993), Global climate change and terrestrial net primary production. *Nature*, *63*, 234-240.

Mitchell, T. D., and P. D. Jones (2005), An improved method of constructing a database of monthly climate observations and associated high-resolution grids, *International Journal of Climatology, 25(6)*, 693-712.

Mouillot, F., A. Narasimha, Y. Balkanski, J-F Lamarque, and C. B. Field (2006), Global carbon emissions from biomass burning in the 20th century, *Geophys. Res. Lett., 33*, L01801 doi:10.1029/2005GL024707.

Myneni, R. B., J. Dong, C. J. Tucker, R. K. Kaufmann, P. E. Kauppi, J. Liski, L. Zhou, V. Alexeyev, and M. K. Hughes (2001), A large carbon sink in the woody biomass of northern forests, *PNAS, 98*, 14784-14789.

Naelapea, O., and J. Nickeson (1998), SERM Forest Fire Chronology of Saskatchewan in Vector Format, Oak Ridge National Laboratory Distributed Active Archive Center, Oak Ridge, Tennessee, U.S.A.

National Geophysical Data Center (NGDC) (1994), TerrainBase v. 1.1, 5-minute digital terrain model data. Boulder, Colorado.

Nemani, R. R., C. D. Keeling, H. Hashimoto, W. M. Jolly, S. C. Piper, C. J. Tucker, R. B. Myneni, and S. W. Running (2003), Climate-driven increases in global terrestrial net primary production from 1982-1999, *Science, 300*, 1560-1563.

Norby, R. J., E. H. DeLucia, B. Gielen, C. Calfapietra, C. P. Giardina, J. S. King, J. Ledford, H. R. McCarthy, D. J. P. Moore, R. Ceulemans, P. De Angelis, A. C. Finzi, D. F. Karnosky, M. E. Kubiske, M. Lukac, K. S. Pregitzer, G. E. Scarascia-Mugnozza, W. H. Schlesinger, and R. Oren (2005), Forest response to elevated CO_2 is conserved across a broad range of productivity, *PNAS, 102(50)*, 18052-18056.

Peng, C. and M. J. Apps (1999), Modelling the response of net primary productivity (NPP) of boreal forest ecosystems to changes in climate and fire disturbance regimes, *Ecological Modelling, 122*, 175-193.

Potter, C., P-N. Tan, M. Steinbach, S. Klooster, V. Kumar, R. Myneni, and V. Genovese (2003a), Major disturbance events in terrestrial ecosystems detected using global satellite data sets, *Global Change Biology*, *9*, 1005-1021.

Potter, C., S. Klooster, P. Tan, M. Steinbach, V. Kumar and V. Genovese (2003b), Variability in terrestrial carbon sinks over two decades. Part 1: North America, *Earth Interactions*, *7*, 1-14.

Potter, C., S. Klooster, P. Tan, M. Steinbach, V. Kumar, and V. Genovese (2005), Variability in terrestrial carbon sinks over two decades: Part 2 – Eurasia, *Global and Planetary Change*, *49*, 177-186.

Raich, J. W., E. B. Rastetter, J. M. Melillo, D. W. Kicklighter, P. A. Steudler, B. J. Peterson, A. L. Grace, B. Moore III, and C. J. Vörösmarty (1991), Potential net primary productivity in South America: application of a global model, *Ecol. Appl., 1(4)*, 399-429.

Serreze, M.C. and J. A. Francis (2006), The Arctic amplification debate, *Climatic Change, 76,* 241-264.

Serreze, M. C., J. E. Walsh, F. S. Chapin III, T. Osterkamp, M. Dyurgerov, V. Romanovsky, W. C. Oechel, J. Morison, T. Zhang, and R. G. Barry (2000), Observational evidence of recent change in the northern high-latitude environment, *Climatic Change*, *46*, 159-207.

Schimel, D. S., J. I. House, K. A. Hibbard, P. Bousquet, P. Ciais, P. Peylin, B. H. Braswell, M . J. Apps, D. Baker, A. Bondeau, J. Canadell, G. Churkina, W. Cramer, A. S. Denning, C. B. Field, P. Friedlingstein, C. Goodale, M. Heimann, R. A. Houghton, J. M. Melillo, B. Moore III, D. Murdiyarso, I. Noble, S. W. Pacala, I. C. Prentice, M. R. Raupach, P. J. Rayner, R. J. Scholes, W. L. Steffen, and C. Wirth (2001), Recent patterns and mechanisms of carbon exchange by terrestrial ecosystems, *Nature*, *414*, 169-172.

Shvidenko, A. Z. and S. Nilsson (2000), Fire and the carbon budget of Russian forests, in *Fire, Climate Change, and Carbon Cycling in the Boreal Forest*, Ecological Studies vol. 138, edited by E. S. Kasischke and B. J. Stocks, pp. 289-311, Springer-Verlag, New York.

Shvidenko, A. and S. Nilsson (2002), Dynamics of Russian forests and the carbon budget in 1961-1998: an assessment based on long-term forest inventory data, *Climatic Change*, *55*, 5-37.

Shvidenko, A. and S. Nilsson (2003), A synthesis of the impact of Russian forests on the global carbon budget for 1961-1998, *Tellus*, *55B*, 391-415.

Soja, A. J., W. R. Cofer, H. H. Shugart, A. I. Sukhinin, P. W. Stackhouse, Jr., D. J. McRae, and S. G. Conard (2004), Estimating fire emissions and disparities in boreal Siberia (1998-2002), *J. Geophys. Res.*, *109*, D14S06, doi:10.1029/2004JD004570.

Stocks, B. J., M. A. Fosberg, T. J. Lynham, L. Mearns, B. M. Wotton, Q. Yang, J-Z. Jin, K. Lawrence, G. R. Hartley, J. A. Mason, and D. W. McKenney (1998), Climate change and forest fire potential in Russian and Canadian boreal forests, *Climatic Change*, *38*, 1-13.

Sukhinin, A. I., N. H. F. French, E. S. Kasischke, J. H. Hewson, A. J. Soja, I. A. Csiszar, E. J. Hyer, T. Loboda, S. G. Conrad, V. I. Romasko, E. A. Pavlichenko, S. I. Miskiv and O. A. Slinkina, (2004), AVHRR-based mapping of fires in Russia: New products for fire management and carbon cycle studies, *Remote Sens. Environ.*, *93(4)*, 546-564.

Thompson, C. D., A. D. McGuire, J. S. Clein, F. S. Chapin III, and J. Beringer (2006), Net carbon exchange across the arctic tundra-boreal forest transition in Alaska 1981-2000, *Mitigation and Adaptation Strategies for Global Change, 11,* 805-827.

Thonicke K., S. Venevsky, S. Sitch, and W. Cramer (2001), The role of fire disturbance for global vegetation dynamics: coupling fire into a Dynamic Global Vegetation Model, *Global Ecology & Biogeography*, *10*, 661-677.

Tian, H., J. M. Melillo, D. W. Kicklighter, A. D. McGuire, and J. Helfrich (1999), The sensitivity of terrestrial carbon storage to historical climate variability and atmospheric CO_2 in the United States, *Tellus*, *51B*, 414-452.

Turetsky, M., K. Wieder, L. Halsey, and D. Vitt (2002), Current disturbance and the diminishing peatland carbon sink, *Geophys. Res. Lett.*, *29*, 10.1029/2001GL014000.

Turetsky, M. R., J. Harden, H. R. Friedli, M. Flannigan, N. Payne, J. Crock, and L. Radke (2006), Wildfires threaten mercury stocks in northern soils, *Geophys. Res. Lett.*, *33*, doi:10.1029/2005GL025595.

Turner, M. G., and W. H. Romme (1994), Landscape dynamics in crown fire ecosystems, *Landscape Ecology*, *9(1)*, 59-77.

van der Werf, G. R., J. T. Randerson, L. Giglio, G. J. Collatz, P. S. Kasibhatla, and A. F. Arellano Jr. (2006), Interannual variability in global biomass burning emissions from 1997 to 2004, *Atmospheric Chemistry and Physics*, *6*, 3423-3441.

Venevsky, S., K. Thonicke, S. Sitch, and W. Cramer (2002), Simulating fire regimes in human-dominated ecosystems: Iberian Peninsula case study, *Global Change Biology*, *8*, 984-998.

Wang, S., D. Hui, and Y. Luo (2001), Fire effects on nitrogen pools and dynamics in terrestrial ecosystems: a meta-analysis, *Ecol. Appl.*, *11(5)*, 1349-1365.

Weber, M. G. and M. D. Flannigan (1997), Canadian boreal forest ecosystem structure and function in a changing climate: impact on fire regimes, *Environmental Reviews*, *5*, 145-166.

Wirth, C. (2005), Fire regime and tree diversity in boreal forests: implications for the carbon cycle, in *Forest Diversity and Function: Temperate and Boreal Systems*, Ecological Studies vol. 176, edited by M. Scherer-Lorenzen, C. Körner, and E. – D. Schulze, pp 309-344. , Springer, Berlin.

Wirth. C., E. –D. Schulze, B. Lühker, S. Grigoriev, M. Siry, G. Hardes, W. Ziegler, M. Backor, G. Bauer, and N. N. Vygodskaya (2002a), Fire and site type effects on the long-term carbon and nitrogen balance in pristine Siberian Scots pine forests, *Plant and Soil*, *242*, 41-63.

Wirth, C., C. I. Czimczik, and E. D. Schulze (2002b), Beyond annual budgets: carbon flux at different temporal scales in fire-prone Siberian Scots pine forests, *Tellus*, *54B*, 611-630.

Wotton, B.M. and M. D. Flannigan (1993), Length of the fire season in a changing climate, *For. Chron.*, *69*, 187-192.

Wotton, B.M., Martell, D.L. and Logan, K.A. (2003), Climate change and people-caused forest fire occurrence in Ontario, *Climatic Change*, *60*, 275-295.

Xiao, X., D. W. Kicklighter, J. M. Melillo, A. D. McGuire, P. H. Stone and A. P. Sokolov (1997), Linking a global terrestrial biogeochemical model and a 2-dimensional climate model: implications for the carbon budget, *Tellus*, *49B*, 18-37.

Yurganov, L. N., T. Blumenstock, E. I. Grechko, F. Hase, E. J. Hyer, E. S. Kasischke, M. Koike, Y. Kondo, I. Kramer, F.-Y Leung, E. Mahieu, J. Mellqvist, J. Notholt, P. C. Novelli, C. P. Rinsland, H. E. Scheel, A. Schulz, A. Strandberg, R. Sussmann, H. Tanimoto, V. Velazco, R. Zander, and Y. Zhao (2004), A quantitative assessment of the 1998 carbon monoxide emission anomaly in the Northern Hemisphere based on total column and surface concentration measurements, *J. Geophys. Res., 109,* D15305, doi:10.1029/2004JD004559.

Zhuang, Q., V. E. Romanovsky, and A. D. McGuire (2001), Incorporation of a permafrost model into a large-scale ecosystem model: Evaluation of temporal and spatial scaling issues in simulating soil thermal dynamics, *J. Geophys. Res.*, *106*, 33649-33670.

Zhuang, Q., A. D. McGuire, J. Harden, K. P. O'Neill, V. E. Romanovsky, and J. Yarie. (2002), Modeling soil thermal and carbon dynamics of a fire chronosequence in interior Alaska. *J. Geophys. Res.*, *107*, 8147, doi:10.1029/2001JD001244.

Zhuang, Q., A. D. McGuire, J. M. Melillo, J. S. Clein, R. J. Dargaville, D. W. Kicklighter, R. B. Myneni, J. Dong, V. E. Romanovsky, J. Harden, J. E. Hobbie (2003), Carbon cycling in extratropical terrestrial ecosystems of the Northern Hemisphere during the 20th Century: A modeling analysis of the influences of soil thermal dynamics, *Tellus*, *55B*, 751-776.

Zhuang, Q., J. M. Melillo, B. S. Felzer, D. W. Kicklighter, A. D. McGuire, M. C. Sarofim, A. Sokolov, R. G. Prinn, P. A. Steudler, and S. Hu (2006), CO_2 and CH_4 exchanges between land ecosystems and the atmosphere in northern high latitudes over the 21st century, *Geophys. Res. Lett.*, *33*, L17403, doi:10.1029/2006GL026972.

CHAPTER 2

MODELING HISTORICAL AND FUTURE AREA BURNED OF BOREAL NORTH AMERICA USING A MULTIVARIATE ADAPTIVE REGRESSION SPLINES (MARS) APPROACH[1]

2.1 Abstract

Fire is a common disturbance in the North American boreal forest that influences ecosystem structure and function. The temporal and spatial dynamics of fire are likely to be altered as the climate continues to change. In this study, we develop temporally and spatially explicit relationships between air temperature and fuel moisture codes derived from the Canadian Fire Weather Index System to estimate annual area burned at 2.5° (latitude x longitude) resolution using a Multivariate Adaptive Regression Splines (MARS) approach across Alaska and Canada. At the Alaska-Canada scale, the empirical fire models explain on the order of 80% of the variation in annual area burned for the period 1960-2002. Mean July temperature was the most frequent predictor across all models, but the fuel moisture codes for months June through August (as a group) entered the models as the most important predictors of annual area burned. Predictability was higher in the western portion of the study region and lower in eastern Canada, which both include substantial topographic relief, and the transition between boreal forest and tundra. To understand how the temporal and spatial dynamics of fire might be altered by future climate change, the empirical fire models were driven by output from the Canadian

[1] M. S. Balshi, A. D. McGuire, P. Duffy, M. Flannigan, J. Walsh, and J. Melillo (submitted), Modeling historical and future area burned of boreal North America using a Multivariate Adaptive Regression Splines (MARS) approach, *Global Change Biology*.

Climate Center CGCM2 global climate model to predict annual area burned through year 2100. Relative to 1991-2000, the results suggest that average decadal area burned will double by 2041-2050 and will increase on the order of 3.5-5.7 times by the last decade of the 21st Century. The majority of this increase is suggested to occur across Alaska and western/central Canada. While this study highlights the vulnerability of boreal North America to future climate change, a major limitation is that the empirical models based on current conditions do not consider how changes in vegetation influence the relationships between climate and fire. To improve the ability to better predict wildfire across Alaska and Canada, future research should focus on incorporating the effects of long-term and successional vegetation changes on area burned to account more fully for interactions among fire, climate, and vegetation dynamics.

2.2 Introduction

The North American boreal forest is part of one of the world's most extensive biomes. Wildfire is common in this region and affects both the structure and function of the forest. The frequency and size of fires has a close association with climate (Clark, 1990; Flannigan and Van Wagner, 1991; Johnson and Wowchuk, 1993; Skinner et al., 1999, 2002; Duffy et al., 2005) and future climate changes are likely to have pronounced effects on the fire regime (Wotton and Flannigan, 1993; Flannigan et al., 2000, 2005; Carcaillet et al., 2001). Changes in the fire regime, defined as the frequency, intensity, seasonal timing, type, severity, and size of fire (Weber and Flannigan, 1997), have implications for the climate system though a variety of feedbacks (Kasischke et al., 1995). Trace gas emissions due to fire can increase the concentrations of greenhouse gases, creating a positive feedback on climate warming (Gillett et al., 2004). Alteration in surface energy exchange as a result of successional dynamics following fire also alters feedbacks to regional climate (Chapin et al., 2000; Chambers and Chapin, 2003; Randerson et al., 2006). Given the potential for future climate change in this region, it is important to assess its effect on the future fire regime. In this study, we specifically evaluate how future climate change may affect area burned in boreal North America.

The fire season in the North American boreal forest typically begins in April and continues through September (Skinner et al., 2002). Lightning is the primary source of wildfire ignition in boreal North America and usually results in fires that account for the majority of the area burned in a given season (Nash and Johnson, 1996). Smaller fires occur most frequently in the boreal region; however, the majority of the area burned in

the boreal forest is the result of large, infrequent fires (Stocks et al., 2002) during extended periods of high pressure systems that result in fuel drying (Johnson and Wowchuk, 1993). Weather plays a major role in the ignition, growth and death of a wildfire at daily to monthly time scales (Johnson, 1992; Campbell and Flannigan, 2000; Flannigan et al., 2000). Weather influences fire activity through impacts on fuel moisture, ignitions by lightning, and wildfire behavior. Of these factors, fuel moisture content is one of the most important as it integrates information about temperature and precipitation through time and hence is a useful indicator of whether or not a fire will start and spread (Flannigan and Harrington, 1988). Fuels for fires may consist of both living vegetation ("live" fuels), detritus on the soil surface, and organic matter in the soil itself ("dead" fuels). Live fuels generally contain significantly more moisture than dead fuels. Prolonged periods of low rainfall and elevated temperatures can lead to a decrease in dead fuel moisture and therefore an increase in the probability of a fire event. Factors that contribute to a change in dead fuel moisture include the amount and duration of a precipitation event, temperature, relative humidity, and wind. Each of these factors, in combination with the fuel size and shape, influences the rate at which fuels can retain or lose moisture content.

A variety of studies have addressed how fire weather indices will change under current (Amiro et al., 2004) and future climate change scenarios (Flannigan et al., 1998, 2000; Stocks et al., 1998). Empirical relationships between weather/climate and historical area burned have also been developed for the boreal forest (Harrington et al., 1983; Flannigan and Harrington, 1988; Flannigan and Van Wagner, 1991; Skinner et al.,

1999, 2002; Duffy et al., 2005; Flannigan et al., 2005; McCoy and Burn, 2005) and for regions in the western United States (Swetnam and Betancourt, 1990; Westerling et al., 2006). While these studies have been successful at regional levels, it is desirable to develop a more temporally and spatially explicit fire model for the North American boreal forest that can be easily coupled to global climate models.

The temporal coverage of historical fire data sets for the North American boreal forest now makes it possible to model relationships between fire weather and area burned across this region. Identification of these relationships can aid in the prediction of future spatial and temporal changes in area burned. The focus of this study is to improve our ability to predict the response of historical wildfire regime to fuel moisture indices and air temperature with the overall goal of predicting future area burned across the North American boreal region. Our first objective was to take an alternative approach to modeling area burned by developing temporally and spatially explicit empirical models using a multivariate adaptive regression spline (MARS) approach (Friedman, 1991). MARS does not require assumptions about the form of the relationship between the independent and dependent variables. Consequently, it can identify patterns and relationships that are difficult, if not impossible, for other regression methods to reveal. Previous studies have used MARS to model topographic effects on Antarctic sea ice (De Veaux et al., 1993), map forest characteristics in the western United States (Moisen and Frescino, 2002), and predict distributions of anadromous fish species in response to various environmental variables (Leathwick et al., 2005). A second objective of our

study was to use MARS models to generate predictions of annual area burned across boreal North America in response to future scenarios of climate change.

2.3 Data and Methods

2.3.1 Overview

In this study, we evaluated the response of historical wildfires to monthly air temperature and fuel moisture for boreal North America north of 45° N. We develop temporally (1950-2002) and spatially explicit empirical models at 2.5° (latitude x longitude) resolution driven by monthly air temperature, fuel moisture codes, and monthly severity rating using a multivariate adaptive regression splines (MARS) modeling approach to predict annual area burned. Climate predictors were derived from the NCEP Reanalysis I project (Kalnay et al., 1996) at 2.5° spatial resolution. These climate data were also used to calculate spatially and temporally explicit fuel moisture codes using the equations defined in the Canadian Fire Weather Index System (see section 2.3.4.3). We assumed all fires are the result of lightning ignition. The MARS approach was used to identify relationships between historical annual area burned and monthly air temperature and fuel moisture. We then evaluated model performance by comparing predictions with observations over the period 1960-2002 across the study region. Following model development we used climate model output from the second generation of the Canadian Center for Climate Modeling and Analysis Coupled Global Climate Model to calculate fuel moisture codes for the period 2006-2100 based on the Intergovernmental Panel on Climate Change (IPCC) Third Assessment (IPCC, 2001).

We then used the future air temperature and fuel moisture codes to drive each MARS model through year 2100.

2.3.2 Multivariate adaptive regression splines (MARS)

Multivariate adaptive regression spline (MARS) models use a non-parametric modeling approach that does not require assumptions about the form of the relationship between the predictor and dependent variables (Friedman, 1991). As a consequence, MARS models have the ability to characterize relationships between explanatory and response variables that are difficult, if not impossible, for other regression methods (e.g., linear models) to reveal. MARS modeling, in the simplest form, partitions the parameter hyper-space of explanatory variables into disjoint hyper-regions. Within each of these hyper-regions, a linear relationship is used to characterize the impact of explanatory variables on the response. The point where the slope changes among hyper-regions is called a knot and the collection of knots identified by the MARS algorithm is used to generate basis functions (splines), representing either single variable transformations or multivariable interactions.

The MARS algorithm operates in two basic parts. The first part can be thought of as a selection of a suitable collection of explanatory variables, and the second part is elimination of the least useful explanatory variables among the previously selected set. The first part of the MARS algorithm constructs models in a parsimonious manner by minimizing Mean Square Error (MSE) across the model space while searching in a forward stepwise manner for combinations of variables and knot locations that improve

the model fit. Specifically, the basic algorithm cycles through each predictor variable, x_i and every possible knot value, k of x_i, and breaks the data into two parts, one on either side of the knot, k. The algorithm keeps the knot and variable pair that gives the best fit and then fits the response using linear functions that are both non-zero on one side of the knot. After a variable is selected, splits on subsequent variables can depend on the previous split by splitting on one side of the previous knot (i.e., dependent on the parent basis function).

The number of basis functions can be constrained by a user-defined maximum. The set of explanatory variables is then pruned back (i.e., variables are assessed for potential removal from the model) based on a residual sum of squares criteria using a reverse stepwise procedure. The optimal model is then chosen based on a generalized cross-validation (GCV) measure of the MSE. The GCV procedure is used to determine which variables to keep in a given model by introducing a penalty on adding variables to the model. The procedure determines which variables to keep in the model and which to eliminate. Furthermore the GCV is used to rank variables in terms of their importance by computing the GCV with and without each variable in the model.

2.3.3 Model development and extrapolation

In this study, we used MARS v2.0 (© Salford Systems, 2001) to develop 127 independent models at 2.5° spatial resolution (total of 127 boreal cells across Alaska and Canada). The total number of models developed depended on the spatial and temporal coverage of historical fire records across the North American boreal region. The

parameterization approach was designed to capture variation in the influence of predictor variables across the spatial extent of our domain (e.g., Alaska to Eastern Canada). The response variable was annual area burned, and the predictor variables are monthly (April-September) air temperature and the monthly fuel moisture codes and severity rating of the Canadian Fire Weather Index System (see section 2.3.4.3). This resulted in a total of 30 possible predictor variables for each grid cell (6 months x 5 predictors: air temperature, fine fuel moisture code, drought code, duff moisture code, monthly severity rating). Models were only developed for cells where the number of fire years (i.e., years where area burned is non-zero) in a given 2.5° cell is equal to or greater than 10.

We evaluated the response of annual area burned to future climate change by calculating the Canadian Fire Weather Index fuel moisture and severity rating components using the CGCM2 global climate model A2 and B2 SRES scenario data sets and then extrapolated each MARS model from year 2006 to year 2100 for each scenario.

2.3.4 Data sets for model development and application

2.3.4.1 Historical fire records

As lightning is caused by weather related factors, and because our overall goal is to model the influence of fire weather on annual area burned, we did not include human-caused fires in this study. Although human-caused fires account for the majority of fires in the North America boreal region, they account for a small portion of the total area burned (Kasischke et al., 2006). For this study, we considered only lightning-caused fires

from each data set for years 1960-2002. The fire data were aggregated by year within each 2.5° grid cell.

A database of fire point location data and 1-km resolution fire scar data sets was acquired for Alaska and Canada. For Alaska, we used the Alaska fire scar location database initially developed by Kasischke et al. (2002) and maintained by the Bureau of Land Management, Alaska Fire Service (2005). The database contains point and boundary location information for fires in Alaska from 1950-2002. Fires greater than 1000 acres (~404 ha) are included from 1950-1987, inclusive, and fires greater than 100 acres (~40.4 ha) are included from 1988-2002, inclusive.

For Canada we used a combination of point location data from the Canadian Large Fire Database (LFDB) and provincial polygon data. The LFDB is a compilation of provincial and territorial wildfire data that represent all fires from 1959-1999 that are greater than 200 ha. For the point location datasets for Canada (Flannigan and Little, 2002), we used the longitudinal and latitudinal point locations to calculate a radius for each location based on the area of the historical fire area. Circular fire boundaries were then created for each point by buffering each point by a distance equal to the calculated radius. The provincial polygon data represent fires in all provinces from 1980-2002 (Stocks et al., 2002; Flannigan, unpublished data). Historical fire data for Saskatchewan (Naelapea and Nickeson, 1998) and Alberta (Government of Alberta, 2005) were also obtained as polygon coverages for the periods 1945-1979 and 1931-1979, respectively.

2.3.4.2 Daily weather data and GCM scenarios

Daily maximum air temperature, wind speed, and relative humidity were obtained from the NCEP Reanalysis 1 data set (Kalnay et al., 1996) at the NOAA Office of Oceanic and Atmospheric Research, Earth Sciences Research Laboratory, Physical Sciences Division, Boulder, Colorado, USA (http://www.cdc.noaa.gov/) at 2.5° resolution for 1960-2005. For daily precipitation, we used the statistically reconstructed NCEP precipitation obtained online from the Arctic Regional Integrated Modeling System data server (http://rims.unh.edu/data/data.cgi) at 2.5° resolution for the same time period. The daily NCEP data were used to calculate the fuel moisture components of the Canadian Fire Weather Index System (refer to section 2.3.4.3). The fuel moisture codes and air temperature were then aggregated to monthly resolution to develop empirical relationships with historical area burned using the MARS modeling approach (refer to section 2.3.2).

To predict annual area burned for future climate change scenarios, we derived daily data from 1961-2100 at approximately 3.75° by 3.75° resolution for air temperature, precipitation, specific humidity, and wind speed from the second generation of the Canadian Center for Climate Modeling and Analysis Coupled Global Climate Model (CGCM2) (http://www.cccma.bc.ec.gc.ca/data/cgcm2/cgcm2.shtml). A detailed description of the CGCM2 can be found in Flato and Boer (2001). CGCM2 has been used to produce ensemble climate change projections using the IPCC Third Assessment A2 and B2 scenario storylines. The A2 and B2 emissions storylines are discussed in detail in the IPCC Special Report on Emissions Scenarios (Nakićenović and Swart, 2000). The

emissions are based on assumptions about socioeconomic, demographic, and technological changes. These scenarios were then converted into greenhouse gas concentration equivalents that are used as driving variables for GCM projections. The A2 scenario represents a world where energy usage is high, economic and technological development is slow, and population growth reaches 15 billion by year 2100. The B2 scenario represents a world where energy usage is lower, economies evolve more rapidly, environmental protection is greater, and population growth is slower (10.4 billion by year 2100). The B2 scenario therefore produces lower emissions and less future warming.

Both scenarios have a baseline period of 1961-1990 that corresponds to the IS92a scenario and was used to initialize the A2 and B2 scenarios for CGCM2. These data were downscaled from 3.75° to 2.5° spatial resolution by area-weighting the CGCM2 cells that intersected a given 2.5° grid cell. To account for differences between the model development data and the GCM predictions (air temperature, relative humidity, precipitation, and wind speed), we adjusted the CGCM2 data relative to the absolute difference from the 1961-1990 NCEP mean by:

$$CGCM2_{adjusted\ daily} = NCEP\mu + (CGCM2_{daily} - CGCM2\mu) \quad (2.1)$$

in which NCEPμ is the mean daily value for the period 1961-1990 derived from the NCEP model development data, $CGCM2_{daily}$ is the daily value output by CGCM2, and CGCMμ is the mean daily value for the period 1961-1990 derived from the CGCM2 daily data. Taking the absolute difference between different climate data sets can result in unrealistic values, particularly for precipitation (e.g., negative values for precipitation).

Very few precipitation data points (calculated by Equation 2.1) across the study area resulted in negative values and were set to zero for those instances.

2.3.4.3 Canadian fire weather index

The Canadian Fire Weather Index System (CFWI) was developed for the prediction of forest fire behavior in response to weather data (Van Wagner, 1987). The CFWI is composed of three fuel moisture codes, the drought code (DC), duff moisture code (DMC), and the fine fuel moisture code (FFMC) and three behavioral indices which are the buildup index (BUI), initial spread index (ISI), and fire weather index (FWI). Of the three behavioral indices, the FWI represents the intensity of a spreading fire and is derived from the three moisture codes and surface wind speed. The daily severity rating (DSR) is derived from the FWI and is designed to capture the non-linear aspect of fire spread (area burned) (Van Wagner, 1987). By averaging the DSR over a period, one can obtain the monthly severity rating (MSR) or seasonal severity rating (SSR), which is used as an index of fire weather from month to month (MSR) and from season to season (SSR). Each component of the CFWI system is calculated from a combination of daily weather data which include air temperature, precipitation, relative humidity, and wind speed. It should be noted that many of the components of the CFWI System are highly non-linear.

For the purpose of this study, we used the fuel moisture codes and severity rating. The unitless codes represent the amount of moisture present in organic matter, with higher values reflecting less moisture content in fuels. The FFMC represents the

moisture content of surface litter and other fine fuels in a forest stand and is an indicator of sustained flaming ignition and fire spread. The DMC represents the moisture content of loosely compacted, decomposing organic matter of moderate depth and relates to the probability of lightning ignition and fuel consumption. The DC represents a deep layer of compact organic matter and relates to the consumption of heavier fuels and the effort required to extinguish a fire. The MSR, which is a monthly average of the DSR represents the fire weather from month to month.

We used the CFWI algorithm (provided by Mike Wotton, personal communication) to calculate 2.5° estimates of the fuel moisture and DSR codes for each day for months April to September (years 1960-2005) across Alaska and Canada. For the period 1960-2005, we used the daily air temperature, precipitation, relative humidity, and wind speed values from the NCEP Reanalysis I data set to calculate the fuel moisture codes and DSR which were then aggregated to monthly resolution for model input. For evaluating fire regime for future scenarios of climate change, a second set of CFWI fuel moisture and severity codes was calculated for years 2006-2100 based on the CGCM2 A2 and B2 scenarios.

2.4 Results

We first present our model estimates that correspond to the temporal period of the development data sets (1960-2005) and discuss model performance at different spatial scales. We then present estimates of annual area burned for future scenarios of climate change.

2.4.1 Model estimates for Alaska & Canada, 1960-2005

To understand the level of predictability at the scale of Alaska and Canada combined, we aggregated the predicted annual area burned for the period 1960-2002 and compared it with observations contained in all model cells over that period. At this scale (Alaska and Canada combined), the MARS models explain 82% ($p < 0.0001$) of the variation in annual area burned in response to April-September air temperature, FFMC, DMC, DC, and MSR (Figure 2.1a). The models captured the inter-annual variation in observed annual area burned, from small fire years to large fire years (Figure 2.1b). The models tended to overestimate annual area burned on average by approximately 50% during the early- to mid-1960s and underestimate area burned during large fire years from the late 1970s through 2002.

At 2.5° resolution, our models captured the variation in annual area burned across Alaska and Canada with varying levels of success (Figure 2.2). On average, the models explained 53% of the variation in annual area burned at 2.5° resolution. Across all models (see Appendix), monthly air temperature was found to be the most frequently occurring variable followed by monthly severity rating (Table 2.1a). Across all variables, months June through August corresponded to the most frequently occurring months across all models (Table 2.1). The starting (April and May) and ending (September) months for all variables generally had the fewest occurrences across all models. On an individual basis, July air temperature entered the models most frequently as the variable of greatest importance (Table 2.1b). However, if the CFWI codes are grouped together,

they enter the models most frequently for months June through August as the most important predictors of area burned, followed by July temperature (Table 2.1b).

Differences in the level of predictability at 2.5° are related to the region in which a given model was developed (Figures 2.2 and 2.3). The models appear to consistently capture the variability in annual area burned in the western portion of the study area, extending from the interior region of Alaska through portions of western and central Canada. However, the models are less consistent in the areas along the boreal forest-tundra border in western North America as well as the eastern portion of the study region, extending from southeast of the Canadian Shield through Ontario and Quebec. Areas with substantial topographic relief, such as the MacKenzie Mountains and eastern edges of the Rocky Mountains, also have lower levels of predictability. To give a better picture of the level of predictability aggregated to the regional scale, we divided the study area into three regions: Alaska (defined as west of 145° W), western Canada (defined as east of 142.5° W and west of 92.5° W; extending southeast from the Yukon Territory to eastern Manitoba), and eastern Canada (defined as east of 90° W) extending from western Ontario to western Newfoundland). For Alaska (N_{models} = 17; Figure 2.3a) and western Canada (N_{models} = 91; Figure 2.3b), the MARS approach explains on the order of 80% of the variation in annual area burned, with greater predictability in western Canada. In contrast, the models for eastern Canada (N_{models} = 19; Figure 2.3c) explain on the order of 40% of the variation in annual area burned. The regression trend in eastern Canada is largely driven by an outlying data point from an anomalously large fire year. Removing

this data point caused the models to collectively explain only 9% of the variation in annual area burned.

2.4.2 Future area burned, 2006-2100

At the Alaska-Canada scale, future area burned showed substantial inter-annual variability from year to year when forced by the A2 and B2 climate scenarios (Figure 2.4a). Predicted area burned between the A2 and B2 scenarios was similar through 2050, but diverged for the last 50 years of the 21st Century, with the A2 scenario resulting in greater area burned (Figure 2.4a). We averaged area burned by decade from 1991-2100 to highlight the differences between each scenario. The period 1991-2000 was defined as the baseline comparison period. This corresponds to a period with high fire activity across Alaska and Canada and is used to compare with future decades that are assumed to also experience high levels of fire activity in response to climate change. Across Alaska and Canada, average area burned approximately doubled by the middle of the 21st Century for both the A2 and B2 scenarios. After 2050, the A2 scenario area burned continued to increase on the order of 1.2 times per decade through 2100 (Figure 2.5a). Relative to 1991-2000, area burned increased by 5.7 times under the A2 scenario by the last decade of the 21st Century. A period exists under the B2 scenario where average area burned plateaus from the 2040s until the 2060s followed by an increase in the 2070s that remained approximately the same through the remaining decades of the 21st Century (Figure 2.5a). Relative to the baseline period, average area burned increased on the order of 3.5 times under the B2 scenario.

To understand the differences in future area burned from Alaska to Eastern Canada, we divided the study area into regions as defined earlier in section 2.4.1. Across Alaska (Figure 2.4b), western Canada (Figure 2.4c), and eastern Canada (Figure 2.4d) annual area burned showed considerable variation from year to year under the A2 and B2 scenarios. Relative to the baseline period, average decadal area burned approximately doubled by the 2040s for both Alaska (Figure 2.5b) and western Canada (Figure 2.5c) under both scenarios. In contrast, average decadal area burned approximately tripled for eastern Canada (Figure 2.5d). For all three subregions, the A2 scenario generally resulted in an increase in average decadal area burned from the baseline period through the 2090s. Comparing the baseline period with the last decade of the 21st Century, the A2 scenario resulted in an increase in average decadal area burned by 4.0 and 5.7 times for Alaska (Figure 2.5b) and western Canada (Figure 2.5c), respectively, while it increased on the order of 7.0 times for eastern Canada (Figure 2.5d). For the B2 scenario, however, area burned appeared to plateau from 2050-2090 in Alaska (Figure 2.5b) and from 2040-2070 in western Canada (Figure 2.5c). For Alaska, this was followed by an increase in average decadal area burned for the period 2091-2100, while for western Canada an increase in average decadal area burned was observed in 2071-2080 and then remained similar through the end of the 21st Century. A similar pattern was observed for the last three decades in eastern Canada (Figure 2.5d). It should be noted, however, that the average decadal area burned in eastern Canada was quite variable for the previous decades of the 21st Century. Relative to the baseline period, average decadal area burned for the 2090s increased on the order of 3.0-3.5 times for all sub-regions.

2.5 Discussion

The results presented here represent a first attempt at using a non-parametric regression spline approach for understanding the response of historical wildfire regime to fuel moisture indices and weather with the overall goal of predicting future area burned. Below we address the overall performance of the MARS modeling approach, the effectiveness of this approach at different spatial and temporal scales, and uncertainties and limitations of this study.

2.5.1 Model fitting and overall performance

While several methods have been successful at regional levels, they are often based on classical linear regression approaches when in fact the underlying relationships between climate and fire are inherently non-linear (Stocks, 1993). The use of classical regression techniques such as simple or multiple linear regression for describing complex relationships is limited, as the models may be too simplistic to accurately represent the study system. Additionally, these methods tend to be cumbersome in terms of meeting assumptions of data normality, often require variable transformations, and are not efficient for investigating relationships hidden in data sets of high dimensionality. Improvements in identifying complex relationships can be made through the use of more complicated modeling approaches, such as neural networks, but it is often difficult to interpret the meaning of these models. The MARS approach is a means of overcoming these hurdles when modeling complex systems by forming a series of regressions on different intervals (hyper-regions) of the independent variable space without having to

meet the assumptions of data normality. An additional concern when modeling observational data is the problem of extreme collinearity of predictor variables (Friedman, 1991). The effects of having variables that are highly correlated are reduced in the MARS approach by introducing a penalty on added variables through the generalized cross-validation criterion used in the forward selection procedure as well as by increasing the number of interaction terms in the model. Furthermore, models developed using the MARS approach are easier to interpret in comparison to other modeling and mathematical techniques (e.g., neural networks, principal components analysis).

2.5.2 Spatial and temporal dynamics of historical wildfire regime

It is clear that a linkage exists between fire and climate; however, this relationship can vary from one geographic region to another. Understanding the spatial and temporal dynamics of historical area burned is essential prior to predicting area burned for future scenarios of climate change. Our results are a first attempt at understanding wildfire regime through the use of the MARS modeling approach. We found considerable spatial variation in the level of predictability at 2.5° but were able to explain on the order of 80% of the variation in annual area burned at the Alaska-Canada scale. Fire weather indices have been used to establish relationships with area burned by wildfire across Canada in previous studies. Harrington et al. (1983) explained up to 38% of the variability in provincial area burned while Flannigan et al. (2005) explained between 36%-64% of the

variation in area burned by ecozone. Both of these studies used forward-stepwise linear regression approaches.

Accounting for the spatial influences on wildfire regime is important when developing models that are driven by fuel moisture and temperature. For example, the fire regime across Alaska and western Canada has more continental influences than that in eastern Canada, where the fire regime is influenced by Atlantic moisture sources and large water bodies (e.g., Great Lakes, Hudson and James Bays). As a result, short-lived drought periods will have a greater influence on fire regime in regions characterized by drier climates while regions characterized by a wetter climate require longer drought periods to realize similar effects (Skinner et al., 1999). The fire return interval, defined as the time it takes to burn an area equal in size to an existing burn area, can also influence model development and overall performance. In eastern Canada, the fire return interval tends to be longer (Campbell and Flannigan, 2000), and there is a greater proportion of broad-leaf forests (leading to lower flammability). Therefore the number of historical fires would be less in comparison to western Canada and Alaska.

The level of predictability was generally higher in the western portion of our study area, with some areas of low predictability near the Mackenzie Mountains and along the eastern border of the Rocky Mountains. Predictability was low in areas along the boreal forest-tundra border in western North America. Although we did not incorporate topographic influences on fire regime in this study, it has been shown to be an important factor in previous studies at regional scales (Dissing and Verbyla, 2003). In the eastern portion of the study region, the level of predictability was considerably lower,

as also observed in previous studies (Harrington et al., 1983; Flannigan and Van Wagner, 1991) and may be attributed to factors such as maritime influences and more extensive fire suppression.

Accounting for the seasonality of wildfire regime is an important component of attempts to model the variation in annual area burned. Generally, the mid-summer (June and July) months will correspond to periods of high fire activity in the North American boreal region as they are, on average, the warmest months on record and support favorable conditions for fire ignition and spread. Our models demonstrate the ability to capture this period, as the most frequent months that entered a given model across our study area were either June or July. Stocks et al. (1998) used the Canadian GCM under a 2x CO_2 scenario and found significant increases in areas experiencing extreme fire weather danger across Canada and Russia, primarily in June and July. It has been observed, however, that in extreme fire years, favorable conditions for fire ignition and spread can continue well beyond this period (e.g., 2004 fire season in Alaska). Air temperature has been demonstrated in previous empirical studies to be an important predictor of area burned by wildfire (see Duffy et al., 2005, Flannigan et al., 2001; 2005). Duffy et al. (2005) explained 79% of the variation in annual area burned for Alaska using monthly air temperature, precipitation, and atmospheric teleconnection indices. While we did not incorporate the role of atmospheric teleconnections, which are synoptic in scale, our results support the role of air temperature as a predictor of area burned as it entered the models as one of the most important predictors (Table 2.1b). Other studies have found that the fuel moisture codes of the CFWI (FFMC, DMC, DC), were the most

frequently occurring predictors of area burned for Canadian ecozones (Flannigan et al., 2005). The FFMC, DMC, and DC (in increasing order of importance) were also found to be important in the prediction of area burned in our study; however, air temperature and MSR were the most frequently occurring predictors in the models across Alaska and Canada (Table 2.1a). With respect to variable importance, however, the CFWI codes, as a group, entered the models more frequently across the study area (Table 2.1b).

2.5.3 Future wildfire regimes

The projected changes in climate across the boreal region are expected to have far reaching effects on fire regime. Shifts in fire size, frequency, and severity would have major implications for the carbon cycle (Zhuang et al., 2006; Balshi et al., 2007) across this region as well as for energy feedbacks to the climate system (Randerson et al., 2006) and potential impacts on regional socio-economic conditions (Chapin et al., 2003). Various forcing scenarios that drive global climate models make it possible to understand how fire regime might change by the end of the 21st Century. In this study, we were limited to using the daily output variables from one GCM, as other data sets that were publicly available were not temporally continuous (i.e., they were only represented as time slices for different periods of the 21st Century). However, the CGCM ranks among the top GCMs currently used by the IPCC with respect to the level of predictability in northern high latitudes (Table 2.2).

Future area burned across North America predicted for the period 2006-2050 indicates marginal differences between the A2 and B2 forcing scenarios (Figure 2.4a).

Although an increase in average area burned is predicted for the entire study region over this period, the increase in the frequency of the largest fire events is not evident until the late 2040s. Across Alaska and Western Canada, annual area burned under the A2 and B2 scenarios are similar through 2050, but diverge in the last 50 years of the 21st Century with the climate under the A2 scenario resulting in greater area burned in both regions.

The projected increase in annual area burned across the North American boreal region is similar to those estimates presented in previous studies. Flannigan et al. (2005) explained between 36-64% of the variation in area burned for Canadian ecozones using a linear forward stepwise regression approach. They suggest that under a 3x CO_2 scenario, area burned will increase by 74-118% by the end of the 21st Century. An earlier study by Flannigan and Van Wagner (1991) explored relationships between seasonal severity rating and annual provincial area burned. They found that under a 2x CO_2 scenario climate, seasonal severity rating (SSR) increased by 46% and suggested that an increase in area burned could be expected under similar conditions, but assuming that the relationship between area burned and SSR is linear.

Flannigan et al. (2000) investigated the influence of future climate on SSR for forests across the United States. They suggest that under a 2x CO_2 climate scenario, SSR will increase by approximately 30% in parts of Alaska, which translates into an increase in area burned of between 25-50% by the middle of the 21st Century. Relative to the period 1991-2000, we predict an approximate doubling of average decadal area burned for Alaska by the 2040s under both the A2 and B2 climate scenarios. Large future increases in area burned for western and central Canada under future climate change

scenarios have been suggested by Flannigan et al. (2001) due to increases in the fire weather index. McCoy and Burn (2005) suggest an approximate doubling of area burned for central Yukon Territory by 2069. Tymstra et al. (2007) estimate an increase in area burned of between 12.9-29.4% for Alberta under 2x and 3x CO_2 climate scenarios. We estimate that the western Canada sub-region (which also encompasses central Canada) will be responsible for the majority of future area burned across North America. By the mid-21st Century we estimate that average decadal area burned will double under the CGCM2 A2 and B2 scenarios and increase by a factor of 3.6-5.6 times by 2091-2100 (Figure 2.5c). Historically, this region has accounted for the majority of area burned across boreal North America.

While an increase in area burned has been suggested across most of central and western Canada, it has been suggested that a reduction in area burned would be expected for regions of eastern Canada based on analyses that examine the relation between components of the CFWI and future climate (Flannigan et al., 2001; Bergeron and Flannigan, 1995). Across eastern Canada, we predict an increase in average decadal area burned by approximately 2-3 times (Figure 2.5d). The differences in our results may be due to the different climate model scenarios used to simulate future area burned. The greatest variability in annual area burned is in eastern Canada, and is most prevalent under the A2 scenario (Figure 2.4d). Of all sub-regions across the study area, the models describing the fire regime of eastern Canada have the lowest level of predictability. The influence of fire frequency on model development is therefore more evident across this

region in comparison to Alaska and western Canada, where fire return intervals are much shorter.

2.5.4 Limitations and uncertainties

Several factors introduce uncertainty in our ability to predict area burned, including the assumptions underlying the use of the CFWI to estimate fuel moisture and severity components for different forest types, the quality and resolution of future climate data sets, and variables not considered in the present analysis.

The present study assumes that the CFWI, which is based on relationships developed with jack pine and Douglas fir (Van Wagner, 1970), can be applied to other forest types that may have different fuel moisture characteristics. However, seasonal trends in duff moisture dynamics in black spruce feather moss stands were predicted well by the CFWI fuel moisture codes (Wilmore, 2001), suggesting that the CFWI may be robust for the North American conifer forests.

Despite the many shortcomings of GCMs, they are the only available tool for estimating future changes in climate. The coarse spatial resolution of GCM output often requires downscaling to an appropriate resolution for conducting analyses relevant to the objectives of a study. The availability of daily GCM output also restricted our options to the use of only one GCM. Many GCMs provide outputs only for certain time-slices (e.g., 2080-2100), which precludes their use in our study, which sought to understand changes from the historical fire record through the entire 21st Century. Availability of restricted time slices also precludes the direct coupling of fire predictions to biogeochemical

models to understand the role of fire on carbon dynamics for future scenarios of climate change. For these reasons we were limited to the CGCM2 coupled ocean-atmosphere global climate model. Other issues related to GCM data stem from the calculation of additional variables (e.g., deriving relative humidity from specific humidity) that, in principle can be obtained, but may yield unrealistic values.

Other variables that we did not consider might also influence future fire regime. While we were able to explain about 82% of the variation in annual area burned driven by fuel moisture, air temperature, and monthly severity rating, variables such as lightning strikes, fire suppression, and the successional dynamics following fire may help to predict area burned on an annual basis more accurately. Incorporating spatially and temporally explicit lightning ignition information into future analyses could be useful with respect to understanding the initial location and subsequent spread of fire, especially at fine spatial scales. However, the Alaska Fire Service and Canadian lightning strike detection network data have only recently become available (since 1986 for Alaska; 1988 for Canada) and do not have temporal coverage spanning the entire length of the historical fire record. Furthermore, current GCMs do not incorporate an explicit component that models cloud to ground lightning strike activity, which would make it difficult to use this variable to project future area burned in response to climate change. Other studies have focused on using satellite data to reconstruct ignition location and fire development, which may have potential for predicting future fire threats (Loboda and Csiszar, 2007).

Fire activity in Canada has been increasing since the 1970s (Podur et al., 2002; Gillett et al., 2004). All things being equal, we would expect that area burned would be

decreasing due to increased spatial coverage of fire suppression and increased efficiency in fire suppression activities including the use of water bombers (Van Wagner 1988; Bergeron et al., 2004, 2006). There is some debate on the effects of fire suppression over large areas and longer timescales (Miyanishi and Johnson, 2001; Ward et al., 2001), but we would expect a decrease in area burned over the short term due to fire management (Cumming, 2005). While fire management agencies operate with a narrow margin between success and failure, a disproportionate number of fires may escape initial attack under a warmer climate, resulting in an increase in area burned much greater than the corresponding increase in fire weather severity (Stocks, 1993). In northern California Fried et al. (2004) used an initial attack model under a 2x CO_2 climate scenario and found that increased fire severity produced faster spreading and more intense fires, which led to increases in escape fires by 50 to 125% over current levels.

Modeling the linkage between climate and fire through empirical relationships limits the potential to incorporate intervening processes. For example, we do not incorporate an available fuels component, which is commonly used in more process-based approaches (see Arora et al., 2005). It has been shown that forest composition can influence fire initiation patterns in the boreal forest (Krawchuck et al., 2007). In addition, fire-induced changes in the proportion of deciduous stands to conifer stands could alter climate-fire interactions in response to changes in future climate. Increases in the frequency and extent of fire could cause a shift from a conifer dominated landscape to a deciduous dominated landscape (Rupp et al., 2001), or might cause regional shifts in the distribution of vegetation types. Coupling our area burned estimates to models that

simulate successional trajectories and biome shifts in response to fire and climate (e.g., Alaska Frame Based Ecosystem Code (ALFRESCO); see Rupp et al., 2002) could provide information with respect to the amount and flammability of fuels across the landscape for future scenarios of climate change.

Finally, future studies should examine the role of future climatic change on the number and sizes of human-caused fires across the boreal region. Wotton et al. (2003) suggested that up to a 50% increase in the total number of human-caused fires could be expected in Ontario, Canada by the end of the 21st Century. Incorporating human-caused fires into future wildfire area estimates will give a more complete picture with respect to the influence of future fire on the carbon dynamics of this region.

2.6 Conclusions

The projected changes in climate across high-latitude regions could significantly alter the current wildfire regimes across the North American boreal forest. These changes in climate could range from increased burning (Flannigan et al., 2000) and extended fire seasons (Wotton and Flannigan, 1993) in portions of the western boreal forest to a reduction in fire frequency in eastern Canadian forests (Carcaillet et al., 2001). These changes in the fire regime have major implications for the carbon dynamics (Zhuang et al., 2006; Balshi et al., 2007) of this region as well as potential energy feedbacks to the climate system (Randerson et al., 2006) through the influence of altered successional pathways.

The empirical relationships developed in this study show that we can accurately predict area burned across the historical fire record for boreal North America. However, incorporating the effects of changes in vegetation composition and structure at large spatial scales (e.g., biome shifts) remains a significant challenge that is best addressed by dynamic vegetation model (DVM) development. Several studies have focused on developing methods for incorporating fire into DVMs at global (Thonicke et al., 2001; Venevsky et al., 2002) and landscape scales (Keane et al., 1996; He and Mladenhoff, 1999; Rupp et al., 2001, 2002). The integration of understanding gained from our study into DVMs is important for predicting the role of fire in the coupled vegetation-climate system. Together, a more accurate representation of interactions among fire, climate, and vegetation dynamics can improve our ability to predict how carbon and energy exchange of the North America boreal region may change in response to future climate regimes.

(a)

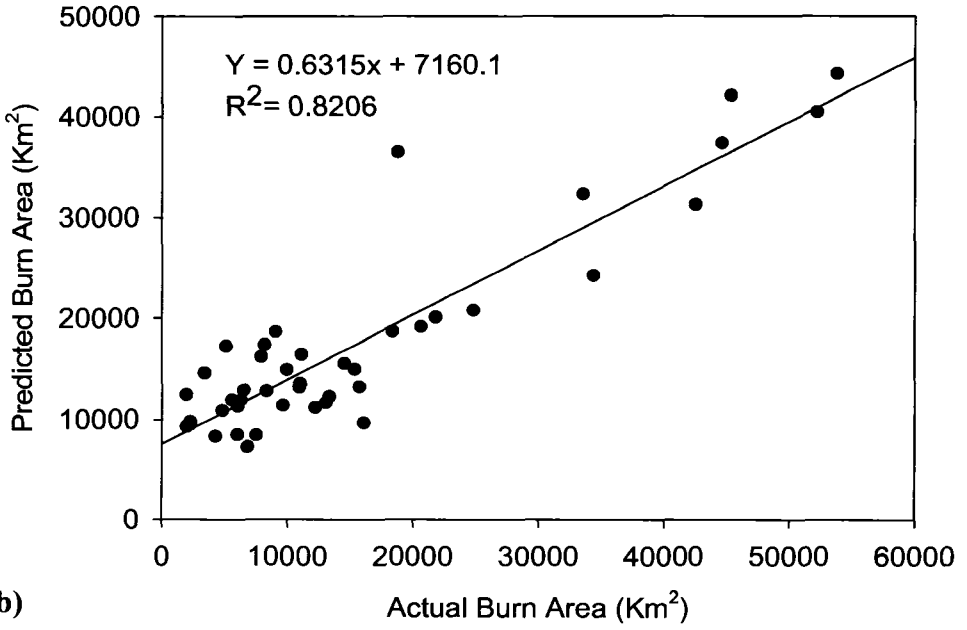

(b)

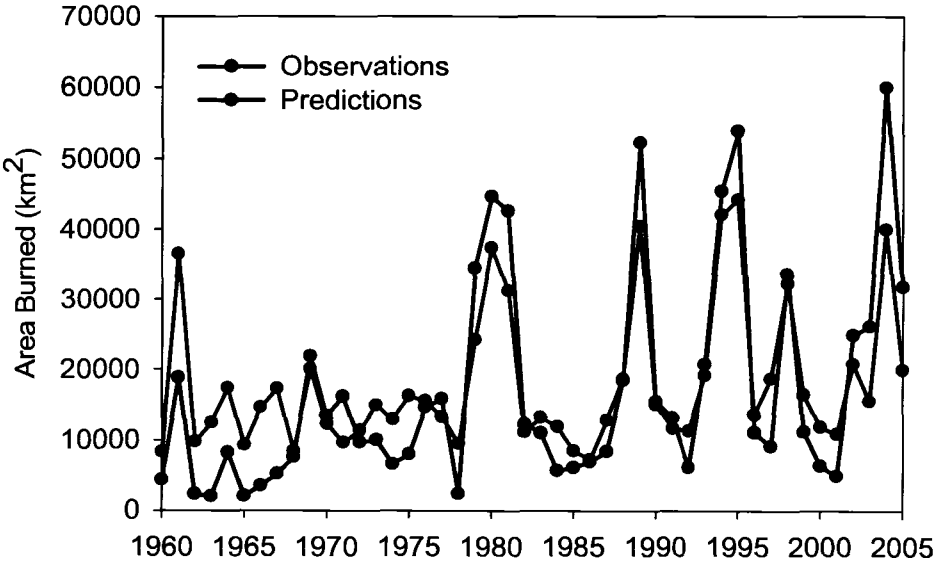

Figure 2.1. (a) Observed vs. predicted annual area burned for Alaska and Canada for years 1960-2002. $R^2 = 0.8206$ ($p < 0.0001$). (b) Comparison of observed and predicted area burned for years 1960-2005.

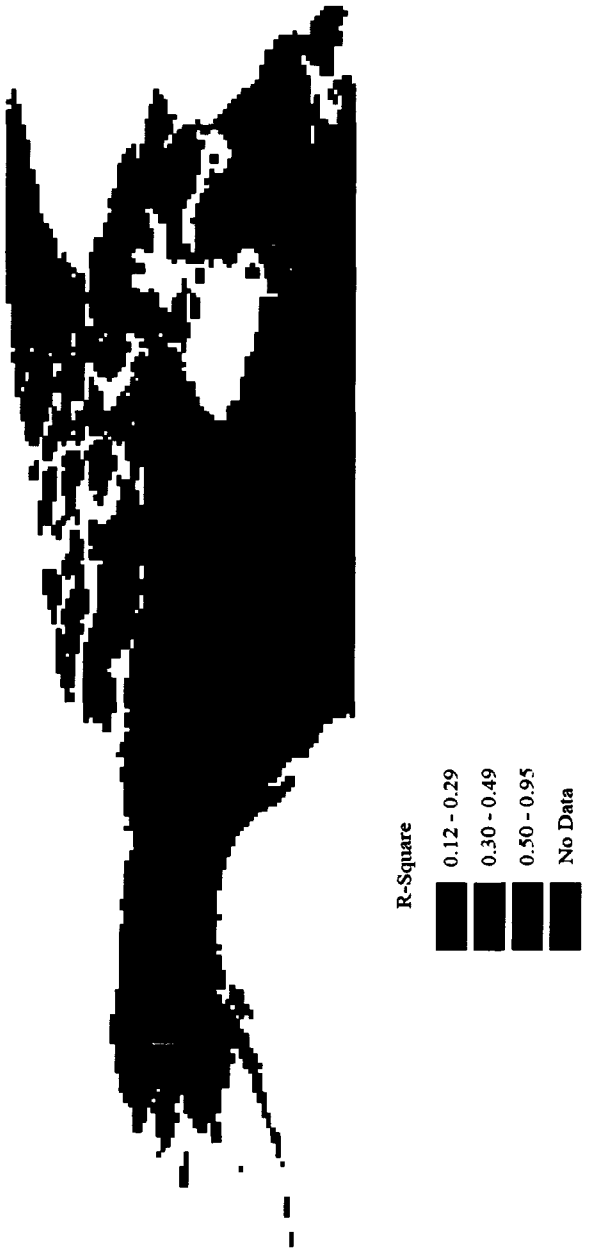

Figure 2.2. R-square values for each 2.5° model for Alaska and Canada. Larger R^2 values represent models with greater level of predictability.

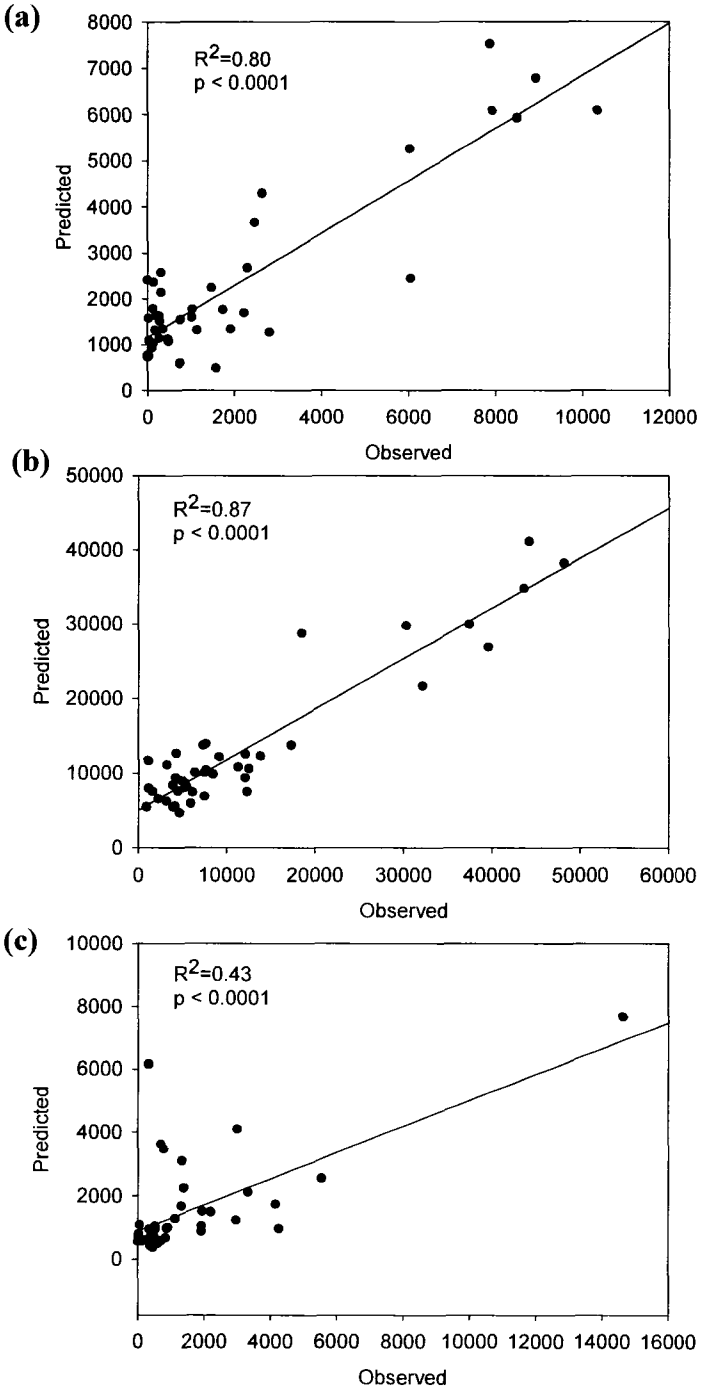

Figure 2.3. Observations vs. MARS model predictions (km^2) of burn area aggregated to regional scales for (a) Alaska (N = 17), (b) western Canada (N = 91), and (c) eastern Canada (N = 19). N indicates the number of models representing the regional aggregate.

Figure 2.4. Predicted annual area burned ($km^2\ yr^{-1}$) driven by the CGCM2 A2 and B2 scenarios from 1990-2100 for (a) Alaska and Canada, (b) Alaska, (c) western Canada, and (d) eastern Canada. Dark circles represent the estimates driven by the A2 scenario while the open circles represent the estimates driven by the B2 scenario.

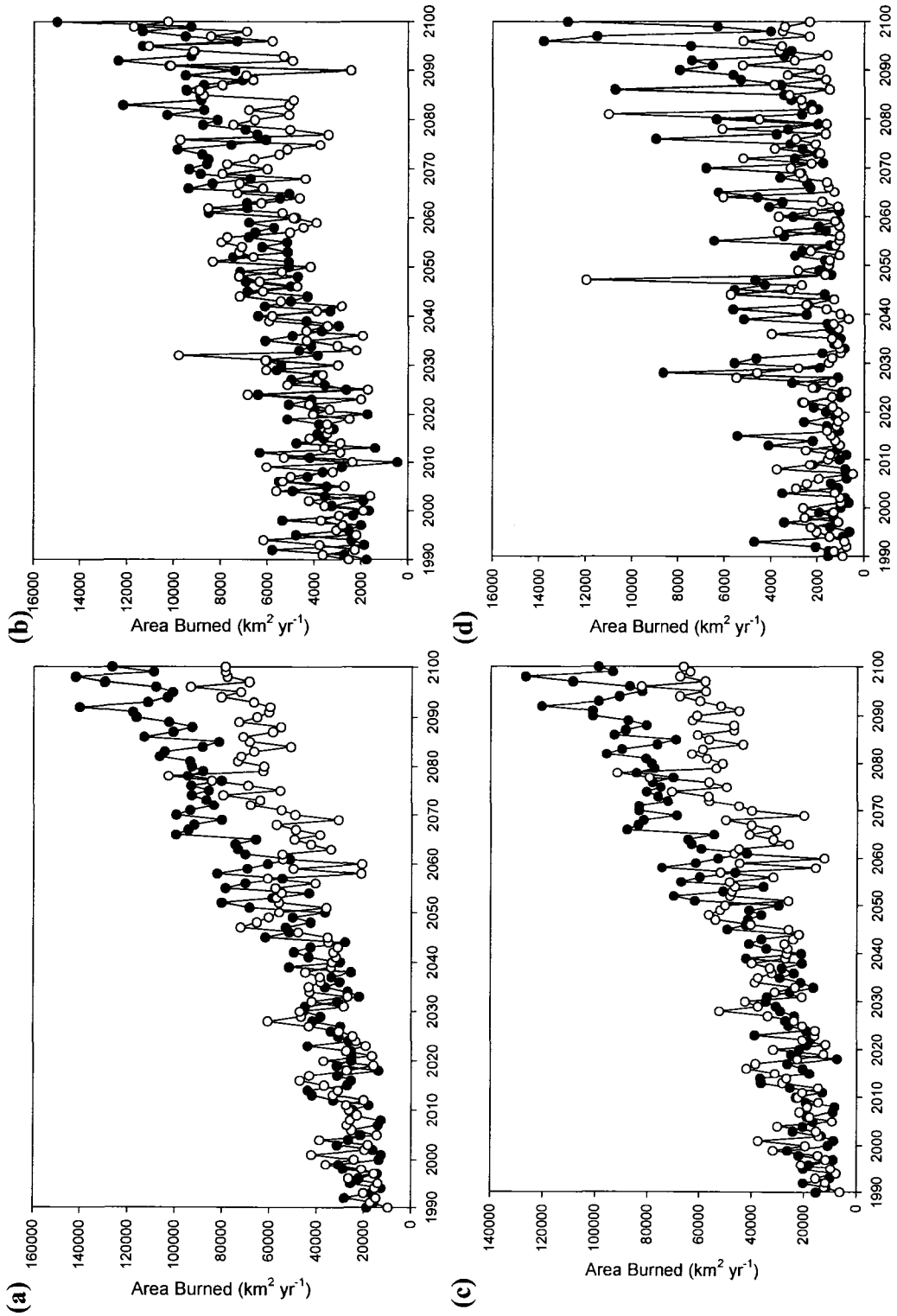

Figure 2.5. Average decadal area burned (km^2 $decade^{-1}$) across (a) North America (b) Alaska, (c) western Canada, and (d) eastern Canada predicted using the NCEP model development datasets ("Observed") and the CGCM2 A2 and B2 climate scenarios. "Observed" represents the baseline period (1991-2000) used for comparison with subsequent decades.

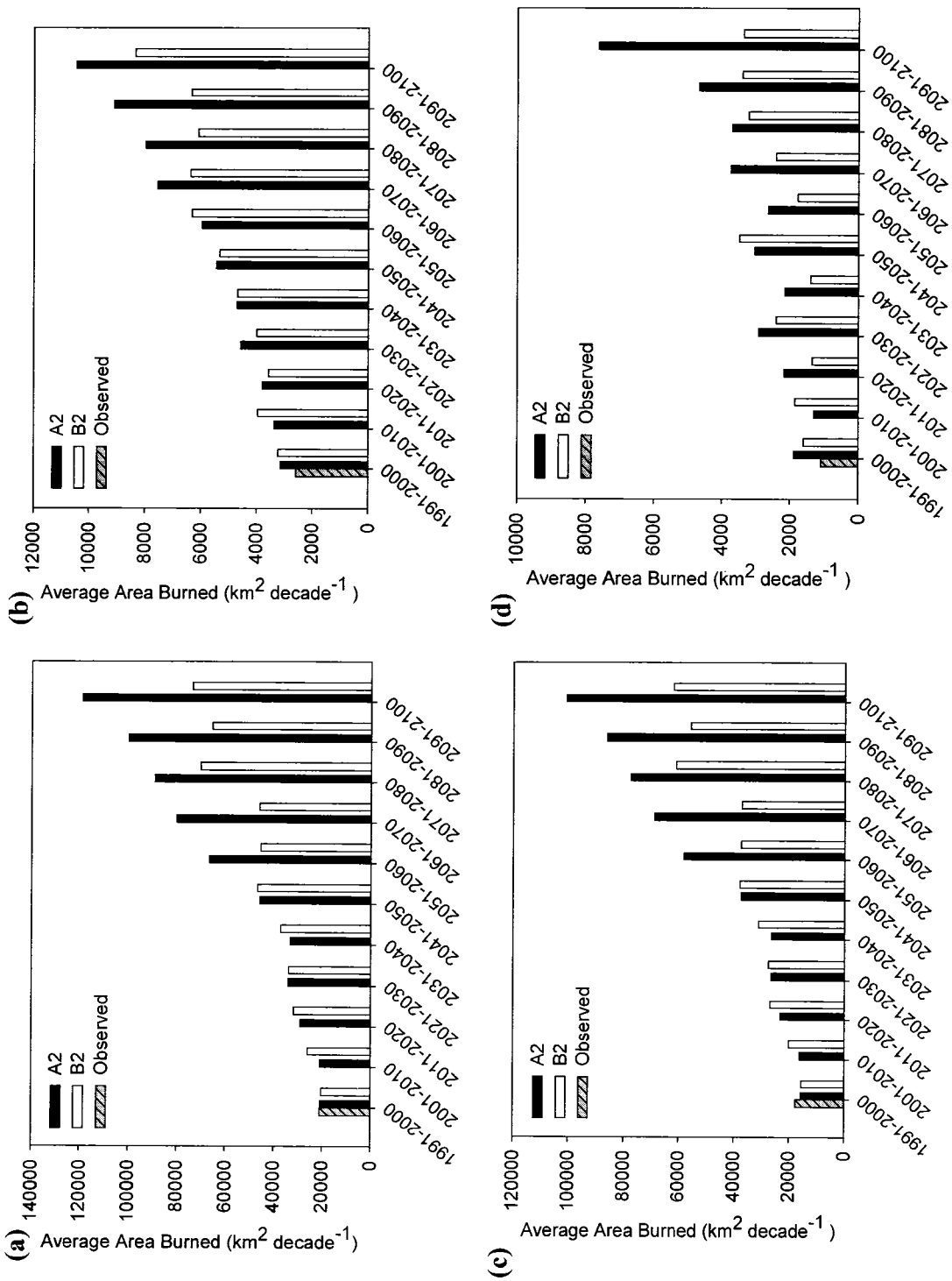

Table 2.1. (a) Model variables and the number of times they occurred across all 2.5 degree models (N = 127) for Alaska and Canada and (b) the number of times a variable entered the model as the most important predictor. MSR is monthly severity rating, DC is drought code, DMC is duff moisture code, and FFMC is fine fuel moisture code.

(a) Variable Count

Model Variable	April	May	June	July	August	September
Air Temperature	22	10	18	33	22	8
MSR	20	12	21	17	12	8
DC	6	10	6	23	16	6
DMC	3	6	18	11	1	3
FFMC	5	4	7	3	6	6

(b) Variable Importance

Model Variable	April	May	June	July	August	September
Air Temperature	6	2	8	16	11	2
MSR	8	2	5	8	7	3
DC	3	5	1	8	10	0
DMC	1	1	8	3	0	1
FFMC	1	1	3	0	2	1
Sum of CFWI codes	13	9	17	19	19	5

Table 2.2. IPCC climate model ranks based on root mean square errors (RMS) averaged over latitudinal ranges 60°N-90°N and 20°N-90°N for surface air temperature (T), precipitation (PREC), and sea level pressure (SLP). In all cases, the RMS errors were summed over the seasonal cycle (12 calendar months) to obtain the ranks. The last column in the table is the sum of the ranks in the preceding columns. CGCM is highlighted in bold.

		60°N-90°N			20°N-90°N			
Rank	Model	T	PREC	SLP	T	PREC	SLP	Total
1	MPI ECHAM5 (Germany)	1	1	3	1	1	1	**8**
2	GFDL CM2.1 (U.S.)	3	4	1	5	2	2	17
3	MIROC3.2_MEDRES (Japan)	4	3	6	3	5	8	29
4	**CCCMA CGCM3.1 (Canada)**	**11**	**2**	**8**	**10**	**4**	**2**	**37**
5	UKMO HADCM3 (U.K.)	8	6	2	6	7	9	38
6	MRI CGM2.3.2A (Japan)	13	11	5	7	6	4	46
7	NCAR CCSM3.0 (U.S.)	2	15	8	2	13	7	47
8	GFDL CM2.0 (U.S.)	9	8	10	14	4	6	51
9	INMCM3.0 (Russia)	6	7	13	10	9	12	57
10	CNRM CM3 (France)	5	12	12	5	11	13	58
11	NCAR PCM1 (U.S.)	13	5	5	14	12	10	59
12	CSIRO MK3.0 (Australia)	14	9	11	12	9	5	60
13	IPSL CM4 (France)	7	11	9	12	15	11	65
14	GISS MODEL ER (U.S.)	10	14	14	10	14	15	77
15	IAP FGOALS1.0.G (China)	15	13	15	15	10	14	82

2.7 Acknowledgements

Funding for this study was provided by grants from the National Science Foundation Biocomplexity Program (ATM-0120468) and Office of Polar Programs (OPP-0531047, OPP-0328282, and OPP-0327664); the National Aeronautics and Space Administration North America Carbon Program (NNG05GD25G); and the Bonanza Creek LTER (Long-Term Ecological Research) Program (funded jointly by NSF grant DEB-0423442 and USDA Forest Service, Pacific Northwest Research Station grant PNW01-JV11261952-231). This study was also supported in part by a grant of HPC resources from the Arctic Region Supercomputing Center at the University of Alaska Fairbanks as part of the Department of Defense High Performance Computing Modernization Program.

2.8 References

Amiro, B. D., K. A. Logan, B. M. Wotton, M. D. Flannigan, B. J. Stocks, and D. L. Martell (2004), Fire weather index system components for large fires in the Canadian boreal forest, *International Journal of Wildland Fire, 13*, 391-400.

Arora, V. K. and G. J. Boer (2005), Fire as an interactive component of dynamic vegetation models. *J. Geophys. Res., 110*, G02008, doi:10.1029/2005JG000042.

Balshi, M. S., A. D. McGuire, Q. Zhuang, J. Melillo, D. W. Kicklighter, E. Kasischke, C. Wirth, M. Flannigan, J. Harden, J. S. Clein, T. J. Burnside, J. McAllister, W. A. Kurz, M. Apps, and A. Shvidenko (2007), The role of historical fire disturbance in the carbon dynamics of the pan-boreal region: a process-based analysis, *J. Geophys. Res., 112*, G02029, doi:10.1029/2006JG000380, 2007.

Bergeron, Y. and M. D. Flannigan (1995), Predicting the effects of climate change on fire frequency in the southeastern Canadian boreal forest, *Water, Air and Soil Pollution, 82*, 437-444.

Bergeron, Y., M. Flannigan, S. Gauthier, A. Leduc, and P. Lefort (2004), Past, current, and future fire frequency in the Canadian boreal forest: implications for sustainable forest management, *Ambio, 33(6)*, 356-360.

Bergeron, Y., D. Cyr, C. R. Drever, M. Flannigan, S. Gauthier, D. Kneeshaw, E. Lauzon, A. Leduc, H. Le Goff, D. Lesieur, and K. Logan (2006), Past, current, and future fire frequencies in Quebec's commercial forests: implications for the cumulative effects of harvesting and fire on age-class structure and natural disturbance-based management, *Can. J. For. Res., 36*, 2737-2744.

Bureau of Land Management, Alaska Fire Service (2005), Alaska Fire History, 1950-2004, Vector Digital Data: http://agdc.usgs.gov/data/blm/fire/index.html

Campbell, I. D. and M. D. Flannigan (2000), Long-term perspectives on fire-climate-vegetation relationships in the North American boreal forest, in *Fire, Climate Change, and Carbon Cycling in the Boreal Forest*, Ecological Studies vol. 138, edited by E. S. Kasischke and B. J. Stocks, pp. 152-172, Springer-Verlag, New York.

Carcaillet, C., Y. Bergeron, P. J. H. Richard, B. Fréchette, S. Gauthier, and Y. T. Prairie (2001), Change of fire frequency in the eastern Canadian boreal forests during the Holocene: does vegetation composition or climate trigger the fire regime?, *Journal of Ecology*, *89*, 930-946.

Chambers, S. D. and F.S. Chapin III (2003), Fire effects on surface-atmosphere exchange in Alaskan black spruce ecosystems: implications for feedbacks to regional climate, *J. Geophys. Res.*, *108(D1)*, doi: 10.1029/2001JD000530.

Chapin III, F. S., A. D. McGuire, J. Randerson, R. Pielke Sr., D. Baldocchi, S. E. Hobbie, N. Roulet, W. Eugster, E. Kasischke, E. B. Rastetter, S. A. Zimov, and S. W. Running (2000), Arctic and boreal ecosystems of western North America as components of the climate system, *Global Change Biology*, *6(Suppl. 1)*, 211-223.

Chapin III, F. S., T.S. Rupp, A. M. Starfield, L. DeWilde, E. S. Zavaleta, N. Fresco, J. Henkelman and A. D. McGuire (2003), Planning for resilience: modeling change in human-fire interactions in the Alaskan boreal forest. *Frontiers in Ecology and the Environment*, *1*, 255-261.

Clark, J. S. (1990), Effect on climate change on fire regimes in northwestern Minnesota, *Nature*, *334*, 233-235.

Cumming, S.G., 2005. Effective fire suppression in boreal forests. *Can. J. For. Res.*, *35*, 772–786.

De Veaux, R. D., A. L. Gordon, J. C. Comiso, and N. E. Bacherer (1993), Modeling of topographic effects on Antarctic sea ice using multivariate adaptive regression splines, *J. Geophys. Res.*, *98(C11)*, 20307-20320.

Dissing, D. and D. L. Verbyla (2003), Spatial patterns of lightning strikes in interior Alaska and their relations to elevation and vegetation, *Can. J. For. Res.*, *33*, 770-782.

Duffy, P. A., J. E. Walsh, J. M. Graham, D. H. Mann, and T. S. Rupp (2005), Impacts of large-scale atmospheric-ocean variability on Alaskan fire season severity, *Ecological Applications*, *15(4)*, 1317-1330.

Flannigan, M. D. and J. B. Harrington (1988), A study of the relation of meteorological variables to monthly provincial area burned by wildfire in Canada (1953-80), *Journal of Applied Meteorology*, *27*,441-452.

Flannigan, M. D. and C. E. Van Wagner (1991), Climate change and wildfire in Canada, *Can. J. For. Res.*, *21*, 66-72.

Flannigan, M. D., Y. Bergeron, O. Engelmark, and B. M. Wotton (1998), Future wildfire in circumboreal forests in relation to global warming, *Journal of Vegetation Science*, *9*, 469-476.

Flannigan, M. D., B. J. Stocks, and B. M. Wotton (2000), Climate change and forest fires, *The Science of the Total Environment*, *262*, 221-229.

Flannigan, M. D., I. Campbell, M. Wotton, C. Carcaillet, P. Richard, and Y. Bergeron (2001), Future fire in Canada's boreal forest: paleoecology results and general circulation model – regional climate model simulations, *Can. J. For. Res.*, *31*, 854-864.

Flannigan, M. D. and J. Little (2002), Canadian Large Fire Database, 1959-1999 point dataset, Canadian Forest Service http://www.nofc.forestry.ca/fire/research/climate_change/lfdb/lfdb_download_e.htm

Flannigan, M. D., K. A. Logan, B. D. Amiro, W. R. Skinner, and B. J. Stocks (2005), Future area burned in Canada, *Climatic Change*, *72*, 1-16.

Flato, G.M. and G.J. Boer (2001), Warming Asymmetry in Climate Change Simulations. *Geophys. Res. Lett.*, *28*, 195-198.

Fried, J. S., M. S. Torn, and E. Mill (2004), The impact of climate change on wildfire severity: A regional forecast for Northern California, *Climate Change*, *64*, 169-191.

Friedman, J. H. (1991), Multivariate adaptive regression splines, *The Annals of Statistics*, *19(1)*, 1-141

Gillett, N. P., A. J. Weaver, F. W. Zwiers, and M. D. Flannigan (2004), Detecting the effect of climate change on Canadian forest fires, *Geophys. Res. Lett.*, 31, L18211, doi:10.1029/2004GL020876

Government of Alberta (2005), Historical Wildfires: 1931-1979, PFFC.GIS@gov.ab.ca, Wildfire Resource Information Section, Forest Protection Division, Sustainable Resource Development, Government of Alberta, Edmonton, Alberta.

Harrington, J. B., M. D. Flannigan, and C. E. Van Wagner (1983), A study of the relation of components of the Fire Weather Index System to monthly provincial area burned by wildfire in Canada 1953-80. Canadian Forestry Services, Information Report PI-X-25, Petawawa, National Forestry Institute.

He, H. S., and D. J. Mladenoff (1999), Spatially explicit and stochastic simulation of forest-landscape fire disturbance and succession, *Ecology*, *80(1)*, 81-99.

IPCC (2001), *Climate Change 2001: The Scientific Basis. Contribution of Working Group I to the Third Assessment Report of the Intergovernmental Panel on Climate Change*., J.T. Houghton, Y. Ding, D. J. Griggs, M. Noguer, P. J. van der Linden, X. Dai, K. Maskell, and C. A. Johnson (eds), Intergovernmental Panel on Climate Change, Cambridge University Press, 572pp.

Johnson, E. A. (1992), *Fire and Vegetation Dynamics: Studies from the North American boreal forest*, 129 pp., Cambridge University Press, Cambridge.

Johnson, E. A. and D. R. Wowchuk (1993), Wildfires in the southern Canadian Rocky Mountains and their relationship to mid-tropospheric anomalies, *Can. J. For. Res.*, *23*, 1213-1222.

Kalnay, E., M. Kanamitsu, R. Kistler, W. Collins, D. Deaven, L. Gandin, M. Iredell, S. Saha, G. White, J. Woolen, Y. Zhu, M. Chelliah, W. Ebisuzaki, W. Higgens, J. Janowiak, K.C. Mo, C. Ropelewski, J. Wang, A. Leetma, R. Reynolds, R. Jenne, and D. Joseph (1996), The NCEP/NCAR 40-year reanalysis project, *Bull. Amer. Meteor. Soc.*, *77*, 437-470.

Kasischke E., N. L. Christensen, Jr, and B. J. Stocks (1995), Fire, global warming, and the carbon balance of boreal forests. *Ecol. Appl., 5*, 437-451.

Kasischke, E. S., D. Williams, and D. Barry (2002), Analysis of the patterns of large fires in the boreal forest region of Alaska, *International Journal of Wildland Fire*, *11*, 131-144.

Kasischke, E. S., T. S. Rupp, and D. L. Verbyla (2006), Fire trends in the Alaskan boreal forest, in *Alaska's Changing Boreal Forest*, edited by F. S. Chapin, III, M. W. Oswood, K. Van Cleve, L. A. Viereck, and D. L. Verbyla, pp. 285-301. Oxford University Press, New York.

Keane, R. E., K. C. Ryan, and S. W. Running (1996), Simulating effects of fire on northern Rocky Mountain landscapes with the ecological process model FIRE-BGC, *Tree Physiology*, *16*, 319-331.

Krawchuk, M. A., S. G. Cumming, M. D. Flannigan, and R. W. Wein (2007), Biotic and abiotic regulation of lightning fire initiation in the mixedwood boreal forest, *Ecology*, *87(2)*, 458-468.

Leathwick, J. R., D. Rowe, J. Richardson, J. Elith, and T. Hastie (2005), Using multivariate adaptive regression splines to predict the distributions of New Zealand's freshwater diadromous fish, *Freshwater Biology*, *50*, 2034-2052.

Loboda, T. V. and I. A. Csiszar (2007), Assessing the risk of ignition in the Russian far east within a modeling framework of fire threat, *Ecol. Appl., 17(3)*, 791-805.

McCoy, V. M. and C. R. Burn (2005), Potential alteration by climate change of the forest-fire regime in the boreal forest of Central Yukon Territory, *Arctic, 58(3)*, 276-285.

Miyanishi, K., and E. A. Johnson (2001), Comment - A reexamination of the effects of fire suppression in the boreal forest, *Can. J. For. Res., 31*, 1462–1466.

Moisen, G. G. and T. S. Frescino (2002), Comparing five modeling techniques for predicting forest characteristics, *Ecological Modelling, 157*, 209-225.

Naelapea, O., and J. Nickeson (1998), SERM Forest Fire Chronology of Saskatchewan in Vector Format, Oak Ridge National Laboratory Distributed Active Archive Center, Oak Ridge, Tennessee, U.S.A.

Nakićenović, N. and R. Swart (eds.) (2000), *Intergovernmental Panel on Climate Change, Special Report on Emissions Scenarios*. Cambridge University Press, 599 pages.

Nash, C. H. and E. A. Johnson (1996), Synoptic climatology of lightning-caused forest fires in subalpine and boreal forests, *Can. J. For. Res., 26*, 1859-1874.

Podur, J., D. L. Martell, and K. Knight (2002), Statistical quality control analysis of forest fire activity in Canada, *Can. J. For. Res., 32*, 195–205.

Randerson, J. T., H. Liu, M. G. Flanner, S. D. Chambers, Y. Jin, P. G. Hess, G. Pfister, M. C. Mack, K. K. Treseder, L. R. Welp, F. S. Chapin, J. W. Harden, M. L. Goulden, E. Lyons, J. C. Neff, E. A. G. Schuur, and C. S. Zender (2006), The impact of boreal forest fire on climate warming, *Science, 314(5802)*, 1130-1132.

Rupp, T. S., F. S. Chapin III, and A. M. Starfield (2001), Modeling the Influence of Topographic Barriers on Treeline Advance of the Forest-Tundra Ecotone in Northwestern Alaska, *Clim. Change*, *48*, 399–416.

Rupp, T. S., A. M. Starfield, F. S. Chapin III, and P. Duffy (2002), Modeling the impact of black spruce on the fire regime of Alaskan boreal forest, *Climatic Change*, *55*, 213-233.

Salford Systems (2001), MARS™ v2.0, San Diego, CA, USA.

Skinner, W. R., B. J. Stocks, D. L. Martell, B. Bonsal, and A. Shabbar (1999), The association between circulation anomalies in the mid-troposphere and area burned by wildland fire in Canada, *Theoretical and Applied Climatology*, *63*, 89-105.

Skinner, W. R., M. D. Flannigan, B. J. Stocks, D. L. Martell, B. M. Wotton, J. B. Todd, J. A. Mason, K. A. Logan, and E. M. Bosch (2002), A 500 hPa synoptic wildland fire climatology for large Canadian forest fires, 1959-1996, *Theoretical and Applied Climatology*, *71*, 157-169.

Stocks, B. J. (1993), Global warming and forest fires in Canada, *Forestry Chronicle*, *69*, 290-293.

Stocks, B. J., M. A. Fosberg, T. J. Lynham, L. Mearns, B. M. Wotton, Q. Yang, J-Z. Jin, K. Lawrence, G. R. Hartley, J. A. Mason, and D. W. McKenney (1998), Climate change and forest fire potential in Russian and Canadian boreal forests, *Climatic Change*, *38*, 1-13.

Stocks, B. J., J. A. Mason, J. B. Todd, E. M. Bosch, B. M. Wotton, B. D. Amiro, M. D. Flannigan, K. G. Hirsch, K. A. Logan, D. L. Martell, and W. R. Skinner (2002), Large forest fires in Canada, 1959– 1997, *J. Geophys. Res.*, *108*, D1, 8149, doi:10.1029/2001JD000484, 2003.

Swetnam, T. W., and J. L. Betancourt (1990), Fire-Southern Oscillation relations in the southwestern United States, *Science*, *249*, 1017-1020.

Thonicke K., S. Venevsky, S. Sitch, and W. Cramer (2001), The role of fire disturbance for global vegetation dynamics: coupling fire into a Dynamic Global Vegetation Model, *Global Ecology & Biogeography*, *10*, 661-677.

Tymstra, C., M. D. Flannigan, O. B. Armitage, and K. Logan (2007), Impact of climate change on area burned in Alberta's boreal forest, *International Journal of Wildland Fire*, *16*, 153-160.

Van Wagner, C. E. (1970), An index to estimate the current moisture content of the forest floor. Can. For. Serv., Dept. of For. And Fisheries. Pub. No. 1288

Van Wagner, C. E. (1987), Development and structure of the Canadian Forest Fire Weather Index System. Canadian Forest Service, Forestry Technical Report 35.

Van Wagner, C. E. (1988), The historical pattern of annual burned area in Canada, *For. Chron.*, *64*, 182–185.

Venevsky, S., K. Thonicke, S. Sitch, and W. Cramer (2002), Simulating fire regimes in human-dominated ecosystems: Iberian Peninsula case study, *Global Change Biology*, *8*, 984-998.

Ward, P. C., A. G. Tithecott, and B. M.Wotton (2001), Reply - A re-examination of the effects of fire suppression in the boreal forest, *Can. J. For. Res.*, *31*, 1467–1480.

Weber, M. G., and M. D. Flannigan (1997), Canadian boreal forest ecosystem structure and function in a changing climate: Impact on fire regimes, *Environ. Rev.*, *5*, 145–166.

Westerling, A. L., H. G. Hidalgo, D. R. Cayan, and T. W. Swetnam (2006), Warming and earlier spring increases western U.S. forest wildfire activity, *Science*, *313*, 940-843.

Wilmore, B. (2001), Duff moisture dynamics in black spruce feather moss stands and their relation to the Canadian forest fire danger rating system, M. S. Thesis, University of Alaska Fairbanks, 117pp.

Wotton, B. M. and M. D. Flannigan (1993), Length of the fire season in a changing climate, *Forestry Chronicle*, *69*, 187-192.

Wotton, B. M., D. L. Martell, and K. A. Logan (2003), Climate change and people-caused forest fire occurrence in Ontario, *Climatic Change*, *60*, 275-295.

Zhuang, Q., J. M. Melillo, B. S. Felzer, D. W. Kicklighter, A. D. McGuire, M. C. Sarofim, A. Sokolov, R. G. Prinn, P. A. Steudler, and S. Hu (2006), CO_2 and CH_4 exchanges between land ecosystems and the atmosphere in northern high latitudes over the 21st century, *Geophys. Res. Lett.*, *33*, L17403, doi:10.1029/2006GL026972.

2.9 Appendix Multivariate Adaptive Regression Spline (MARS) models and associated basis functions listed by spatial location. Location corresponds to the lower left hand corner of each 2.5° grid cell.

Location	Model
65 W, 52.5N	Y = max(0, 2.692 + 1314.078 * BF3) BF1 = max(0, DCJULY - 37.187) BF3 = max(0, .300000E-03 - MSRJUNE) * BF1
67.5 W, 52.5 N	Y = max(0, 34.447 + 9449.171 * BF1) BF1 = max(0, MSRJULY + .564563E-10)
72.5 W, 50 N	Y = max(0, 7.635 + 116393.727 * BF8) BF8 = max(0, MSRJUNE - .300000E-03)
72.5 W, 52.5 N	Y = max(0, -15.499 + 1.217 * BF9 + 42.377 * BF18) BF9 = max(0, DCJULY - 148.781) BF18 = max(0, TEMPJULY - 11.993)
75 W, 47.5 N	Y = max(0, -54.370 + 282.784 * BF1) BF1 = max(0, DMCJUNE - 0.230)
75 W, 50 N	Y = max(0, 8.710 + 20312.041 * BF1 + 1891.058 * BF4) BF1 = max(0, MSRAUG - .600000E-03) BF4 = max(0, 0.287 - DMCMAY)
75 W, 52.5 N	Y = max(0, 45.326 + 5.356 * BF1) BF1 = max(0, DCAUG - 194.548)
77.5 W, 47.5 N	Y = max(0, 19.448 + 7.991 * BF21 BF21 = max(0, FFMCJUNE - 38.283)
77.5 W, 52.5 N	Y = max(0, 64.709 + 22.090 * BF1) BF1 = max(0, DCAUG - 259.319)
80 W, 47.5 N	Y = max(0, 25.683 + 12.619 * BF7) BF7 = max(0, FFMCAUG - 60.823)
80 W, 50 N	Y = max(0, 14.305 + 75.321 * BF2 + 8.835 * BF3) BF2 = max(0, 6.061 - TEMPMAY) BF3 = max(0, DCMAY - 61.274)
80 W, 52.5 N	Y = max(0, -8.242 + 15.303 * BF1) BF1 = max(0, DCAUG - 274.942)
82.5 W, 45 N	Y = max(0, -3.860 + 16.655 * BF1 - 1385.199 * BF8 + 765.408 * BF10) BF1 = max(0, MSRJUNE - 0.006) BF8 = max(0, MSRMAY - 0.043) BF10 = max(0, MSRMAY - 0.064)
82.5 W, 47.5 N	Y = max(0, -28.142 + 8.910 * BF1 + 9.189 * BF3 + 695.768 * BF5) BF1 = max(0, DMCJUNE - 0.367) BF3 = max(0, 7.964 - TEMPMAY) BF5 = max(0, 0.038 - MSRJUNE)
82.5 W, 50 N	Y = max(0, -57.475 + 43.509 * BF2 + 61.148 * BF5 + 33202.270 * BF8+ 41.718 * BF12 + 16.708 * BF19) BF2 = max(0,TEMPAPRI - 2.890) BF5 = max(0, TEMPJUNE - 13.697) BF8 = max(0, 0.002 - MSRJUNE) BF12 = max(0, 2.230 - DMCAPRIL) BF19 = max(0, TEMPAUG - 14.916)
85 W, 47.5 N	Y = max(0, -1.187 + 364.088 * BF1 + 17.542 * BF3) BF1 = max(0, MSRMAY - .491275E-09) BF3 = max(0, 1.307 - TEMPAPRI)
87.5 W, 47.5 N	Y = max(0, -11.579 + 44.028 * BF3 + 42.080 * BF4 + 221.875 * BF15) BF3 = max(0, 2.057 - TEMPAPRI) BF4 = max(0, TEMPSEPT - 14.377) BF15 = max(0, MSRMAY - 0.047)
87.5 W, 50 N	Y = max(0, -4.899 + 158.199 * BF2 + 19.599 * BF3) BF2 = max(0, - 1.660 - TEMPAPRI) BF3 = max(0, FFMCAUG - 61.074)
87.5 W, 52.5 N	Y = max(0, 2.283 + 282.371 * BF1) BF1 = max(0, MSRAUG + .305807E-08)

2.9 Appendix continued

Location	Model
90 W, 50 N	Y = max(0, -7.181 + 2.238 * BF1 + 79.287 * BF4 + 70.789 * BF6) BF1 = max(0, DCJULY - 196.600) BF4 = max(0, - 1.013 - TEMPAPRI) BF6 = max(0, 16.152 - TEMPJULY)
92.5 W, 47.5 N	Y = max(0, -9.871 + 83.208 * BF2 + 337.940 * BF3) BF2 = max(0, 2.187 - TEMPAPRI) BF3 = max(0, MSRMAY - 0.078)
92.5 W, 50 N	Y = max(0, -128.762 + 3978.068 * BF1 + 1.776 * BF15) BF1 = max(0, MSRJUNE - .566064E-09) BF15 = max(0, DCAUG - 144.552)
92.5 W, 52.5 N	Y = max(0, -34.891 + 3.153 * BF1 + 160.570 * BF4) BF1 = max(0, DCMAY - 15.093) BF4 = max(0, TEMPJUNE - 14.720)
95 W, 47.5 N	Y = max(0, -42.907 + 297.328 * BF1 + 313.240 * BF2 + 1.474 * BF3+ 57.445 * BF5) BF1 = max(0, MSRMAY - 0.135) BF2 = max(0, 0.135 - MSRMAY) BF3 = max(0, DCJUNE - 177.180) BF5 = max(0, MSRJULY - 0.001)
95 W, 50 N	Y = max(0, -205.171 + 845.936 * BF1 + 4.494 * BF3 + 7.441 * BF4) BF1 = max(0, TEMPJULY - 19.884) BF3 = max(0, DCJUNE - 115.090) BF4 = max(0, 115.090 - DCJUNE)
95 W, 52.5 N	Y = max(0, -22.889 + 284.661 * BF1 + 305.591 * BF3 + 100.778 * BF5) BF1 = max(0, TEMPJUNE - 15.700) BF3 = max(0, TEMPJULY - 18.594) BF5 = max(0, TEMPMAY - 8.871)
95 W, 55 N	Y = max(0, -24.846 + 486.335 * BF1 + 45601.629 * BF4) BF1 = max(0, TEMPJULY - 17.294) BF4 = max(0, 0.004 - MSRAPRIL)
97.5 W, 47.5 N	Y = max(0, 12.417 + 2.108 * BF1) BF1 = max(0, DCMAY - 112.958)
97.5 W, 50 N	Y = max(0, -94.648 + 1892.714 * BF1 + 502.313 * BF2 + 352.734 * BF4+ 119.890 * BF5) BF1 = max(0, MSRAPRIL - .699998E-03) BF2 = max(0, TEMPJULY - 21.110) BF4 = max(0, MSRMAY - .363630E-08) BF5 = max(0, TEMPJUNE - 17.460)
97.5 W, 52.5 N	Y = max(0, 36.779 + 800.542 * BF1) BF1 = max(0, TEMPJULY - 19.613)
97.5 W, 55 N	Y = max(0, 57.223 + 1414.958 * BF1) BF1 = max(0, TEMPJULY - 17.852)
100 W, 50 N	Y = max(0, -31.976 + 62.135*BF1 + 68.646 * BF2 * BF3) BF1 = max(0,DMCJUNE - 9.710) BF2 = max(0,TEMPJULY - 19.839) BF3 = max(0,9.710 - DMCJUNE)
100 W, 52.5 N	Y = max(0, -31.312 + 537.808 * BF1 + 3.517 * BF2) BF1 = max(0,MSRJULY-0.655) BF2 = max(0,DCJULY-318.332)
100 W, 55 N	Y = max(0, -1291.159 + 4.343 * BF2 + 887.734 * BF3 + 209.611 * BF4 + 5.834 * BF5 + 864.193 * BF6 + 971.245 * BF7) BF2 = max(0, 339.671 - DCAUG) BF3 = max(0, TEMPJULY - 18.061) BF4 = max(0, 18.061 - TEMPJULY) BF5 = max(0, DCJULY - 121.881) BF6 = max(0, MSRSEPT - 0.002) BF7 = max(0, MSRJUNE - .700000E-03)
100 W, 57.5 N	Y = max(0, -83.796 + 5805.285 * BF1 + 5023.921 * BF3) BF1 = max(0, MSRJULY - 0.076) BF3 = max(0, MSRSEPT - 0.046)

2.9 Appendix continued

Location	Model
102.5 W, 50 N	Y = max(0, -203.056 + 43.121 * BF1 + 20.587 * BF2 + 1.984 * BF3) BF1 = max(0, DMCJUNE - 10.503) BF2 = max(0, 10.503 - DMCJUNE) BF3 = max(0, DCMAY - 35.210)
102.5 W, 52.5 N	Y = max(0, -24.705 + 434.277 * BF1 + 478.899 * BF3) BF1 = max(0, MSRJULY - 0.670) BF3 = max(0, MSRMAY - 0.020)
102.5 W, 55 N	Y = max(0, -2220.454 + 1250.298 * BF1 + 270.639 * BF2 + 89.393 * BF3 + 18.598 * BF4 + 47.616 * BF7 + 63295.504 * BF9) BF1 = max(0, TEMPJULY - 17.797) BF2 = max(0, 17.797 - TEMPJULY) BF3 = max(0, DMCJUNE - 0.740) BF4 = max(0, FFMCSEPT - 38.600) BF7 = max(0, FFMCAPRI - 37.883) BF9 = max(0, 0.015 - MSRAPRIL)
102.5 W, 57.5 N	Y = max(0, -126.101 + 2747.822 * BF1 + 233.166 * BF3 + 28.128 * BF5) BF1 = max(0, MSRSEPT - 0.035) BF3 = max(0, TEMPJULY - 15.297) BF5 = max(0, TEMPAPRI + 8.493)
105 W, 52.5 N	Y = max(0, -304.954 + 130.275 * BF1 + 60.349 * BF3 + 43.616 * BF4+ 50.088 * BF5 + 57.388 * BF12) BF1 = max(0, MSRAUG - 1.149) BF3 = max(0, TEMPJUNE - 11.670) BF4 = max(0, TEMPAPRI - 0.967) BF5 = max(0, 0.967 - TEMPAPRI) BF12 = max(0, 18.539 - TEMPAUG)
105 W, 55 N	Y = max(0, 171.338 + 150.583 * BF2) BF2 = max(0, 22.083 - DCAPRIL)
105 W, 57.5 N	Y = max(0, -548.324 + 14951.786 * BF3 + 226.436 * BF4 + 157.459 * BF5) BF3 = max(0, MSRAPRIL + .128952E-09) BF4 = max(0, TEMPJULY - 12.223) BF5 = max(0, FFMCAUG - 62.787)
105 W, 60 N	Y = max(0, -254.888 + 2913.429 * BF2 + 213.817 * BF3 + 2596.765 * BF18) BF2 = max(0, 0.090 - MSRAUG) BF3 = max(0, TEMPJULY - 14.355) BF18 = max(0, MSRAUG - 0.010)
107.5 W, 52.5 N	Y = max(0, -81.741 + 12.452 * BF3 + 7.123 * BF4 + 0.894 * BF5+ 16.283 * BF7) BF3 = max(0, FFMCSEPT - 72.220) BF4 = max(0, 72.220 - FFMCSEPT) BF5 = max(0, DCJULY - 279.303) BF7 = max(0, FFMCMAY - 68.681)
107.5 W, 55 N	Y = max(0, -13.193 + 34.389 * BF3 + 2.155 * BF8) BF3 = max(0, DMCJUNE - 0.820) BF8 = max(0, DCSEPT - 365.537)
107.5 W, 57.5 N	Y = max(0, -411.566 + 14737.769 * BF1 + 54324.848 * BF2 + 93.209 * BF3+ 25.552 *BF5) BF1 = max(0, MSRAPRIL - 0.010) BF2 = max(0, 0.010 - MSRAPRIL) BF3 = max(0, FFMCSEPT - 62.563) BF5 = max(0, FFMCJUNE - 35.497)
107.5 W, 60 N	Y = max(0, -9.153 + 617.092 * BF1 + 737.360 * BF3) BF1 = max(0, TEMPJULY - 15.668) BF3 = max(0, MSRJULY - .806750E-10)
110 W, 52.5 N	Y = max(0, 27.357 + 5.554 * BF1) BF1 = max(0, DCJULY - 347.845)

2.9 Appendix continued

Location	Model
110 W, 55 N	Y = max(0, -549.253 + 133.138 * BF2 + 40.932 * BF3 + 5.406 * BF6 + 12.582 * BF13 + 29293.217 * BF15) BF2 = max(0, 53.742 - FFMCAUG) BF3 = max(0, DMCJUNE - 0.687) BF6 = max(0, DCSEPT - 409.260) BF13 = max(0, 199.273 - DCJUNE) BF15 = max(0, 0.021 - MSRAPRIL)
110 W, 57.5 N	Y = max(0, -578.903 + 78963.859 * BF2 + 37332.512 * BF14) BF2 = max(0, 0.017 - MSRAPRIL) BF14 = max(0, MSRAPRIL - 0.004)
110 W, 60 N	Y = max(0, -372.184 + 8674.142 * BF1 + 409.678 * BF12) BF1 = max(0, MSRSEPT - 0.072) BF12 = max(0, TEMPJULY - 14.871)
112.5 W, 52.5 N	Y = max(0, -23.827 + 33.411 * BF1 + 7.589 * BF2 + 0.436 * BF4+ 236.183 * BF5) BF1 = max(0, TEMPAPRI - 3.903) BF2 = max(0, 3.903 - TEMPAPRI) BF4 = max(0, 332.977 - DCSEPT) BF5 = max(0, MSRAPRIL - .999997E-03)
112.5 W, 55 N	Y = max(0, -26.734 + 39.066 * BF1) BF1 = max(0, DMCJUNE - 0.580)
112.5 W, 57.5 N	Y = max(0, 215.883 + 742.065 * BF1 + 225.569 * BF3 - 66.951 * BF5+ 47.767 * BF7) BF1 = max(0, TEMPAUG - 16.852) BF3 = max, (0, FFMCAPRI - 67.870) BF5 = max(0, FFMCAPRI - 53.967) BF7 = max(0DMCSEPT - 4.283)
112.5 W, 60 N	Y = max(0, 78.188 + 1231.887 * BF1) BF1 = max(0, TEMPJULY - 17.132)
112.5 W, 62.5 N	Y = max(0, -7.636 + 212.035 * BF1 + 236.977 * BF10) BF1 = max(0, MSRJULY - 0.680) BF10 = max(0, MSRSEPT - 0.030)
115 W, 47.5 N	Y = max(0, -0.585 + 0.045 * BF1 + 1.112 * BF3 + 0.502 * BF5 BF1 = max(0, DCAUG - 426.555) BF3 = max(0, TEMPJULY - 17.048) BF5 = max(0, FFMCAUG - 83.439)
115 W, 52.5 N	Y = max(0, 185.396 - 1151.687 * BF3 - 403.731 * BF4 + 22694.453 * BF6+ 1203.894 * BF7 + 6311.835 * BF14) BF3 = max(0, DMCJUNE - 2.383) BF4 = max(0, 2.383 - DMCJUNE) BF6 = max(0, 0.019 - MSRJUNE) BF7 = max(0, DMCJUNE - 2.773) BF14 = max(0, 0.027 - MSRAUG)
115 W, 55 N	Y = max(0, 43.668 + 4.303 * BF16) BF16 = max(0, DCAUG - 376.123)
115 W, 57.5 N	Y = max(0, -54.613 + 574.023 * BF3 + 6213.206 * BF19) BF3 = max(0, TEMPAUG - 17.161) BF19 = max(0, MSRAPRIL - 0.011)
115 W, 60 N	Y = max(0, 16.029 + 324.355 * BF1 + 6618.464 * BF3 BF1 = max(0, TEMPAUG - 16.987) BF3 = max(0, MSRAPRIL - 0.020)
115 W, 62.5 N	Y = max(0, -9.330 + 551.633 * BF1 + 24.723 * BF18) BF1 = max(0, TEMPJULY - 16.965) BF18 = max(0, DCMAY - 80.429)
117.5 W, 50 N	Y = max(0, -31.660 + 27.374 * BF2 - 227.389 * BF3 + 14488.044 * BF6+ 238.291 * BF15) BF2 = max(0, 7.077 - TEMPSEPT) BF3 = max(0, MSRJULY - 0.241) BF6 = max(0, 0.003 - MSRJUNE) BF15 = max(0, MSRJULY - 0.074)

2.9 Appendix continued

Location	Model
117.5 W, 52.5 N	Y = max(0, -16.168 + 27.913 * BF1 + 95.058 * BF5) BF1 = max(0, DMCSEPT - 4.973) BF5 = max(0, TEMPMAY - 3.977)
117.5 W, 55 N	Y = max(0, -7.520 + 56.752 * BF1 + 43.487 * BF4 + 420.004 * BF5) BF1 = max(0, TEMPJUNE - 11.727) BF4 = max(0, 0.077 - TEMPAPRI) BF5 = max(0, MSRJUNE - 0.120)
117.5 W, 57.5 N	Y = max(0, 82.382 + 11.487 * BF1) BF1 = max(0, DCJULY - 386.023)
117.5 W, 60 N	Y = max(0, -169.191 + 116052.242 * BF2 + 156.086 * BF4) BF2 = max(0, 0.006 - MSRAPRIL) BF4 = max(0, TEMPMAY - 6.632)
117.5 W, 62.5 N	Y = max(0, -14.839 + 497.510 * BF1 + 117.188 * BF4 + 139.758 * BF5) BF1 = max(0, TEMPJULY - 17.203) BF4 = max(0, - 6.177 - TEMPAPRI) BF5 = max(0, TEMPSEPT - 8.373)
117.5 W, 65 N	Y = max(0, -29.564 + 285.071 * BF1 + 0.444 * BF3 + 9.651 * BF5) BF1 = max(0, MSRSEPT - 0.087) BF3 = max(0, DCJULY - 266.239) BF5 = max(0, 4.826 - DMCAUG)
120 W, 50 N	Y = max(0, 0.034 + 31.576 * BF1 + 26.000 * BF3) BF1 = max(0, TEMPAUG - 14.381) BF3 = max(0, MSRJULY - .120340E-07)
120 W, 52.5 N	Y = max(0, -1.440 + 5.112 * BF3 + 43.522 * BF5 + 4.834 * BF7+ 0.093 * BF17) BF3 = max(0, TEMPJUNE - 7.193) BF5 = max(0, MSRJULY - 0.012) BF7 = max(0, TEMPAUG - 11.652) BF17 = max(0, 142.810 - DCJULY)
120 W, 55 N	Y = max(0, 0.012 + 275.859 * BF1) BF1 = max(0, TEMPAPRI - 1.447)
120 W, 57.5 N	Y = max(0, -19.033 + 84.265 * BF1 + 12.206 * BF4 + 49.972 * BF10) BF1 = max(0, TEMPAUG - 15.807) BF4 = max(0, 55.367 - FFMCAPRI) BF10 = max(0, TEMPMAY - 7.997)
120 W, 60 N	Y = max(0, -112.038 + 30759.729 * BF7 + 4318.878 * BF9) BF7 = max(0, MSRAPRIL - 0.008) BF9 = max(0, MSRJUNE - 0.302)
120 W, 62.5 N	Y = max(0, -664.354 + 1148.508 * BF1 + 2708.429 * BF3 + 3602.749 * BF4 + 16.967 * BF5 + 13.570 * BF7 + 330.752 * BF9+ 2687.791 * BF12 - 503.358 * BF16) BF1 = max(0, TEMPJULY - 16.929) BF3 = max(0, MSRJUNE - 0.103) BF4 = max(0, 0.103 - MSRJUNE) BF5 = max(0, DCJULY - 384.523) BF7 = max(0, DCSEPT - 577.560) BF9 = max(0, TEMPSEPT - 8.457) BF12 = max(0, 0.186 - MSRSEPT) BF16 = max(0, TEMPJUNE - 13.497)
120 W, 65 N	Y = max(0, 11.578 + 48.703 * BF5) BF5 = max(0, TEMPJULY - 14.523)
122.5 W, 52.5 N	Y = max(0, -7.078 + 527.881 * BF1 + 33.652 * BF2) BF1 = max(0, MSRAUG + .154813E-08) BF2 = max(0, TEMPJUNE - 7.677)
122.5 W, 55 N	Y = max(0, 26.693 + 0.756 * BF4 + 24.028 * BF5) BF1 = max(0, TEMPJULY - 11.397) BF4 = max(0, 189.410 - DCJULY) * BF1 BF5 = max(0, TEMPAUG - 13.126) * BF1

2.9 Appendix continued

Location	Model
122.5 W, 60 N	Y = max(0, 10.112 + 709.577 * BF1) BF1 = max(0, TEMPSEPT - 9.080)
122.5 W, 62.5 N	Y = max(0, -53.670 + 2342.579 * BF1 + 3.807 * BF4 - 735.708 * BF6+ 5013.730 * BF8) BF1 = max(0, TEMPJULY - 15.493) BF4 = max(0, DCAUG - 437.239) BF6 = max(0, TEMPJULY - 14.777) BF8 = max(0, MSRJUNE - 0.036)
122.5 W, 65 N	Y = max(0, -33.329 + 377.958 * BF10 + 0.782 * BF13 - 0.500 * BF14) BF10 = max(0, 0.099 - MSRJULY) BF13 = max(0, DCAUG - 308.061) BF14 = max(0, DCSEPT - 336.347)
125 W, 52.5 N	Y = max(0, 4.296 + 549.942 * BF1) BF1 = max(0, MSRAUG - 0.008)
125 W, 55 N	Y = max(0, -2.790 + 2092.266 * BF1 + 9.695 * BF2 + 54.186 * BF7) BF1 = max(0, MSRJULY - .111872E-09) BF2 = max(0, TEMPAUG - 10.861) BF7 = max(0, 0.400 - DMCSEPT)
125 W, 57.5 N	Y = max(0, -30.978 + 0.779 * BF1 + 221.309 * BF4 + 41194.836 * BF6) BF1 = max(0, DCAUG - 255.929) BF4 = max(0, 0.563 - DMCJUNE) BF6 = max(0, 0.001 - MSRMAY)
125 W, 60 N	Y = max(0, -452.895 + 2.344 * BF1 + 6.828 * BF3 + 3708.129 * BF13+ 9.575 * BF14) BF1 = max(0, DCAUG - 407.019) BF3 = max(0, FFMCMAY - 30.352) BF13 = max(0, 0.057 - MSRSEPT) BF14 = max(0, FFMCSEPT - 26.063)
125 W, 62.5 N	Y = max(0, -1264.668 + 709.783 * BF1 + 30160.254 * BF4 + 30.960 * BF5+ 560.206 * BF8 + 128.881 * BF9 + 50.675 * BF12 - 14.431 * BF15) BF1 = max(0, TEMPJUNE - 10.180) BF4 = max(0, 0.015 - MSRJUNE) BF5 = max(0, DCAUG - 440.003) BF8 = max(0, TEMPSEPT - 5.493) BF9 = max(0, 5.493 - TEMPSEPT) BF12 = max(0, DCAPRIL - 5.820) BF15 = max(0, DCAUG - 404.358)
125 W, 65 N	Y = max(0, -11.055 + 29.840 * BF1 + 1.943 * BF4) BF1 = max(0, DMCJULY - 5.245) BF4 = max(0, 357.981 - DCAUG)
127.5 W, 55 N	Y = max(0, -2.304 + 349392.094 * BF2 + 144999.281 * BF4 + 7349344.500 * BF5) BF1 = max(0, MSRAUG - .250340E-10) BF2 = max(0, MSRJULY + .306515E-10) * BF1 BF3 = max(0, MSRAPRIL + .345107E-09) BF4 = max(0, MSRMAY - .600000E-03) * BF3 BF5 = max(0, .600000E-03 - MSRMAY) * BF3
127.5 W, 57.5 N	Y = max(0, -42.072 + 11501.986 * BF1 + 4.536 * BF3 + 89.207 * BF5) BF1 = max(0, MSRAPRIL - 0.009) BF3 = max(0, DCSEPT - 360.953) BF5 = max(0, DMCJUNE - 0.723)
127.5 W, 60 N	Y = max(0, 20.158 + 1.583 * BF3) BF1 = max(0, DCJULY - 257.645) BF3 = max(0, TEMPJULY - 6.306) * BF1
127.5 W, 62.5 N	Y = max(0, -344.948 + 214.326 * BF1 + 266.348 * BF7 + 10.813 * BF8 + 215.752 * BF18) BF1 = max(0, TEMPMAY - 1.990) BF7 = max(0, 10.761 - TEMPJULY) BF8 = max(0, DCJULY - 294.245) BF18 = max(0, TEMPJULY - 9.800)

2.9 Appendix continued

Location	Model
127.5 W, 65 N	Y = max(0, 61.503 + 275.888 * BF1) BF1 = max(0, DCAPRIL - 22.230)
130 W, 57.5 N	Y = max(0, -145.141 + 14.729 * BF1 + 5.735 * BF2 + 6.038 * BF4+ 3.381 * BF6 + 6291.277 * BF8) BF1 = max(0, FFMCJUNE - 45.143) BF2 = max(0, 45.143 - FFMCJUNE) BF4 = max(0, FFMCSEPT - 26.843) BF6 = max(0, DCJULY - 251.174) BF8 = max(0, MSRAPRIL - 0.011)
130 W, 60 N	Y = max(0, -120.089 + 77.844 * BF1 + 121.595 * BF2 + 7067.656 * BF3+ 36.058 * BF8 + 3.117 * BF10) BF1 = max(0, TEMPJULY - 8.184) BF2 = max(0, 8.184 - TEMPJULY) BF3 = max(0, MSRAPRIL - 0.011) BF8 = max(0, - 6.207 - TEMPAPRI) BF10 = max(0, 52.610 - FFMCAUG)
130 W, 65 N	Y = max(0, -779.663 + 11414.481 * BF1 + 532.687 * BF3 + 28.231 * BF5+ 136.821 * BF8 + 104.526 * BF10) BF1 = max(0, MSRJUNE - 0.017) BF3 = max(0, DCAPRIL - 22.143) BF5 = max(0, FFMCJULY - 46.532) BF8 = max(0, 6.364 - DMCJULY) BF10 = max(0, TEMPMAY + 0.129)
132.5 W, 57.5 N	Y = max(0, 1.600 + 9.041 * BF1 + 29.740 * BF3 - 3.067 * BF5 BF1 = max(0, FFMCMAY - 47.768) BF3 = max(0, TEMPJUNE - 7.767) BF5 = max(0, FFMCMAY - 40.516)
132.5 W, 60 N	Y = max(0, -39.327 + 5.941 * BF1 + 52.576 * BF5) BF1 = max(0, DCAUG - 433.606) BF5 = max(0, TEMPAPRI + 5.057)
132.5 W, 62.5 N	Y = max(0, -84.355 + 48.232 * BF2 + 45.496 * BF8) BF2 = max(0, 8.055 - TEMPAUG) BF8 = max(0, TEMPAUG - 6.342)
132.5 W, 65 N	Y = max(0, -87.901 + 53.018 * BF5 + 175.081 * BF8) BF5 = max(0, DMCJULY - 0.316) BF8 = max(0, TEMPAPRI + 7.100)
135 W, 57.5 N	Y = max(0, 10.901 + 221.731 * BF1 - 149.745 * BF5) BF1 = max(0, DMCMAY - 0.784) BF5 = max(0, DMCMAY - 0.661)
135 W, 60 N	Y = max(0, -5.522 - 4919.515 * BF2 + 69.287 * BF4 + 3841.793 * BF6) BF2 = max(0, DMCAPRIL - 6.013) BF4 = max(0, DCAPRIL - 24.463) BF6 = max(0, DMCAPRIL - 6.000)
135 W, 62.5 N	Y = max(0, 62.129 + 170.100 * BF1) BF1 = max(0, TEMPAUG - 8.000)
135 W, 65 N	Y = max(0, 65.846 + 100.220 * BF1) BF1 = max(0, FFMCAPRI - 64.100)
137.5 W, 60 N	Y = max(0, 7.761 + 136.466 * BF1) BF1 = max(0, DCAPRIL - 24.883)
137.5 W, 62.5 N	Y = max(0, -52.037 + 146.903 * BF1 + 307.122 * BF3 + 11.594 * BF17) BF1 = max(0, TEMPJUNE - 6.140) BF3 = max(0, TEMPAPRI + 5.253) BF17 = max(0, FFMCJUNE - 37.153)

2.9 Appendix continued

Location	Model
137.5 W, 65 N	Y = max(0, -39.259 + 29.910 * BF1 + 2963.431 * BF3 + 125766.211 * BF4) BF1 = max(0, TEMPAUG - 8.500) BF3 = max(0, MSRJUNE - .700000E-03) BF4 = max(0, .700000E-03 - MSRJUNE)
140 W, 60 N	Y = max(0, -2.381 + 16150.373 * BF1 + 37.651 * BF2) BF1 = max(0, MSRJUNE + .313671E-10) BF2 = max(0, TEMPSEPT - 5.390)
140 W, 62.5 N	Y = max(0, 27.592 + 7.659 * BF1 + 116.217 * BF3) BF1 = max(0, DCJULY - 281.939) BF3 = max(0, TEMPJUNE - 6.120)
140 W, 65 N	Y = max(0, 11.289 + 1.091 * BF8) BF2 = max(0, 62.700 - DCMAY) BF8 = max(0, TEMPAPRI + 10.547) * BF2
142.5 W, 65 N	Y = max(0, -163.527 + 13.843 * BF1 + 220.481 * BF3 + 62.554 * BF4) BF1 = max(0, DCJULY - 337.674) BF3 = max(0, TEMPJUNE - 9.783) BF4 = max(0, 9.783 - TEMPJUNE)
145 W, 62.5 N	Y = max(0, 13.861 + 7.114 * BF1 + 25035.348 * BF3 - 21217.652 * BF5) BF1 = max(0, DCJUNE - 167.287) BF3 = max(0, MSRJUNE - 0.004) BF5 = max(0, MSRJUNE - 0.001)
145 W, 65 N	Y = max(0, -1231.302 + 314.707 * BF2 + 81.678 * BF4 + 8.472 * BF5+ 64.587 * BF7 + 95.313 * BF8 + 74.166 * BF11) BF2 = max(0, 8.135 - TEMPAUG) BF4 = max(0, 66.700 - DCMAY) BF5 = max(0, DCJULY - 270.303) BF7 = max(0, 36.630 - FFMCJUNE) BF8 = max(0, DMCMAY - 0.084) BF11 = max(0, TEMPAPRI + 10.753)
147.5 W, 62.5 N	Y = max(0, 48.363 + 4891.161 * BF2) BF2 = max(0, MSRAPRIL - 0.021)
147.5 W, 65 N	Y = max(0, 36.584 + 52.402 * BF2) BF2 = max(0, 35.230 - FFMCJUNE)
150 W, 62.5 N	Y = max(0, 12.067 + 34.659 * BF4) BF3 = max(0, 9.465 - TEMPJULY) BF4 = max(0, DMCJUNE - 0.130) * BF3
150 W, 65 N	Y = max(0, -169.078 - 3259.911 * BF6 + 1192.324 * BF8 + 2073.436 * BF10+ 423.590 * BF13) BF6 = max(0, DMCJULY - 1.181) BF8 = max(0, DMCJULY - 1.974) BF10 = max(0, DMCJULY - 0.658) BF13 = max(0, 1.463 - DMCJUNE)
152.5 W, 62.5 N	Y = max(0, 17.677 - 307.055 * BF2 + 262.489 * BF4) BF1 = max(0, DMCJUNE - 0.187) BF2 = max(0, DMCMAY - 3.084) * BF1 BF4 = max(0, DMCMAY - 2.432) * BF1
152.5 W, 65 N	Y = max(0, -623.691 + 175.802 * BF1 + 498.019 * BF2 + 448.783 * BF5+ 4.265 * BF8 - 198.457 * BF11) BF1 = max(0, TEMPAUG - 9.239) BF2 = max(0, 9.239 - TEMPAUG) BF5 = max(0, TEMPAPRI + 4.583) BF8 = max(0, DCJULY - 214.584) BF11 = max(0, TEMPAPRI + 6.827)

2.9 Appendix continued

Location	Model
155 W, 62.5 N	Y = max(0, -560.543 + 30.780 * BF2 + 322.213 * BF3 + 144.693 * BF6 + 20005.117 * BF8 - 0.689 * BF11) BF1 = max(0, DCMAY - 59.242) BF2 = max(0, 59.242 - DCMAY) BF3 = max(0, MSRJULY + .106806E-08) * BF1 BF6 = max(0, TEMPAUG - 6.658) BF8 = max(0, 0.002 - MSRAUG) * BF1 BF11 = max(0, DCJULY - 324.065) * BF1
155 W, 65 N	Y = max(0, 40.693 + 11.303 * BF1) BF1 = max(0, DCJULY - 354.110)
157.5 W, 60 N	Y = max(0, -518.197 + 357.580 * BF3 + 18523.148 * BF6 + 226.227 * BF7 + 78.687 * BF9) BF3 = max(0, TEMPJUNE - 9.460) BF6 = max(0, 0.026 - MSRAUG) BF7 = max(0, TEMPAUG - 9.855) BF9 = max(0, TEMPMAY - 2.681)
157.5 W, 62.5 N	Y = max(0, -979.175 + 15.565 * BF3 + 15085.198 * BF4 + 5.638 * BF5+ 28.716 * BF7) BF3 = max(0, 74.471 - DCMAY) BF4 = max(0, MSRAPRIL - .346190E-09) BF5 = max(0, DCJULY - 220.374) BF7 = max(0, 48.387 - FFMCJULY)
157.5 W, 65 N	Y = max(0, -13.953 + 188.621 * BF1 + 20.525 * BF3 + 7.542 * BF13) BF1 = max(0, TEMPAUG - 11.568) BF3 = max(0, FFMCJULY - 60.616) BF13 = max(0, DCJUNE - 198.307)
160 W, 60 N	Y = max(0, 13.621 + 179.362 * BF1 + 138.743 * BF3 + 63.530 * BF5- 28.852 * BF18) BF1 = max(0, TEMPJUNE - 9.757) BF3 = max(0, TEMPMAY - 4.619) BF5 = max(0, DMCJULY - 5.503) BF18 = max(0, DMCJULY - 1.600)
160 W, 62.5 N	Y = max(0, -41.138 + 252.296 * BF1 + 12.634 * BF3 + 1219.904 * BF10) BF1 = max(0, TEMPJUNE - 11.620) BF3 = max(0, DCJULY - 350.397) BF10 = max(0, MSRAUG - 0.039)
160 W, 65 N	Y = max(0, 52.236 + 620.239 * BF1 + 56.485 * BF12 - 28.481 * BF14+ 355.372 * BF16 - 126.289 * BF18) BF1 = max(0, MSRJULY - 0.299) BF12 = max(0, DMCJULY - 14.877) BF14 = max(0, DMCJULY - 8.271) BF16 = max(0, TEMPAUG - 11.693) BF18 = max(0, TEMPAUG - 10.303)
162.5 W , 62.5 N	Y = max(0, 4.911 - 0.112 * BF9 + 8.838 * BF11) BF1 = max(0, DCAUG - 160.252) BF9 = max(0, 3.719 - DMCJULY) * BF1 BF11 = max(0, 0.033 - MSRJULY) * BF1

CHAPTER 3

THE VULNERABILITY OF CARBON STORAGE IN BOREAL NORTH AMERICA DURING THE 21ST CENTURY TO INCREASES IN WILDFIRE ACTIVITY[1]

3.1 Abstract

The boreal forest contains large reserves of belowground carbon. Across this region, wildfires influence the temporal and spatial dynamics of carbon storage. In this study, we estimate fire emissions and changes in carbon storage for boreal North America over the 21st Century. We use a gridded data set developed with a multivariate adaptive regression spline (MARS) approach to determine how area burned varies each year with changing climatic and fuel moisture conditions. We apply the process-based Terrestrial Ecosystem Model (TEM) to evaluate the effect of future fire on the carbon dynamics of boreal North America in the context of changing atmospheric CO_2 concentration and climate in the A2 and B2 emissions scenarios of the second generation Canadian Center for Climate Modeling and Analysis Coupled Global Climate Model. Relative to the last decade of the 20th Century, decadal total carbon emissions from fire increase on the order of 2.5 to 4.4 times by 2091-2100, depending on the climate scenario and assumptions about CO_2 fertilization. Fire emissions are higher with warmer climates or if CO_2 fertilization is assumed to occur. Despite the increases in fire emissions, our simulations

---

[1] M. S. Balshi, A. D. McGuire, P. Duffy, M. Flannigan, D. W. Kicklighter, and J. Melillo (in preparation), The vulnerability of carbon storage in boreal North America During the 21st Century in response to increases in wildfire activity, *Global Change Biology*.

indicate that boreal North America will be a carbon sink over the 21st Century if CO_2 fertilization is assumed to occur in the future. In contrast, simulations excluding CO_2 fertilization over the same period indicate that the region will change to a carbon source to the atmosphere, with the source being 2.1 times greater under the warmer A2 scenario than the B2 scenario. To improve estimates of wildfire on terrestrial carbon dynamics in boreal North America, future studies should incorporate the role of dynamic vegetation to represent more accurately post-fire successional processes, incorporate fire severity parameters that change in time and space, and integrate the role of other disturbances and their interactions with future fire regime.

3.2 Introduction

The North American boreal forest occupies approximately one third the global boreal biome and contains roughly 40% of the world's soil reactive carbon (McGuire et al., 1995). Wildfire is the dominant disturbance in the North American boreal forest and is strongly linked to climate (Clark et al., 1990; Flannigan and Van Wagner, 1991; Johnson and Wowchuk, 1993; Skinner et al., 1999, 2002; Duffy et al., 2005; Balshi et al., 2007, in review). There is substantial evidence of warming for boreal North America (Chapman and Walsh, 1993; Serreze et al., 2000; Serreze and Francis, 2006; McGuire et al., 2006; Soja et al., 2006) and that warming is affecting ecosystem structure and function through changes in fire regime (McGuire et al., 2007).

Relationships between climate and fire across the North American boreal region indicate a general increasing trend in the area burned historically (Gillett et al., 2004; Kasischke and Turetsky, 2006). It is believed that these trends in area burned will continue into the future (Flannigan et al., 1998, 2000; Stocks et al., 1998; Balshi et al., 2007, in review). An altered fire regime in response to future climatic changes (Wotton and Flannigan, 1993; Flannigan et al., 2000, 2005; Carcaillet et al., 2001) has strong implications for the carbon dynamics of this region. Changes in the carbon emitted due to wildfire in response to changes in climate may act as a potentially strong positive feedback to atmospheric CO_2 concentrations (Kasischke et al., 1995) and either a positive and/or negative feedback to surface energy exchange (Chapin et al., 2000; Chambers and Chapin, 2003; Amiro et al., 2006; Randerson et al., 2006). Wildfire shows a great deal of interannual variation in area burned and severity (Kasischke and Turetsky, 2006), which

makes predicting the effect of wildfire on carbon storage for future scenarios of climate change difficult.

Wildfires influence the carbon dynamics of the North American boreal region at multiple temporal and spatial scales, and understanding the historical effects of fire on carbon storage is critical to predicting future changes in the carbon budget for this region (Kasischke et al., 1995; Balshi et al., 2007). The fire regime in the North American boreal forest is dominated by stand-replacing fires (Johnson, 1992), which influence the carbon dynamics of this region through direct carbon emissions at the time of fire and through processes such as decomposition and vegetation changes that take place over decades to centuries after fire (Kasischke et al., 1995). The amount of carbon released at the time of fire depends on the area burned, the severity of a fire event (i.e., carbon fraction consumed), and the amount of fuel both above- and below-ground that is available for burning. Fire severity can be directly influenced by the time of season a given fire occurs (Kasischke and Turetsky, 2006). In addition, the amount and quality of fuel available for burning depends on the history of previous fire disturbances (Balshi et al., 2007). Biomass and the accumulation of biomass over time following fire varies with stand age (Kurz and Apps, 1999; Hicke et al., 2003), and, as a result, it is critical to represent the distribution of stand-ages across the landscape when calculating regional to global scale carbon dynamics (Chen et al., 2002; Balshi et al., 2007).

Relatively few studies have investigated the influence of future fire disturbance on the carbon dynamics of the North American boreal region in the context of a changing climate and atmospheric CO_2 concentrations. Zhuang et al. (2006) evaluated the role of

fire in pan-boreal carbon dynamics assuming that area burned increases at a fixed rate of 1% per year from 2000 to 2100. However, the assumption of a fixed rate of increase in area burned in the boreal forest is simplistic, as wildfire tends to be episodic, with some years experiencing larger, more catastrophic burn years than others (Murphy et al., 2000; Kasischke et al., 2002). Bachelet et al. (2005) used a dynamic global vegetation model to examine the influence of climate and fire on the carbon dynamics of Alaska. While the area burned in that study was allowed to vary from year to year based on the Palmer Drought Index, the influence of fire disturbance legacies, as represented by the evolution of stand-age distributions across the landscape, was not considered. Balshi et al. (2007, in review) developed spatially and temporally explicit empirical relationships for the North American boreal region that relate area burned with air temperature and the fuel moisture indices and monthly severity rating of the Canadian Fire Weather Index System. The advantage of this approach is that it captures the spatiotemporal variation in the influence of the model predictor variables across the boreal region in addition to incorporating the influence of fuel moisture for different depths of the ground layer. With the overall goal of examining the vulnerability of carbon storage in the North American boreal region to future fire, we build on the cohort approach developed by Balshi et al. (2007), and incorporate the role of the legacy of previous fire disturbances and a climatically-driven future fire regime on the future carbon dynamics of North America north of 45° N (referred to hereafter as "boreal North America"). The objectives of this study are to estimate future fire emissions and carbon storage of this region using estimates of future area burned (Balshi et al., in review), and to evaluate the

carbon dynamics of the region in the context of ecosystem responses to changes in future atmospheric CO_2 concentration and changes in climate. We also identify sources of uncertainty that should be addressed in studies that estimate the role of future fire on the carbon dynamics of this region.

3.3 Methods

3.3.1 Overview

In this study we used the process-based Terrestrial Ecosystem Model (TEM) to evaluate how changes in atmospheric CO_2, climate, and fire disturbance over the 21st Century influence carbon dynamics for North America north of 45° N. We used three steps to initialize our simulations for the state of these ecosystems at the beginning of the year 2003. First, we ran the model to equilibrium (where annual NPP = annual heterotrophic respiration) for each 0.5° latitude x 0.5° longitude grid cell using long term mean monthly climate from 1901-1930. The period 1901-1930 corresponds to a period where climate exhibits less change relative to the latter portion of the 20th Century. Second, a 900 year spin-up (described in Balshi et al., 2007) was conducted to dynamically equilibrate the TEM to variability in climate by using data describing the annual climate conditions for the period 1901-1930, repeatedly. Third, TEM was then run from 1901-2002 using gridded monthly climate based on observations. A backcasting approach (Balshi et al., 2007) was used to account for the influence of fire on carbon dynamics prior to the start of the historical fire record (defined as 1959-2002 for Canada; 1950-2002 for Alaska) including the 900 year spin-up period.

For future conditions, there is much uncertainty as to how atmospheric CO_2 concentrations and climate may change (Intergovernmental Panel on Climate Change, IPCC, 2001). In addition, the importance of CO_2 fertilization on carbon sequestration remains a controversial topic (e.g., Caspersen et al., 2000; Oren et al., 2001; Joos et al. 2002; Hungate et al., 2003; Luo et al., 2004, 2006; Körner et al., 2005; Long et al., 2006; Reich et al., 2006; Canadell et al., 2007). To examine the consequences of these uncertainties on carbon dynamics in boreal North America, we conducted two sets of three simulations for each of two different climate scenarios (12 simulations in total) for the period 2003-2100. In the first set of simulations, photosynthesis was assumed to be sensitive to increasing atmospheric CO_2 concentration (i.e., CO_2 fertilization), while in the second set, no CO_2 fertilization was assumed. For the set considering the effect of atmospheric CO_2 fertilization, we conducted three simulations. In simulation one (S1), atmospheric CO_2 concentrations varied, but a mean monthly climate was used from 1901-1930 to represent the climate for each year. Fire disturbance was not included in this simulation. In simulation two (S2), both atmospheric CO_2 concentrations and monthly climate varied, but disturbance by fire was excluded. In simulation three (S3), atmospheric CO_2 concentrations and monthly climate varied and fire disturbances were incorporated. In the second set of simulations, we conducted the same three simulations as in the first set, but with atmospheric CO_2 fixed at 296 ppm, which was the mole fraction used to initialize each simulation. The changes in atmospheric CO_2 concentration and climate conditions were derived from output of the second generation of the Canadian Center for Climate Modeling and Analysis Coupled Global Climate

Model (CGCM2) driven by either the A2 or B2 emissions scenarios of the IPCC Third Assessment (IPCC, 2001). Future fire disturbance for the period 2003-2100 was derived from an empirical modeling approach presented in Balshi et al. (2007, in review) also using the CGCM2 ouput. We then analyzed our simulation results for the North American region north of 45° N. The effect of CO_2 fertilization on carbon storage was determined by the results of simulation S1. The effect of climate on carbon storage was determined by the difference between simulations S2 and S1. The effect of fire on carbon storage was determined by the difference between the simulations S3 and S2.

3.3.2 The Terrestrial Ecosystem Model (TEM)

The TEM is a large-scale, process-based biogeochemical model that estimates monthly pools and fluxes of carbon and nitrogen for terrestrial ecosystems. TEM is driven by a series of spatially explicit data sets that include climate, elevation, soil texture, and vegetation. The equations and parameters of TEM have been documented in previous studies (Raich et al., 1991; McGuire et al., 1992; Tian et al., 1999; Zhuang et al., 2003; Euskirchen et al., 2006; Balshi et al., 2007), and the model has been applied to regions around the globe, including the high latitudes (McGuire et al., 2000a, 2000b, 2001, 2002, 2004; Clein et al., 2000, 2002, 2007; Zhuang et al., 2001, 2002, 2003, 2006; Euskirchen et al., 2006, 2007; Balshi et al., 2007). Several of the parameters in TEM are based on values obtained in the peer-reviewed literature. However, the rate-limiting parameters are defined by calibrating the model to pools and fluxes of field sites that are representative of particular ecosystems. The model is coupled to a soil thermal model

and can be applied to both permafrost and non-permafrost soils. In this study, we used TEM version 5.1 (Euskirchen et al., 2006; Balshi et al., 2007), which incorporates the effects of fire on both carbon and nitrogen dynamics. To estimate changes in carbon storage we calculated the net ecosystem carbon balance (NECB, Chapin et al., 2006) for outputs generated by the model as:

$$NECB = NPP - R_h - TCE \quad (3.1)$$

where NPP is net primary production, R_h is heterotrophic respiration, and TCE is total carbon emitted due to fire (Equation 3.1). TCE for historical and future area burned was calculated based on the fraction of aboveground and ground-layer carbon consumed at the time of fire (Equation 3.2; Table 3.1):

$$TCE = (ß_a * V_c) + (ß_g * S_c) \quad (3.2)$$

where TCE is the total carbon emitted, $ß_a$ is the aboveground C fraction consumed, $ß_g$ is the ground layer carbon fraction consumed during a fire, V_c is vegetation carbon, and S_c is soil carbon. It was assumed that 85% of soil and vegetation nitrogen was retained at the time of fire (Wirth et al., 2002; Harden et al., 2004). The nitrogen lost from the ecosystem as a result of fire was reintroduced into the system annually in equal increments obtained by dividing the total net nitrogen lost to the atmosphere during the most recent fire event by the fire return interval of the grid cell. Fire return intervals, which are defined as the time required to burn an area equal to the entire 0.5° grid cell, were derived from Balshi et al. (2007). Disturbances due to insects, land-use change, and forest harvest were not included in the calculation of NECB in this study.

3.3.3 Input data sets

To extrapolate the TEM across boreal North America, we used driving data sets that had (1) only temporal variability (atmospheric CO_2 concentration), (2) only spatial variability (elevation, soil texture, and vegetation), and (3) both spatial and temporal variability (air temperature, precipitation, cloudiness, and fire disturbance). These data sets are described in more detail in the following sections.

3.3.3.1 Data used to initialize ecosystem state in year 2003

In this study we simulated the response of carbon dynamics to historical atmospheric CO_2, climate, and fire using the same data sets and procedures as outlined in an earlier study by Balshi et al. (2007). Atmospheric CO_2 data were obtained from the Mauna Loa station (Keeling and Whorf, 2005). TerrainBase v1.1 elevation data were obtained from the National Geophysical Data Center, Boulder, CO (NGDC, 1994) and aggregated to a 0.5° latitude x 0.5° longitude spatial resolution. Soil texture, represented as percent silt plus percent clay in TEM, was based on the Global Gridded Surfaces of Selected Soil Characteristics data set (Global Soil Data Task Group/ IGBP-DIS, 2000) and gridded at a 0.5° latitude x 0.5° longitude spatial resolution. The input vegetation data set, gridded at 0.5° resolution, was represented by a potential natural vegetation map described by Melillo et al. (1993). A time series data set of gridded climate data (0.5° latitude x 0.5° longitude) was obtained from the Climate Research Unit (CRU) of the University of East Anglia (Mitchell and Jones, 2005) and used to prescribe historical climate from 1901 to 2002.

To represent the occurrence and distribution of historical fires (1959-2002 for Canada; 1950-2002 for Alaska), we used the gridded (0.5° latitude x 0.5° longitude) time series of fire disturbance developed by Balshi et al. (2007). With this data set, the legacies of past fire disturbances on carbon storage were determined by stratifying the vegetation in a 0.5° grid cell into cohorts of different stand ages. Each cohort was determined from one of several unique fire histories that may occur in the grid cell (for details, see Balshi et al., 2007). The cohort information in year 2002 was then used to develop cohorts based on area burned for years 2003-2100 (see section 3.3.3.2.4).

3.3.3.2 Simulation of future carbon dynamics

For simulating future carbon dynamics, we used the same static data sets for elevation, soil texture and vegetation that were used for initializing the ecosystem state in 2003. New data sets, however, were developed to represent future climate, atmospheric CO_2 concentrations and fire disturbance as described below.

3.3.3.2.1 Future climate

We derived monthly data for years 2003-2100 at 3.75° x 3.75° resolution for air temperature, precipitation, and downwelling shortwave radiation from CGCM2 (http://www.cccma.bc.ec.gc.ca/data/cgcm2/cgcm2.shtml). A detailed description of the CGCM2 can be found in Flato and Boer (2001). CGCM2 has been used to produce ensemble climate change projections using the IPCC Third Assessment A2 and B2 emissions scenario storylines. The A2 and B2 emissions storylines are discussed in detail

in the IPCC Special Report on Emissions Scenarios (Nakićenović and Swart, 2000). The emissions scenarios act as representations of the future development of radiatively active emissions and are based on assumptions about socioeconomic, demographic, and technological changes. These scenarios are then converted into greenhouse gas concentration equivalents that are used as driving variables for GCM projections. The A2 scenario represents a world where energy usage is high, economic and technological development is slow, and population growth reaches 15 billion by year 2100. The B2 scenario represents a world where energy usage is lower than the A2, economies evolve more rapidly, environmental protection is greater, and population growth is slower than the A2 (10.4 billion by year 2100).

The near term warming effect (through the mid-21st Century) for the A2 scenario is less than the B2 scenario due to the greater cooling effect resulting from higher sulfur dioxide emissions (IPCC, 2001). The temperature changes for the A2 and B2 scenarios cross about the mid-21st Century, with the A2 scenario resulting in greater long-term warming due to higher emissions of radiatively active gases (IPCC, 2001).

Both scenarios have a baseline period of 1961-1990 that corresponds to the IS92a scenario which was used to initialize the A2 and B2 scenarios for CGCM2. Because we apply TEM at 0.5° spatial resolution in this study, these data were linearly interpolated. We then fused the CRU data to the CGCM2 scenarios by adjusting the CGCM2 monthly data relative to the absolute difference from the 1961-1990 CRU monthly mean by:

$$CGCM2_{adjusted\ monthly} = CRU_{\mu} + (CGCM2_{monthly} - CGCM2_{\mu}) \quad (3.3)$$

in which CRU_{μ} was the mean monthly value for the period 1961-1990 derived from the CRU input datasets (described in section 3.3.3.1), $CGCM2_{monthly}$ was the monthly value output by CGCM2, and $CGCM2_{\mu}$ was the mean monthly value for the period 1961-1990 derived from the CGCM2 monthly data.

3.3.3.2.2 Future atmospheric CO_2 concentration

The equivalent CO_2 concentration used for simulating future climate by the CGCM2 includes climate forcing caused by the atmospheric concentrations of other greenhouse gases (e.g., methane, nitrous oxide, ozone, etc) in addition to carbon dioxide. For simulations with TEM, we converted the CO_2 equivalent used to drive the CGCM2 into CO_2 concentration by developing relationships between the observed CO_2 record (Keeling et al., 2005) and CO_2 equivalent concentrations for the period 1901-2000 using a series of regression models. The relationship between the observed CO_2 concentrations and CO_2 equivalent for the B2 scenario appeared to be linear ($R^2 = 0.99$; $p < 0.01$). However, the relationship between the observed CO_2 concentration and the A2 CO_2 equivalent was best described by a power model ($R^2 = 0.99$; $p < 0.01$). We then extrapolated atmospheric CO_2 concentration from year 2003-2100 using the empirical relationships developed for each scenario. These data sets were then appended to the observed atmospheric CO_2 record. The atmospheric CO_2 concentration derived by the empirical relationships show that by the end of the 21st Century, atmospheric CO_2 was greater under the A2 scenario (1100 ppm) than the B2 scenario (766 ppm).

3.3.3.2.3 Future fire disturbance data sets

To represent the area burned by future fires for the years 2003-2100, we used the 2.5° gridded data developed by Balshi et al. (2007, in review) using a multivariate adaptive regression spline (MARS) approach. The fire models used in this approach were developed based on relationships between historically recorded fire and air temperature and fuel moisture codes of the Canadian Fire Weather Index system for the period 1960-2002. The models were then extrapolated for the period 2003-2100 using the SRES A2 and B2 scenario output from CGCM2. Predicted area burned between the A2 and B2 scenarios was similar through 2050, but diverged for the last 50 years of the 21st Century, with the A2 scenario resulting in greater area burned. Relative to the 1991-2000 baseline period defined by Balshi et al. (2007, in review), area burned increased by 5.7 times under the A2 scenario while it increased by 3.5 times under the B2 scenario by the last decade of the 21st Century.

3.3.3.2.4 Accounting for future stand age

We developed an algorithm to downscale the annual area burned estimates from 2.5° resolution to 0.5° resolution by evenly distributing the future area burned estimates to land-based areas that are assumed to burn. Similar to the approach by Balshi et al. (2007) we accounted for differences in stand age resulting from multiple fires within a 0.5° grid cell. We distributed the burn area assigned to each 0.5° grid cell to existing cohorts that were created from the historical fire data, starting with the oldest, until all existing cohorts burned. New cohorts were created if the burn area in a given year was

either smaller or larger than the size of an existing cohort. Burned areas were only distributed to land-based areas within a given 0.5° grid cell containing vegetation types assumed to be burnable (e.g., boreal forest vs. ice/rock).

3.4 Results

We first present estimates of fire emissions across the North American boreal region and sub-regions. Boreal North American and sub-regional carbon dynamics of the 21st Century are then evaluated with respect to the relative importance of atmospheric CO_2, climate, and fire.

3.4.1 Future fire emissions

Mean annual decadal emissions increased from the beginning to the end of the 21st Century, but vary with climate and CO_2 fertilization assumptions (Figure 3.1) and were highly correlated with the mean annual decadal area burned (A2 and B2 scenario R^2 values = 0.97; $p < 0.0001$). For both climate scenarios, the simulations excluding CO_2 fertilization resulted in lower increases in fire emissions across all decades (Figure 3.1b). The greatest difference between the simulations incorporating and excluding CO_2 fertilization was seen in the last 50 years of the 21st Century. The larger emissions from fire for the simulations incorporating atmospheric CO_2 fertilization over this period was due to the greater amount of carbon sequestered during the first 50 years of the 21st Century and therefore more biomass in the ecosystem for burning. Relative to the last decade of the 20th Century, mean annual decadal emissions for the simulations that both

included and excluded CO_2 under the A2 scenario increased 2.2-2.4 times by 2050 and 3.1-4.4 times by 2091-2100 (Figures 3.1a and 3.1b). Mean annual decadal emissions for the simulations that both included and excluded CO_2 for the B2 simulations, increased 2.1-2.3 times by 2050 and 2.5-3.1 times by 2091-2100 (Figures 3.1a and 3.1b). Mean annual decadal emissions were similar among climate scenarios for the first half of the 21st Century but were greater for the A2 scenario in the last 50 years as a result of greater area burned (see Figure 3.4, Balshi et al., 2007, in review). The majority of carbon emissions resulting from fire for both climate scenarios and the sets of simulations that both included and excluded CO_2 were concentrated primarily in Canada (Figure 3.1) due to greater area burned across this region.

3.4.2 21st Century carbon dynamics for boreal North America, 2003-2100

For the period 2003-2100, our simulations that considered the effect of atmospheric CO_2 fertilization on photosynthesis estimated that boreal North America was a carbon sink of 235.6 Tg C yr^{-1} (19.6 g C m^{-2} yr^{-1}) and 178.5 Tg C yr^{-1} (14.8 g C m^{-2} yr^{-1}) for the A2 and B2 scenarios, respectively (Table 3.2). CO_2 and climate variability acted to sequester carbon, while fire acted to release carbon to the atmosphere. For the warmer A2 scenario, CO_2 fertilization was responsible for sequestering carbon at a rate of 245.1 Tg C yr^{-1} (20.5 g C m^{-2} yr^{-1}) while climate variability was responsible for sequestering 176.1 Tg C yr^{-1} (14.7 g C m^{-2} yr^{-1}). For the B2 scenario we estimate that CO_2 fertilization was responsible for sequestering approximately 30% less carbon (171.5 Tg C yr^{-1} or 14.3 g C m^{-2} yr^{-1}) while climate variability was responsible for sequestering

approximately 16% less carbon (147.0 Tg C yr^{-1} or 12.3 g C m^{-2} yr^{-1}), relative to the A2 scenario. The role of fire on carbon storage resulted in a source to the atmosphere at a rate of 185.6 Tg C yr^{-1} (15.6 g C m^{-2} yr^{-1}) and 140.0 Tg C yr^{-1} (11.8 g C m^{-2} yr^{-1}) for the A2 and B2 scenarios, respectively. Greater carbon was released to the atmosphere under the A2 scenario than the B2 scenario due to more area burned throughout the latter half of the 21st Century.

The simulations that exclude CO_2 fertilization estimated a carbon source to the atmosphere of 64.7 Tg C yr^{-1} (5.5 g C m^{-2} yr^{-1}) and 30.0 Tg C yr^{-1} (2.6 g C m^{-2} yr^{-1}) for the A2 and B2 scenarios, respectively (Table 3.2). Alaska remains an overall carbon sink, while Canada became a carbon source to the atmosphere (Table 3.2). The effect of climate variability on carbon storage was similar among the A2 and B2 scenarios. Climate variability was responsible for a carbon sink of 74.7 Tg C yr^{-1} (6.2 g C m^{-2} yr^{-1}) and 76.8 Tg C yr^{-1} (6.4 g C m^{-2} yr^{-1}) for the A2 and B2 scenarios, respectively (Table 3.2). Fire, however, was responsible for releasing carbon to the atmosphere at a rate of 139.4 Tg C yr^{-1} (11.7 g C m^{-2} yr^{-1}) and 106.8 Tg C yr^{-1} (9.0 g C m^{-2} yr^{-1}) for the A2 and B2 scenarios, respectively (Table 3.2). Similar to the simulations incorporating atmospheric CO_2 fertilization, the A2 scenario resulted in greater area burned over the latter half of the 21st Century and therefore resulted in greater carbon release to the atmosphere.

We analyzed the cumulative changes in carbon stocks for vegetation, soil, and total ecosystem carbon pools in response to CO_2, climate, and fire for the period 2003-2100 (Figure 3.2). For the simulations that included atmospheric CO_2 fertilization,

vegetation carbon stocks increased throughout the 21st Century, and were 24% greater for the A2 than B2 scenario by 2100 (Figure 3.2). For the A2 scenario, vegetation carbon stocks showed greater change in the last 35 years of the 21st Century in comparison to the same period for the B2 scenario. Similar to the changes in vegetation carbon stocks, changes in soil carbon stocks resulted in approximately 25% greater carbon storage for the A2 scenario than for the B2 scenario (Figure 3.2). By the end of the 21st Century we estimated that the cumulative changes in total carbon stored, relative to year 2003 was 22,930 Tg C and 17,370 Tg C for the A2 and B2 scenarios, respectively. Thus, the warmer scenario resulted in 24% greater carbon storage over the 21st Century. For the simulations that excluded CO_2, changes in vegetation carbon stocks promote a carbon source for much of the 21st Century (Figure 3.2). The trend of changes in vegetation carbon stocks was similar among the A2 and B2 scenarios until 2060, but the A2 scenario resulted in greater release of carbon than the B2 scenario from 2061-2100 due to greater area burned (Figure 3.2). Changes in soil carbon stocks shifted from promoting carbon storage to a carbon source for this period for both climate scenarios, and were greater for the A2 scenario due to greater area burned over this period (Figure 3.2). Changes in the vegetation carbon stocks for the first 60 years of the 21st Century were responsible for the small total ecosystem carbon losses during this period, while in the last 40 years, vegetation and soil carbon were about equally important in promoting total carbon release to the atmosphere. Total carbon release to the atmosphere was 54% greater for the warmer A2 scenario by the end of the century (Figure 3.2).

In addition to temporal variations in carbon storage, the capacity of terrestrial ecosystems to sequester carbon varied across boreal North America (Figures 3.3 and 3.4). These spatial variations in carbon flux between the land and atmosphere also depended upon the assumptions made about CO_2 fertilization and climate change. Atmospheric CO_2 had a positive effect on carbon storage across North America for the A2 (Figure 3.3a) and B2 (Figure 3.4a) scenarios. The effect of climate, however, showed both carbon sequestration and release to the atmosphere for the A2 (Figure 3.3b) and B2 (Figure 3.4b) climate scenarios. Carbon release was greater for the simulations that excluded CO_2 fertilization and was most evident in the Canadian Archipelago, the Mackenzie Mountain range, and portions of central Canada extending northeast to Hudson Bay (Figures 3.3e; 3.4e). The effect of fire on net ecosystem carbon balance was observed primarily where historical fire records and future fire estimates were concentrated. Carbon losses for the simulations that included a CO_2 fertilization effect were observed in portions of interior Alaska, extending through western and central Canada to portions of Labrador and Newfoundland, with greater losses under the A2 scenario (Figure 3.3c) than the B2 scenario (Figure 3.4c). Carbon losses for the simulations that excluded CO_2 fertilization were lower in comparison to the simulations that included a CO_2 fertilization effect on photosynthesis (Figures 3.3f; 3.4f). Greater carbon losses resulting from fire for the simulations that included CO_2 fertilization were due to greater total ecosystem carbon stocks resulting from the fertilization effect and therefore more biomass for burning. The spatial extent of carbon losses was also different for the simulations excluding CO_2 fertilization. Under both climate scenarios,

carbon losses were observed in portions of interior Alaska, extending southeast through western and central Canada to portions of central Quebec. Thus, although boreal North America acted overall as a carbon sink in response to the combined effect of CO_2, climate, and fire for both climate scenarios, there were regions which act as a carbon source, particularly where fires occurred and in regions that showed losses in response to climatic variability (Figures 3.3d; 3.4d). Similarly, in the simulations that excluded CO_2 fertilization, boreal North America acted overall as a carbon source to the atmosphere in response to climatic variability and fire, but there were regions which still acted as carbon sinks of atmospheric CO_2 (Figures 3.3g; 3.4g).

3.4.3 Decadal-scale carbon dynamics of the 21st Century

To better understand temporal changes in the relative roles of CO_2, climate, and fire effects on carbon dynamics across boreal North America over the 21st Century, we calculated mean decadal changes in carbon storage for the A2 (Figure 3.5) and B2 (Figure 3.6) simulations. For the A2 scenario, carbon storage increased each decade in response to increasing atmospheric CO_2 concentration (Figure 3.5a). A similar pattern was observed for the B2 scenario; however, the effect of increasing carbon storage tended to plateau after 2061-2070 due to the deceleration of increasing atmospheric CO_2 concentration (Figure 3.6a). The effect of increasing air temperature on carbon storage was similar for the A2 (Figure 3.5b) and B2 (Figure 3.6b) scenarios for the simulations incorporating CO_2 fertilization, with warmer mean temperatures promoting more carbon sequestration. In contrast, the set of simulations that excluded atmospheric CO_2

fertilization showed that warming temperatures result in carbon sequestration that was relatively unchanged from decade to decade for the A2 (Figure 3.5b) and B2 (Figure 3.6b) scenarios. However the last four decades did appear to become more variable, which coincide with the warmest average decadal temperatures of the 21st Century. Further analysis of the response of carbon storage to the warmer A2 scenario for the S2 simulation that excluded CO_2 showed that by the last decade of the 21st Century, R_h continued to increase while NPP decreased despite the increased levels of nitrogen availability caused by warming enhanced nitrogen mineralization (Figure 3.7).

The effect of fire on decadal scale carbon dynamics showed that as area burned increased, fire generally released more carbon to the atmosphere, with more carbon released per decade under the A2 climate scenario (Figure 3.5c). Despite greater area burned for the period 2071-2080, relative to the previous decade, fire resulted in less of a carbon source for the simulations that both incorporated and excluded CO_2 fertilization (Figure 3.5c). The fire effect integrates the legacy of how fire influences the balance between NPP and R_h on regrowing stands during each decade in addition to emissions resulting from fire. To show the effect of fire on NPP and R_h, we calculated the difference between the S3 and S2 simulations (Figure 3.8). The decrease in the source resulting from fire for the period 2071-2080 under the A2 scenario was due to a greater increase in NPP than in R_h for the simulations that included (Figure 3.8a) and excluded atmospheric CO_2 fertilization (Figure 3.8c). For the set of simulations that excluded CO_2 fertilization, the last three decades that correspond to the greatest burned area resulted in a carbon source that is relatively unchanged (Figure 3.5c), while the carbon source

increased from decade to decade for the set of simulations that incorporated atmospheric CO_2 fertilization (Figure 3.5c). NPP increases while R_h decreases under the A2 scenario for the simulations excluding atmospheric CO_2 in the last three decades (Figure 3.8c). The simulations under the A2 scenario that incorporated atmospheric CO_2 show a decrease in NPP (Figure 3.8a) over this period as well as an increase in fire emissions (Figure 3.1a). The B2 scenario showed that as area burned increased through 2050, carbon released to the atmosphere also increased in simulations that incorporated CO_2 fertilization (Figure 3.6c). Future area burned under the B2 scenario then plateaus from 2041-2070 due to the relationship between air temperature and fuel moisture indices on area burned (see Figure 2.4 in Balshi et al., in review). The carbon source increased from 2041-2060 then decreased from 2061-2070 as NPP increased (Figure 3.8b). The last three decades of the 21st Century corresponded to greater area burned under the B2 scenario, and the effect of fire resulted in a larger carbon source to the atmosphere than the previous 70 years (Figure 3.6c) due to greater fire emissions (Figure 3.1a) and decreasing NPP (Figure 3.8b). For the simulations that excluded CO_2 fertilization, the period 2061-2070 resulted in a smaller carbon source as NPP increased (Figure 3.8d) and fire emissions were relatively unchanged (Figure 3.1b) relative to the previous decade. The carbon source increased for the period 2071-2080 due to an increase in R_h and decrease in NPP (Figure 3.8d), relative to the previous decade. The source remained relatively unchanged for the remainder of the 21st Century as NPP (Figure 3.8d) and area burned (Figure 3.6c) plateau.

The combined effects of CO_2, climate, and fire on decadal scale carbon dynamics indicated that boreal North America was a carbon sink for the A2 (Figure 3.5d) and the B2 (Figure 3.6d) scenarios for the simulations that incorporated atmospheric CO_2, as NPP increased faster than R_h and TCE (Figures 3.9a, 3.9b). The last three decades under the A2 scenario showed that the net carbon sink flux approximately tripled relative to the period 1991-2000 (Figure 3.5d). For the B2 scenario, the last four decades of the 21st Century show that the carbon sink flux was more than double that of the period 1991-2000 (Figure 3.6d). NPP, R_h and TCE increased faster under the A2 scenario (Figure 3.9a) throughout the 21st Century than under the B2 scenario (Figure 3.9b). The set of simulations that excluded atmospheric CO_2 fertilization indicated that boreal North America was a small carbon sink in the first decade of the 21st Century and became a carbon source in the remaining decades for the A2 scenario (Figure 3.5d) as R_h and TCE increased faster than NPP (Figure 3.9c). For the B2 scenario, North America was a small carbon source from 2011-2100 except for a small sink in 2061-2070 (Figure 3.5d), which was a decade when NPP increased and R_h and TCE decreased relative to the previous decade (Figure 3.9d).

3.5 Discussion

The strong link between climate and fire in the North American boreal forest (Clark, 1990; Flannigan and Van Wagner, 1991; Johnson and Wowchuk, 1993; Skinner et al., 1999, 2002; Duffy et al., 2005) implies that changes in climate will likely correspond to changes in fire regimes (Gillet et al., 2004; Kasischke and Turetsky, 2006)

through increased burning (Flannigan et al., 2000) and extended fire seasons (Wotton and Flannigan, 1993) in portions of the western boreal forest and a reduction in fire frequency in eastern Canadian forests (Carcaillet et al., 2001). It is therefore critical to incorporate the effects of fire when estimating future carbon dynamics of this region. The results presented here represent a first attempt at coupling spatially and temporally explicit empirical estimates of future area burned (Balshi et al., 2007, in review) into a process-based biogeochemical modeling framework for the land-based area of North America, north of 45° N. We discuss the implications of different climate change scenarios on fire emissions and the overall carbon balance of this region. We also discuss uncertainties that should be addressed in future studies to improve the representation of the effects of future fire disturbance on the carbon dynamics of the North American boreal region.

3.5.1 Effect of future climate change on boreal North American fire emissions

In this study, we estimated the effects of two climate scenarios on boreal North American fire emissions, both including and excluding the effects of CO_2 fertilization on photosynthesis. The simulations suggest that climate warming throughout the 21st Century will, on average, result in greater levels of total carbon emitted by future wildfires. Our estimates suggest that by the end of the 21st Century (2091-2100), total carbon emitted by wildfire is between 25-30% higher under the A2 scenario than the B2 scenario and the higher emissions are the result of greater area burned (see Balshi et al., 2007, in review). The A2 and B2 simulations that exclude the effect of CO_2 fertilization

on photosynthesis result in lower total carbon emissions for each decade than the corresponding simulations including the effect of CO_2 fertilization. The effect of CO_2 fertilization results in greater carbon sequestration for that set of simulations and therefore greater carbon emitted at the time of fire due to greater biomass available for burning (Figure 3.2). Balshi et al. (2007) reported minor differences in total carbon emission estimates for the period 1959-2002 for simulations including and excluding CO_2 fertilization on photosynthesis. Our results suggest that CO_2 fertilization plays a much larger role in the emissions resulting from future area burned.

Bachelet et al. (2005) used a dynamic vegetation model that simulates the effects of fire to estimate the role of fire on carbon dynamics for Alaska through year 2100. They report an average loss of 17-19 Tg C yr^{-1} due to fire emissions for the period 2025-2099 based on simulations with two climate scenarios. Our simulations estimate a range of between 18-25 Tg C yr^{-1} emitted at time of fire for Alaska over the same period. The larger range of emissions estimates from our study can be attributed to greater future area burned estimates for the period 2051-2090 (averaged across climate scenarios, our area burned estimates are between 1.4-8.0 times higher than those of Bachelet et al. (2005) for the period 2051-2090). The area burned estimates may be greater because we used different climate model scenarios to simulate future area burned.

3.5.2 Changes in 21st Century carbon storage

Process-based models are useful for understanding the relative roles of CO_2, climate, and fire on the carbon dynamics of the boreal region because individual factors

affecting carbon storage can be isolated. Similar to Balshi et al. (2007) for the historical period 1959-2002, we found that both CO_2 and climatic variability accounted for the majority of the reported carbon sink across boreal North America for the 21st Century for both climate scenarios. The sink activity for the A2 scenario resulted in approximately 24% more carbon stored than the B2 scenario. However, for the simulations that excluded a CO_2 fertilization effect we report a source of carbon from terrestrial ecosystems to the atmosphere. The switch to a source in the simulations that exclude CO_2 fertilization is due to both no carbon sequestration associated with rising CO_2 and lower carbon sequestration in response to climatic variability due to the lack of CO_2 interactions with climate variability.

To our knowledge, this study is the first to simulate the effects of future fire on the carbon dynamics of the North American boreal region. The only study that we know of that report estimates for a portion of our study area is Bachelet et al. (2005). Bachelet et al. (2005) report a range of net ecosystem carbon balance estimates of 10-31 g C m^{-2} yr^{-1} sequestered by terrestrial vegetation for Alaska for the period 2025-2099. Our estimates of carbon storage over the same period indicate carbon storage of 18-28 g C m^{-2} yr^{-1} for the simulations that included CO_2 fertilization, which is within the range of Bachelet et al. (2005). In contrast, our simulations that exclude CO_2 fertilization estimate a range of 3.9-4.7 g C m^{-2} yr^{-1} for Alaska, which is below the range of Bachelet et al. (2005).

Previous studies that used process-based models to simulate carbon dynamics of terrestrial ecosystems indicate that a substantial carbon sink results from atmospheric

CO_2 fertilization (Kicklighter et al., 1999; McGuire et al., 2001; Friedlingstein et al., 2003; Thompson et al., 2004; Balshi et al., 2007). The TEM simulates explicit interactions between the carbon and nitrogen cycles and limits carbon uptake by vegetation based on the availability of nitrogen. The response of TEM to increases in atmospheric CO_2 is highly constrained by the representation of the nitrogen cycle in the model (McGuire et al., 1993, 1997, 2001; Kicklighter et al., 1999). Our simulations for the 21st Century also indicate that atmospheric CO_2 fertilization plays a major role in the carbon dynamics of boreal North America. In our simulations, the A2 and B2 scenarios responded differently to the elevated levels of atmospheric CO_2. Carbon storage increases in response to elevated CO_2 for each decade for the A2 scenario while carbon storage increases then plateaus for the last three decades of the 21st Century for the B2 scenario. This response is likely due to the deceleration of increasing CO_2 concentration.

The increase in carbon storage to warming in our simulations is associated with increases in the availability of soil nitrogen due to warming-enhanced nitrogen mineralization (McGuire et al., 1992; Xiao et al., 1998). The influence of interannual variation in climate on carbon storage simulated by TEM has been documented in previous studies (Tian et al., 1999; McGuire et al., 2001; Nemani et al., 2003; Euskirchen et al., 2006; Kimball et al., 2007; Balshi et al., 2007; Clein et al., 2007). For the simulations incorporating the effect of atmospheric CO_2, both climate scenarios indicate that as average decadal temperatures increase, carbon storage associated with climate variability increases. In contrast, the simulations excluding atmospheric CO_2 fertilization estimate lower sink strength associated with climate variability. Although we isolate the

climate effect from the CO_2 effect by subtracting the S2 simulation from the S1 simulation, interactions between increasing CO_2 and climate are present in this estimate, and it is the interaction between CO_2 and climate that is responsible for greater sink strength associated with climate variability in the simulations that include CO_2 fertilization (see McGuire et al., 2001). For the A2 simulation excluding the effect of CO_2 fertilization, carbon storage (Figure 3.4b) was lower in the last three decades of the 21st Century, relative to the previous 70 years. Throughout the 21st Century, mean decadal air temperature is rising and may result in R_h increasing faster than NPP, despite the increased levels of nitrogen availability caused by warming enhanced nitrogen mineralization. Our simulations that excluded CO_2 fertilization under the warmer A2 scenario indicate that by the last decade of the 21st Century, NPP begins to decrease while R_h continues to increase (Figure 3.7). Despite the warmer temperatures, a decrease in NPP may be related to a drought-induced reduction in photosynthesis (Angert et al., 2005).

Our results indicate that it is important to incorporate fire in estimating future carbon dynamics. For the 21st Century, we estimate that fire results in a net carbon source to the atmosphere in some regions for simulations that include and exclude atmospheric CO_2 and is larger under the A2 scenario than the B2 scenario. The incorporation of fire activity into our analysis reduces total ecosystem carbon storage through changes in vegetation and soil carbon pools across boreal North America for the entire 21st Century. For the simulations excluding CO_2 fertilization, decades with greater area burned resulted in an overall carbon source to the atmosphere (Figures 3.5d and

3.6d) while decades with lower area burned generally resulted in greater carbon sink activity.

While we have attempted to account for the effects of climate, enhanced atmospheric CO_2 concentrations, spatially explicit fire severity, and fuel availability, as represented by stand-age distribution, on fire emissions, there are additional issues that we did not consider that might influence estimates of carbon dynamics in boreal North America. We have yet to evaluate the role of temporally varying fire severity and vegetation under a warming climate. Deeper, later season burns have the potential to release larger amounts of carbon and therefore increase the effect of fire on the carbon dynamics of the North American boreal region, while successional changes in vegetation following fire as well as vegetation redistribution resulting from a changing climate may result in an increase or decline in the overall fire effect. These issues are discussed further in section 3.5.3.2.

3.5.3 Uncertainties and limitations

Similar to projections of future climate and atmospheric CO_2 concentrations, our estimates of the role of future wildfires on the carbon dynamics of boreal North America have limitations. We identify several limitations that introduce uncertainties in our estimates which should be considered in future process-based modeling studies to improve simulating the effect of fire on carbon dynamics. We first identify limitations that are specific to the methodologies used for implementing area burned into the TEM.

We then discuss more general limitations imposed by the current implementation of fire severity and vegetation state following fire.

3.5.3.1 Limitations of coupling future area burned to TEM

Several challenges were encountered when coupling future area burned to the current framework of the TEM. The first challenge we encountered was downscaling future area burned from 2.5° to 0.5° spatial resolution, which required several assumptions. For the sake of simplicity, we evenly distributed the area burned estimates for each year to every 0.5° cell that occurred within a given 2.5° cell. This area was then distributed to cohorts within each 0.5° cell based on the number and age of the cohorts in year 2002. The future stand age distributions therefore rely on the accuracy of the stand ages in year 2002. An added level of uncertainty deals with the assumption that all burnable vegetation types within a given 2.5° cell are available for burning in the future. The assumption does not take into account the issue of vegetation changes through time (i.e., species replacement following fire as well as changes in vegetation distribution in response to climate change), which could have implications on the estimates of future carbon balance estimates (addressed in section 3.5.3.2). A third limitation not taken into consideration in this study is the potential for grid cells that were not explicitly modeled by Balshi et al. (2007, in review) to burn in the future. Changes in climate are likely going to be accompanied by increases in fuel loading in areas that have not burned historically, and therefore are more likely to burn if warmer, drier conditions prevail.

Accounting for future fire in grid cells that are currently assumed not to burn would likely result in a greater carbon source.

3.5.3.2 Additional limitations, uncertainties, and future work

Incorporating the role of dynamic vegetation, temporal changes in fire severity, and other disturbances such as insect outbreaks in future modeling studies is important with respect to capturing a better representation of emissions estimates at the time of fire as well as the carbon dynamics associated with secondary successional processes following fire. The estimates that we present in this study do not take into account changes in vegetation type (i.e., conifer to deciduous) following fire. Different vegetation types may have different responses to elevated atmospheric CO_2 concentrations and a warming climate. One of the main limitations of the current study is that our carbon balance estimates are based on a fixed vegetation distribution that does not change spatially through time. This can be problematic in that regional carbon dynamics can be influenced for several decades following fire due to the differences in the post-fire responses of different vegetation types (e.g., deciduous vs. coniferous) (Amiro et al., 2006). This introduces uncertainty with respect to the calculation of net ecosystem carbon balance and is also important with respect to surface energy feedbacks between terrestrial ecosystems and the climate system (Chapin et al., 2000; McGuire et al., 2006; Randerson et al., 2006). The deciduous stands that dominate following fire have a higher albedo than boreal conifers and are also less flammable. The potential increases in area burned and fire frequency may lead to stands that are dominated

primarily by deciduous forests, which can lead to an overall cooling effect on the climate system and a negative feedback to the climate system (Chapin et al., 2000; McGuire et al., 2004, 2006, 2007; McGuire and Chapin, 2006; Randerson et al., 2006).

Closely related to the role of vegetation changes in response to fire is the influence of fire severity on post-fire vegetation recruitment. For example, it has been shown that lower severity fires result in conditions that are more favorable to recruitment by boreal conifers while high severity fires that consume duff to the mineral soil result in a seedbed that is more favorable to deciduous species (Johnstone and Chapin, 2006). Future studies should attempt to incorporate these processes; however it is recognized that representing these fine-scale processes at a much larger scale is an ongoing challenge (Fosberg et al., 1999).

Under a warming climate, it is also important to recognize the potential of the northward expansion of vegetation types currently absent from particular regions of the boreal forest and the associated implications for future fire regimes. There is increasing evidence of tree line expansion into tundra (Bachelet et al., 2005; Chapin et al., 2005; Scholze et al., 2006; McGuire et al., 2007) as well as the northward expansion of lodgepole pine (Johnstone and Chapin, 2003) that should be taken into account in future work. If fire were to migrate into areas currently dominated by other vegetation types, the contribution to fire emissions and the overall carbon budget could be significant.

Fire severity influences the amount of total carbon emitted at the time of fire as well as long-term carbon accumulation (Kurz and Apps, 1999; Harden et al., 2000; Balshi et al., 2007). Our implementation of fire severity is static, which does not account for

seasonal variations in depth of burn. The importance of accounting for seasonal variation in depth of burn has been addressed in previous studies (Kasischke et al., 2005; Kasischke and Turetsky, 2006) and has great potential to result in different estimates of total carbon emitted than what we report in the current study. Several studies (Wotton and Flannigan, 1993; Flannigan et al., 2000, 2005; Carcaillet et al., 2001; Balshi et al., 2007, in review) have shown that a warmer climate results in greater future area burned, which is partially a consequence of longer fire seasons. If fire seasons become longer, there is potential for the alteration of depth of burn (i.e., greater severity) due to the potential for drier conditions in the duff layer in addition to deeper thaw of the soil. Increases in fire severity have the potential to decrease the amount of insulating moss and soil organic layers, which can also feedback to the soil thermal and permafrost regimes through increasing the active layer depth and thawing of permafrost (Hinzman et al., 2003). Interactions between fire severity, soil thermal, and permafrost regimes are therefore important to consider in future work.

Finally, it is important to consider the role of other disturbances (e.g., insects and disease) and how they interact with fire regime across the North American boreal forest. It has been suggested that as climate warms insect outbreak behavior will intensify (Logan et al., 2003). Because insect outbreaks and disease result in more fuel for future disturbance by wildfire, there is great potential to alter fire regime by increasing the amount of fuel that could contribute to larger, more catastrophic fire events. Greater emissions resulting from an increase in fire activity also has potential to offset the effects of CO_2 fertilization on carbon storage. Incorporating the response of insect disturbance

and disease to future climate change and the interactions between these disturbances and fire regime will be essential to improve current carbon balance estimates of the future.

3.6 Conclusion

Changes in the fire regime in response to a changing climate have strong implications for the carbon dynamics of the North American boreal region. Our analysis suggests that it is important to incorporate the spatial and temporal changes in future wildfire regime as a result of a changing climate in the simulation of large-scale ecosystem carbon dynamics. In addition to moisture content of fuel, changes in atmospheric CO_2 concentration and climate influence the amount of fuel that is available to burn in the future. Fire histories of a stand also influence the amount of fuel available to burn in the future. If CO_2 fertilization presently occurs and continues in the future, we expect boreal North America will be a carbon sink for the period 2003-2100, with larger sink strengths associated with warmer temperatures. In contrast, if CO_2 fertilization does not occur, we expect this region to be a source of atmospheric CO_2 in the future, with a larger source strength associated with warmer temperatures. Consideration of post-fire successional vegetation, vegetation redistribution with climate change, temporal-varying fire severities, and other disturbance regimes, such as insect outbreaks or disease, in future studies will help to reduce the uncertainties present in this study and will be essential to providing a more complete picture of how future carbon storage changes in the North American boreal region.

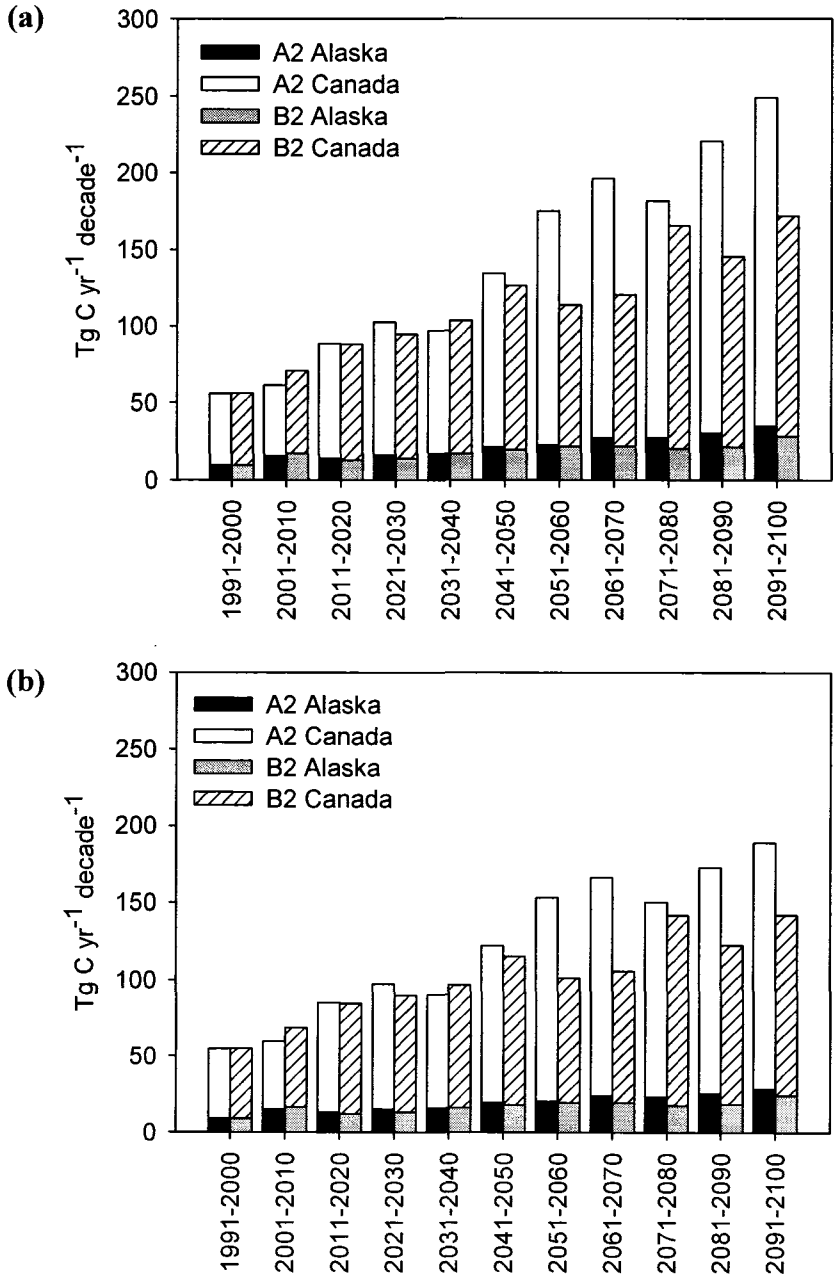

Figure 3.1 Mean decadal total carbon emissions resulting from fire for North America during the 21st Century that (a) incorporate the effect of atmospheric CO_2 on photosynthesis and (b) exclude the role of atmospheric CO_2 on photosynthesis. The decade 1991-2000 is used as a comparison period and corresponds to years where fire emissions are driven by historical fire records. Units are Tg C yr^{-1} $decade^{-1}$.

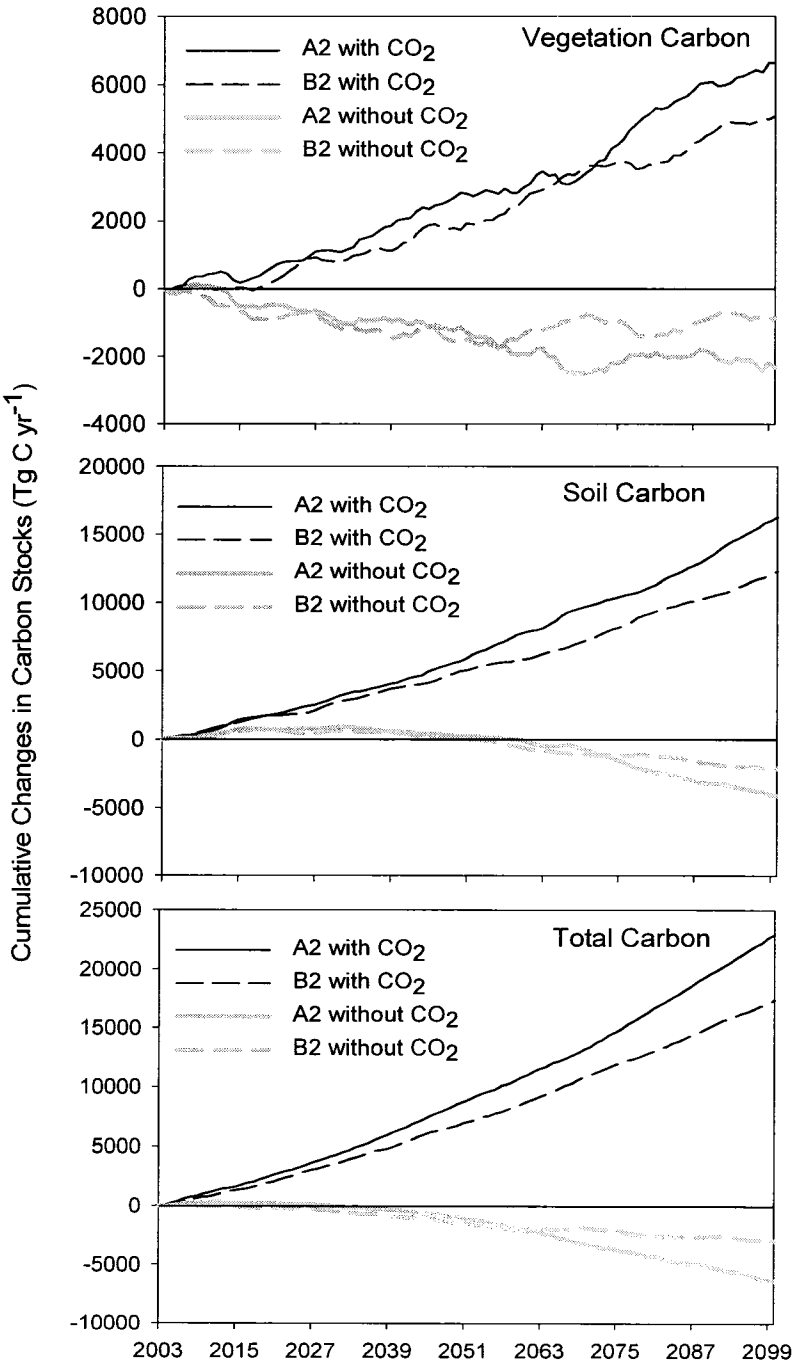

Figure 3.2 Cumulative changes in vegetation, soil, and total ecosystem carbon stocks for North America from 2003-2100. Units are Tg C yr^{-1}.

Figure 3.3 Simulated mean annual net ecosystem carbon balance of North America estimated under the A2 climate scenario from 2003-2100 in response to (a) CO_2 fertilization, (b, e) climate, (c, f) fire, and (d, g) the combination of CO_2, climate, and fire. Results are presented with and without a CO_2 fertilization effect on photosynthesis. Units are g C m^{-2} yr^{-1}. Positive values represent carbon sequestration while negative values represent release of carbon from the land to the atmosphere.

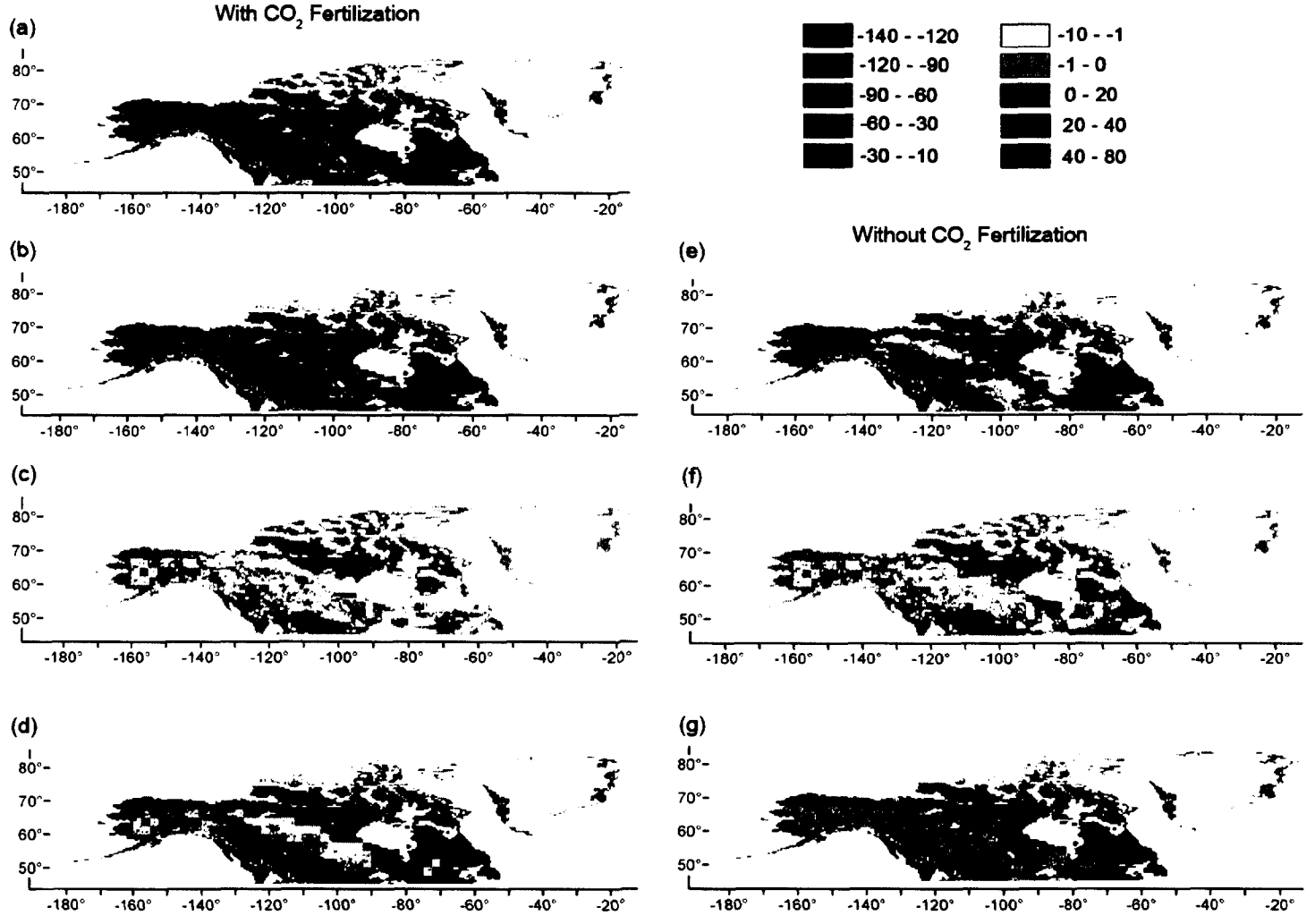

Figure 3.4 Simulated mean annual net ecosystem carbon balance of North America estimated under the B2 climate scenario from 2003-2100 in response to (a) CO_2 fertilization, (b, e) climate, (c, f) fire, and (d, g) the combination of CO_2, climate, and fire. Results are presented with and without a CO_2 fertilization effect on photosynthesis. Units are g C m^{-2} yr^{-1}. Positive values represent carbon sequestration while negative values represent release of carbon from the land to the atmosphere.

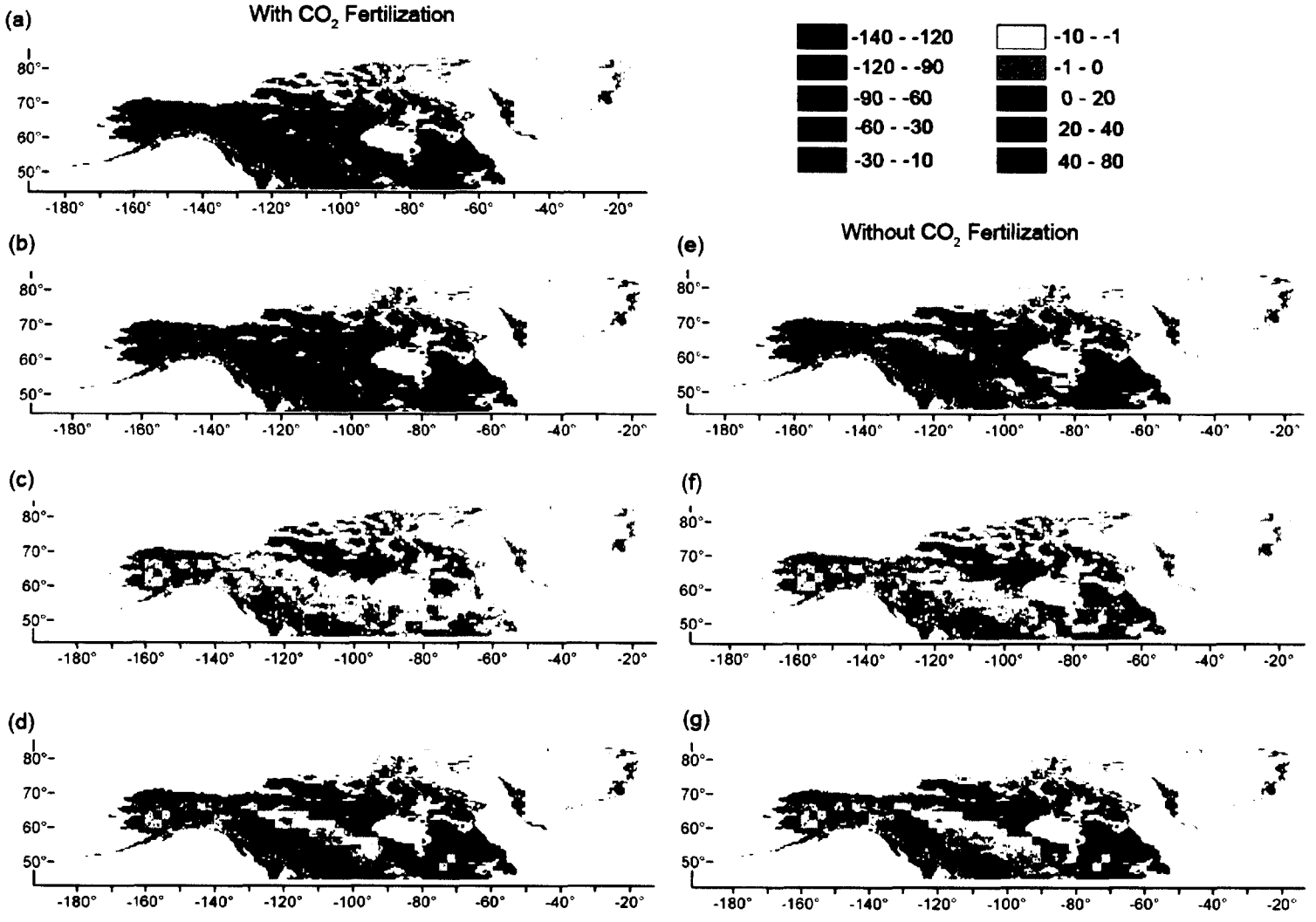

Figure 3.5 Mean decadal effects from the A2 scenario simulations of (a) CO_2, (b) climate, (c) fire, and (d) the combined effects of CO_2, climate, and fire on simulated net ecosystem carbon balance for North America for the 21st Century. Also included is the period 1991-2000, which is used as a baseline comparison period. Each effect is compared with model driving data of mean atmospheric CO_2 concentration, mean air temperature, and mean area burned. Positive values represent carbon sequestration by terrestrial ecosystems, while negative values represent a release of carbon from the land to the atmosphere.

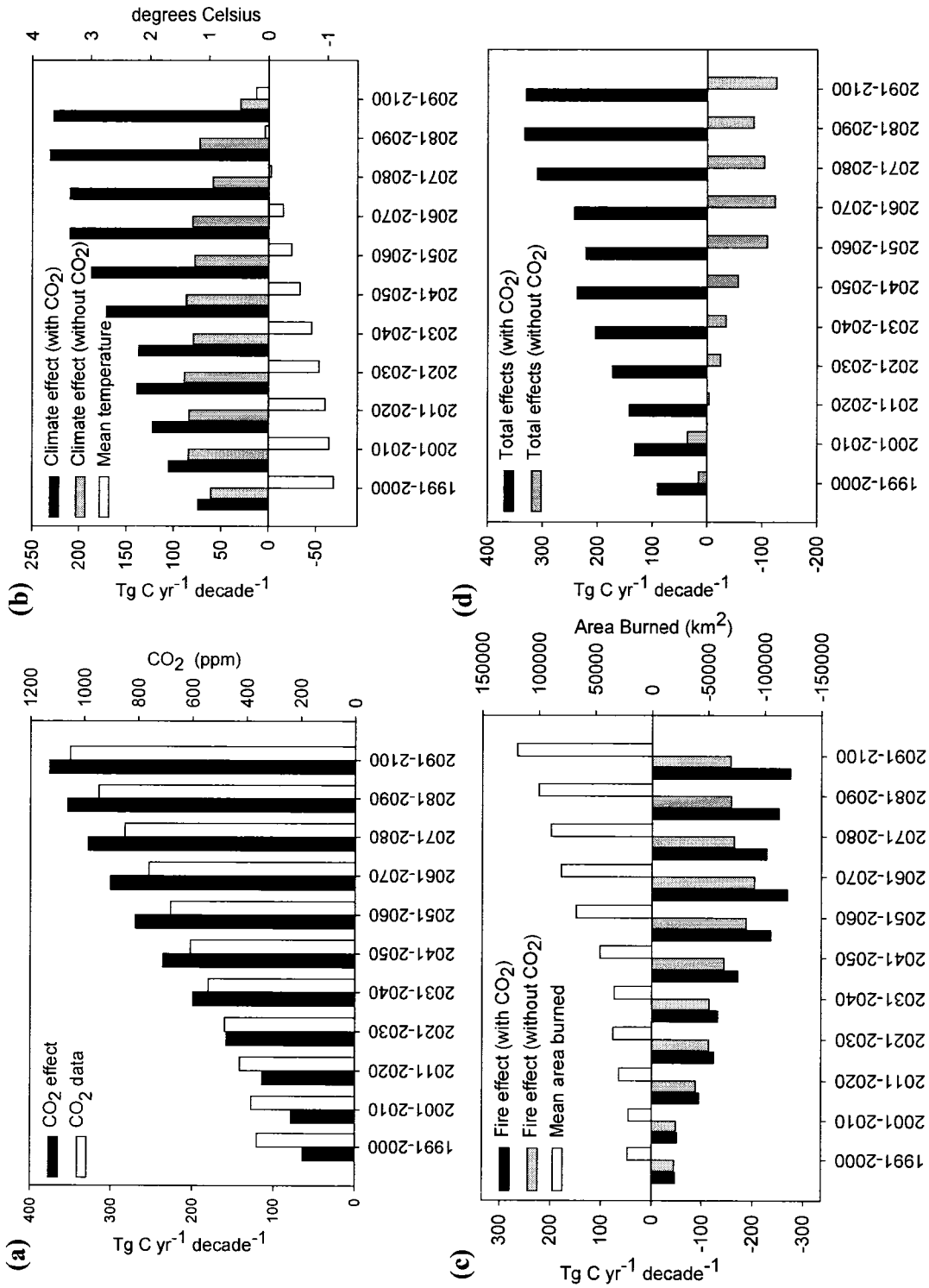

Figure 3.6 Mean decadal effects from the B2 scenario simulations of (a) CO_2, (b) climate, (c) fire, and (d) the combined effects of CO_2, climate, and fire on simulated net ecosystem carbon balance for North America for the 21st Century. Also included is the last decade of the 20th Century for reference. Each effect is compared with model driving data of mean atmospheric CO_2 concentration, mean air temperature, and mean area burned. Positive values represent carbon sequestration by terrestrial ecosystems, while negative values represent a release of carbon from the land to the atmosphere

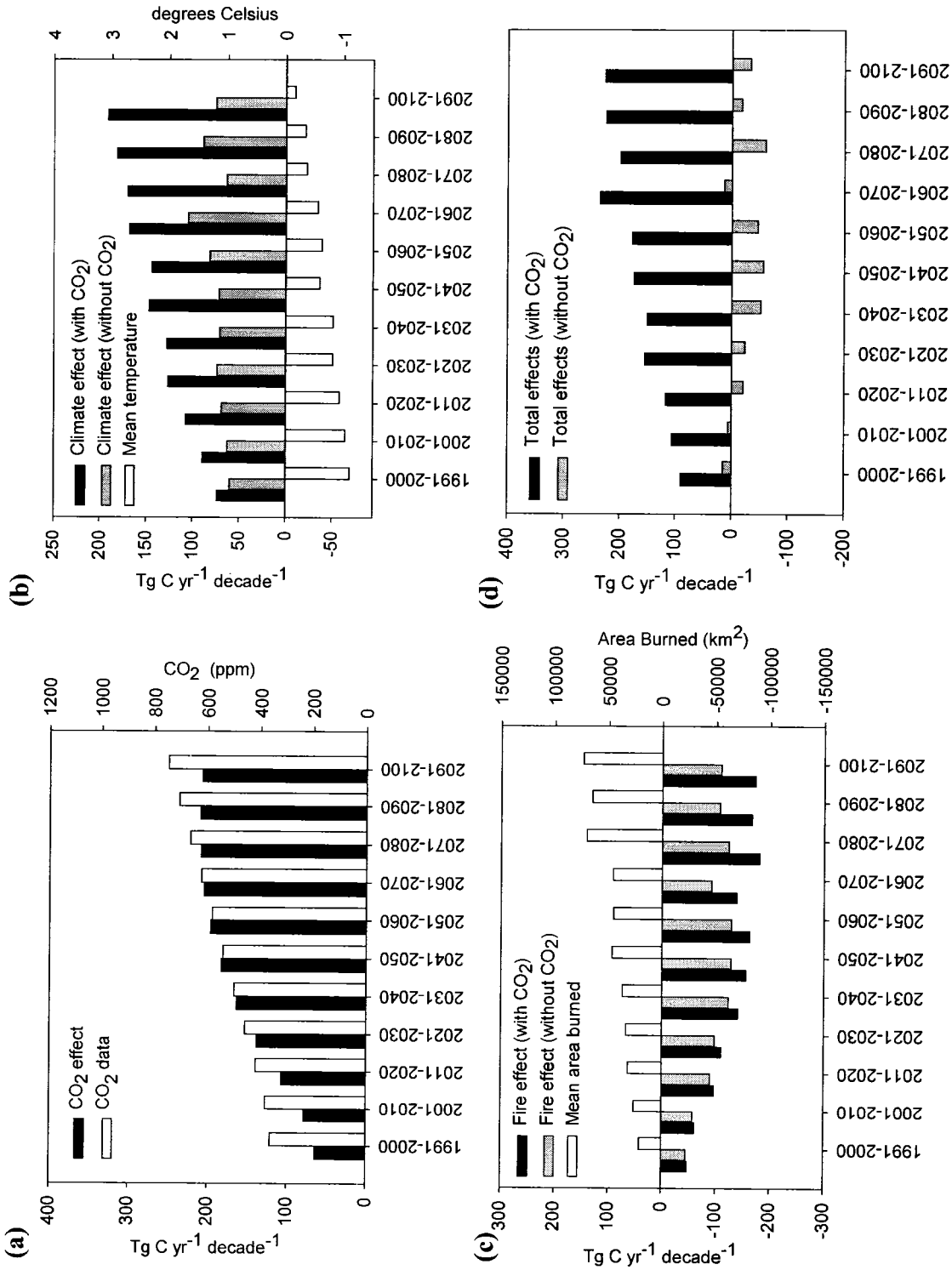

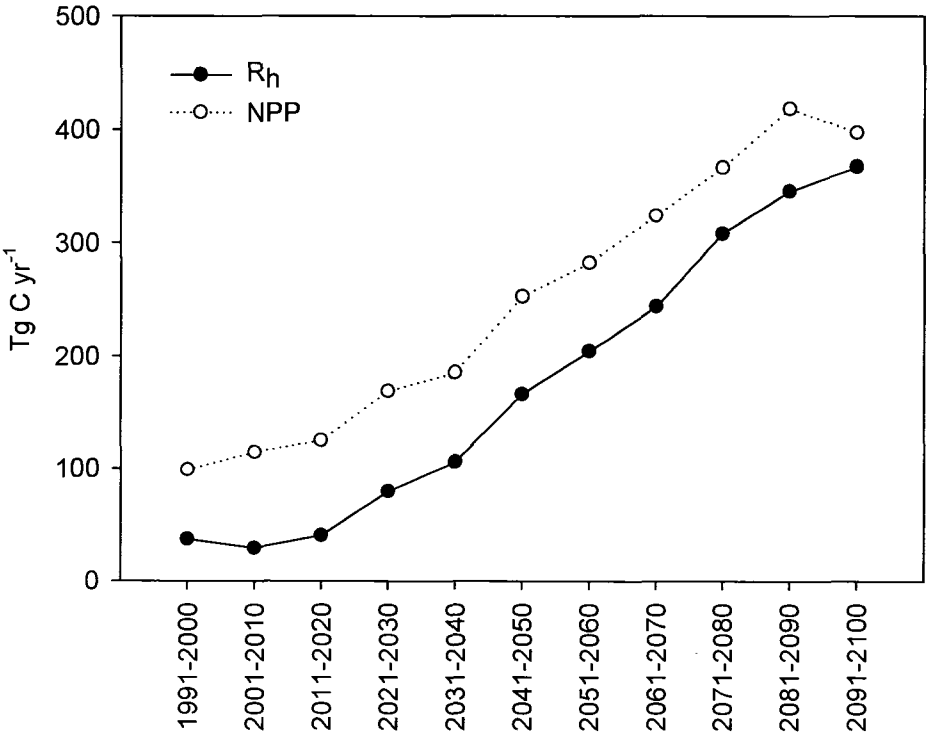

Figure 3.7 Mean decadal net primary production (NPP) and heterotrophic respiration (R_h) in response to climate for the A2 scenario S2 simulation that excluded the effect of atmospheric CO_2 fertilization on photosynthesis. Units are Tg C yr^{-1} $decade^{-1}$.

Figure 3.8 Mean decadal difference between the S3 and S2 simulations representing the effect of fire on net primary production (NPP) and heterotrophic respiration (R_h) for the (a) A2 and (b) B2 scenarios incorporating the effect of atmospheric CO_2 fertilization and the (c) A2 and (d) B2 scenarios excluding the effect of atmospheric CO_2 fertilization on photosynthesis. Regions highlighted in gray indicate areas of interest discussed in section 3.4.3. Units are Tg C yr^{-1} $decade^{-1}$.

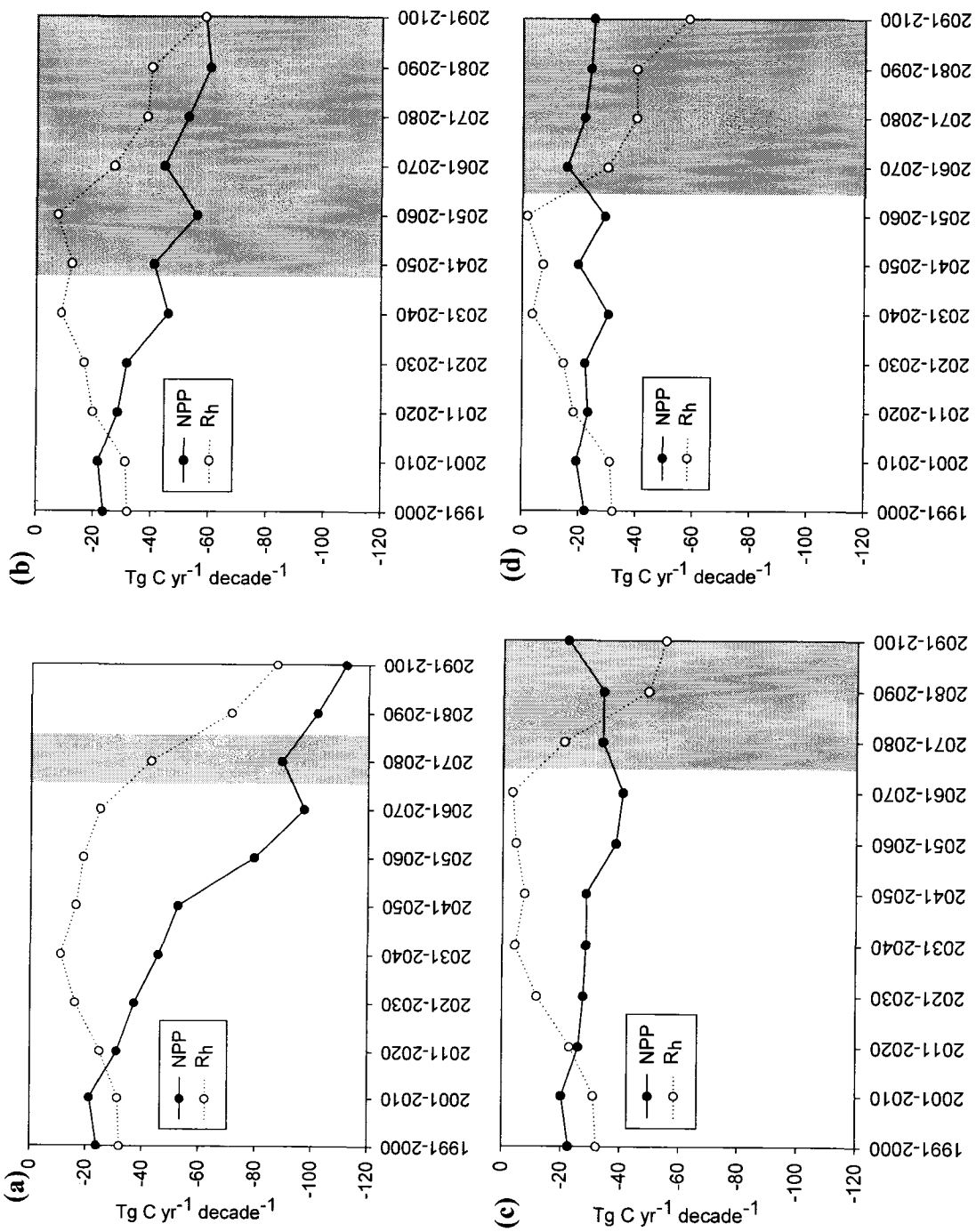

Figure 3.9 Mean decadal net primary production (NPP), heterotrophic respiration (R_h), and the combination of heterotrophic respiration and fire emissions (R_h + TCE) in response to CO_2, climate, and fire for the (a) A2 and (b) B2 scenarios incorporating the effect of atmospheric CO_2 fertilization and the (c) A2 and (d) B2 scenarios excluding the effect of atmospheric CO_2 fertilization on photosynthesis. Units are Tg C yr^{-1} $decade^{-1}$.

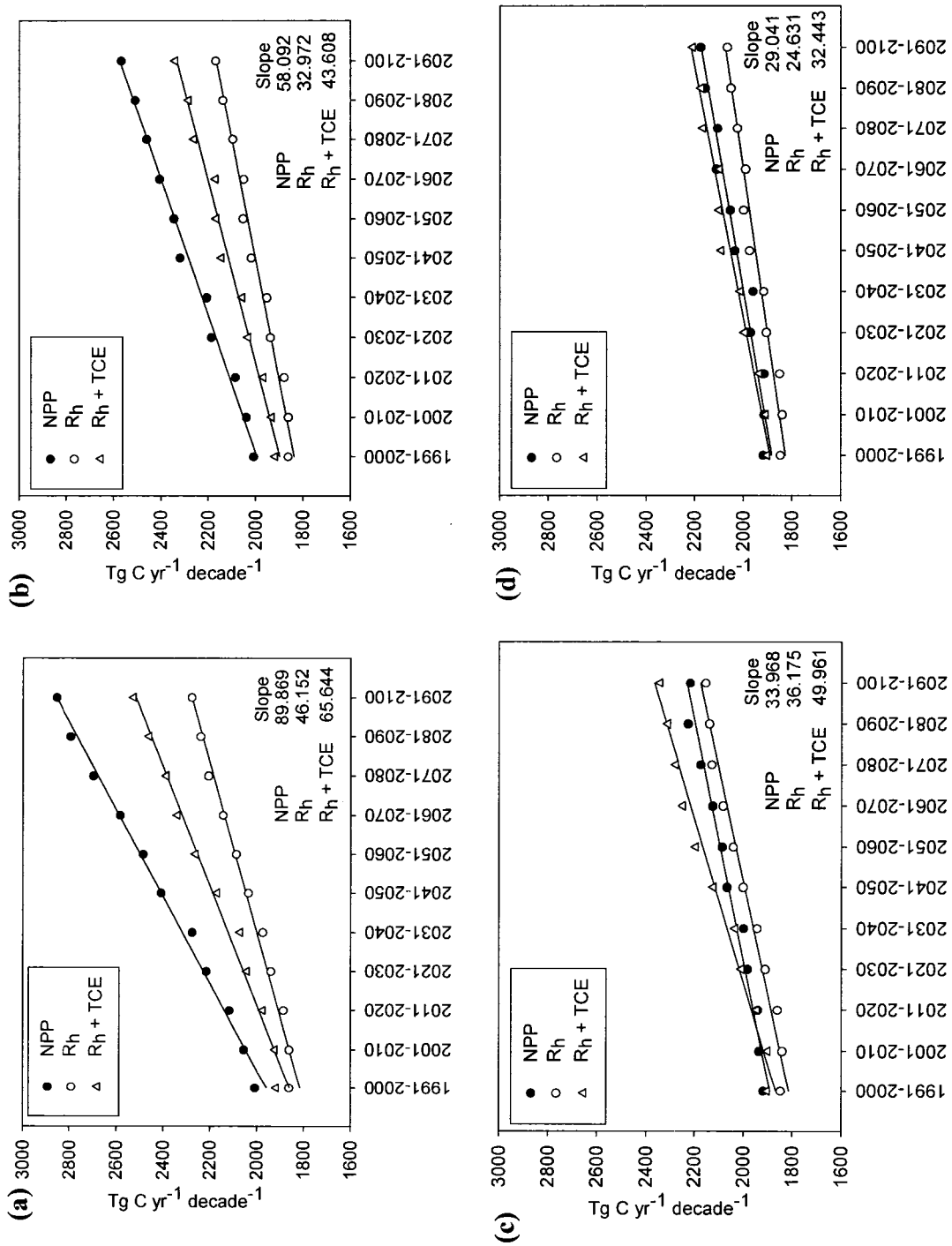

Table 3.1 Literature estimates of average aboveground ($ß_a$) and ground layer ($ß_b$) carbon fraction consumed used for emissions estimates during a fire event for North America (French et al., 2000).

Ecozone	Aboveground ($ß_a$) C fraction consumed	Ground Layer ($ß_b$) C fraction consumed
North America		
Alaska Boreal Interior	0.23	0.36
Boreal Cordillera	0.13	0.38
Taiga Plain	0.25	0.06
West Taiga Shield	0.25	0.05
East Taiga Shield	0.25	0.05
West Boreal Shield	0.26	0.06
East Boreal Shield	0.22	0.06
Boreal Plain	0.24	0.11
Hudson Plain	0.24	0.05

Table 3.2 Mean annual changes in carbon storage for boreal North America from 2003-2100[a] driven by SRES A2 and B2 scenarios output by CGCM2.

		Effects			
Scenario	Region	CO_2	Climate	Fire	Total
	With CO_2 Fertilization				
A2	North America	245.1	176.1	-185.6	235.6
	Alaska	26.7	21.5	-12.0	36.2
	Canada	218.4	154.6	-173.7	199.3
B2	North America	171.5	147.0	-140.0	178.5
	Alaska	18.4	14.9	-9.4	23.9
	Canada	153.1	132.2	-130.6	154.7
	Without CO_2 Fertilization				
A2	North America	0.0	74.7	-139.4	-64.7
	Alaska	0.0	16.9	-11.0	5.9
	Canada	0.0	57.7	-128.4	-70.7
B2	North America	0.0	76.8	-106.8	-30.0
	Alaska	0.0	12.6	-8.3	4.3
	Canada	0.0	64.2	-98.5	-34.3

[a]Units are in Tg C yr^{-1}. Positive values indicate carbon sequestration by terrestrial ecosystems. Negative values indicate a release of carbon from land to atmosphere.

3.7 Acknowledgements

Funding for this study was provided by grants from the National Science Foundation Biocomplexity Program (ATM-0120468) and Office of Polar Programs (OPP-0531047, OPP-0328282, and OPP-0327664); the National Aeronautics and Space Administration North America Carbon Program (NNG05GD25G); and the Bonanza Creek LTER (Long-Term Ecological Research) Program (funded jointly by NSF grant DEB-0423442 and USDA Forest Service, Pacific Northwest Research Station grant PNW01-JV11261952-231). This study was also supported in part by a grant of HPC resources from the Arctic Region Supercomputing Center at the University of Alaska Fairbanks as part of the Department of Defense High Performance Computing Modernization Program.

3.8 References

Amiro, B. D., A. L. Orchansky, A. G. Barr, T. A. Black, S. D. Chambers, F. S. Chapin, III, M. L. Goulden, M. Litvak, H. P. Liu, J. H. McCaughey, A. McMillan, and J. T. Randerson (2006), The effect of post-fire stand age on the boreal forest energy balance, *Agricultural and Forest Meteorology*, *140*, 41-50.

Angert, A., S. Biraud, C. Bonfils, C. C. Henning, W. Buermann, J. Pinzon, C. J. Tucker, and I. Fung (2005), Drier summers cancel out the CO_2 uptake enhancement induced by warmer springs, *PNAS*, *102(31)*, 10823-10827.

Bachelet, D., J. Lenihan, R. Neilson, R. Drapek, and T. Kittel (2005), Simulating the response of natural ecosystems and their fire regimes to climatic variability in Alaska, *Can. J. For. Res.*, *35*, 2244-2257.

Balshi, M. S., A. D. McGuire, P. Duffy, M. Flannigan, J. Walsh, and J. Mellilo (2007), Modeling historical and future area burned of boreal North America using a Multivariate Adaptive Regression Splines (MARS) approach, *Global Change Biology*, in review.

Balshi, M. S., A. D. McGuire, Q. Zhuang, J. Melillo, D. W. Kicklighter, E. Kasischke, C. Wirth, M. Flannigan, J. Harden, J. S. Clein, T. J. Burnside, J. McAllister, W. A. Kurz, M. Apps, and A. Shvidenko (2007), The role of historical fire disturbance in the carbon dynamics of the pan-boreal region: a process-based analysis, *J. Geophys. Res.*, *112*, G02029, doi:10.1029/2006JG000380.

Canadell, J. G., D. E. Pataki, R. Gifford, R. A. Houghton, Y. Luo, M..R. Raupach, P. Smith and W. Steffen (2007), Saturation of the terrestrial carbon sink, in *Terrestrial Ecosystems in a Changing World*, edited by J. G. Canadell, D. Pataki, and L. Pitelka, pp. 59-73, The IGBP Series, Springer-Verlag, Berlin.

Carcaillet, C., Y. Bergeron, P. J. H. Richard, B. Fréchette, S. Gauthier, and Y. T. Prairie (2001), Change of fire frequency in the eastern Canadian boreal forests during the Holocene: does vegetation composition or climate trigger the fire regime?, *Journal of Ecology*, *89*, 930-946.

Caspersen, J. P., S. W. Pacala, J. C. Jenkins, G. C. Hurtt, P. R. Moorcroft and R. A. Birdsey (2000), Contributions of land-use history to carbon accumulation in U. S. forests, *Science, 290*, 1148-1151.

Chambers, S. D. and F.S. Chapin III (2003), Fire effects on surface-atmosphere exchange in Alaskan black spruce ecosystems: implications for feedbacks to regional climate, *J. Geophys. Res., 108(D1)*, doi: 10.1029/2001JD000530.

Chapin, F. S., III, A. D. McGuire, J. Randerson, R. Pielke Sr., D. Baldocchi, S. E. Hobbie, N. Roulet, W. Eugster, E. Kasischke, E. B. Rastetter, S. A. Zimov, and S. W. Running (2000), Arctic and boreal ecosystems of western North America as components of the climate system, *Global Change Biology, 6(Suppl. 1)*, 211-223.

Chapin, F.S., III, M. Sturm, M. C. Serreze, J. P McFadden, J. R. Key, A. H. Lloyd, A. D. McGuire, T. S. Rupp, A. H. Lynch, J. P Schimel, J. Beringer, W. L. Chapman, H. E. Epstein, E. S. Euskirchen, L. D. Hinzman, G. Jia, C. L. Ping, K. D. Tape, C. D. C. Thompson, D. A. Walker, and J. M. Welker (2005), Role of land-surface changes in arctic summer warming, *Science, 310(5748)*, 657-660.

Chapin, F.S., III, G. M. Woodwell, J. T. Randerson, G. M. Lovett, E. B. Rastetter, G.M. Lovett, D. D. Baldocchi, D. A. Clark, M. E. Harmon, D. S. Schimel, R. Valentini, C. Wirth, J. D. Aber, J. J. Cole, M. L. Goulden, J. W. Harden, M. Heimann, R. W. Howarth, P. A. Matson, A. D. McGuire, J. M. Melillo, H. A. Mooney, J. C. Neff, R. A. Houghton, M. L. Pace, M. G. Ryan, S. W. Running, O. E. Sala, W. H. Schlesinger, and E. -D. Schulze (2006), Reconciling carbon-cycle concepts, terminology, and methods. *Ecosystems, 9*, 1041-1050.

Chapman, W. L. and J. E. Walsh (1993), Recent variations of sea ice and air temperatures in high latitudes. *Bull. Amer. Meteor. Soc., 74*, 33-47.

Chen, W., J. M. Chen, D. T. Price, and J. Cihlar (2002), Effects of stand age on net primary productivity of boreal black spruce forests in Ontario, Canada, *Can. J. For. Res., 32*, 833-842.

Clark, J. S. (1990), Effect on climate change on fire regimes in northwestern Minnesota, *Nature, 334*, 233-235.

Clein J. S., B. Kwiatkowski, A. D. McGuire, J. E. Hobbie, E. B. Rastetter, J. M. Melillo, and D. W. Kicklighter (2000), Modeling carbon responses of tundra ecosystems to historical and projected climate: A comparison of a plot- and a global-scale ecosystem model to identify process-based uncertainties, *Global Change Biology*, *6*, S127-S140.

Clein, J. S., A. D. McGuire, X. Zhang, D. W. Kicklighter, J. M. Melillo, S. C. Wofsy, P. G. Jarvis, and J. M. Massheder (2002), Historical and projected carbon balances of mature black spruce ecosystems across North America: The role of carbon-nitrogen interactions, *Plant and Soil*, *242*, 15-32.

Clein, J. S., A.D. McGuire, S. E. Euskirchen, and M. Calef (2007), The effects of different climate input data sets on simulated carbon dynamics in the western Arctic, *Earth Interactions*. In press.

Duffy, P. A., J. E. Walsh, J. M. Graham, D. H. Mann, and T. S. Rupp (2005), Impacts of large-scale atmospheric-ocean variability on Alaskan fire season severity, *Ecol. Appl.*, *15(4)*, 1317-1330.

Euskirchen, S. E., A. D. McGuire, D. W. Kicklighter, Q. Zhuang, J. S. Clein, R. J. Dargaville, D. G. Dye, J. S. Kimball, K. C. McDonald, J. M. Melillo, V. E. Romanovsky, and N. V. Smith (2006), Importance of recent shifts in soil thermal dynamics on growing season length, productivity, and carbon sequestration in terrestrial high-latitude ecosystems, *Global Change Biology*, *12*, doi: 10.1111/j.1365-2486.2006.01113.x.

Euskirchen, E. S., A. D. McGuire, and F. S. Chapin III (2007), Energy feedbacks to the climate system associated with snow cover dynamics in northern high latitudes during warming periods of the 20th Century, Submitted to *Global Change Biology*.

Flannigan, M. D. and C. E. Van Wagner (1991), Climate change and wildfire in Canada, *Can. J. For. Res.*, *21*, 66-72.

Flannigan, M. D., Y. Bergeron, O. Engelmark, and B. M. Wotton (1998), Future wildfire in circumboreal forests in relation to global warming, *J. Veg. Sci.*, *9*, 469-476.

Flannigan, M. D., B. J. Stocks, and B. M. Wotton (2000), Climate change and forest fires, *The Science of the Total Environment*, *262*, 221-229.

Flannigan, M. D., K. A. Logan, B. D. Amiro, W. R. Skinner, and B. J. Stocks (2005), Future area burned in Canada, *Climatic Change*, *72*, 1-16.

Flato, G. M. and G. J. Boer (2001), Warming Asymmetry in Climate Change Simulations. *Geophys. Res. Lett.*, *28*, 195-198.

Fosberg, M. A., W. Cramer, V. Brovkin, R. Fleming, R. Gardner, A. M. Gill, J. G. Goldammer, R. Keane, P. Koehler, J. Lenihan, R. Nielson, S. Stich, K. Thonicke, S. Venvski, M. G. Weber, and U. Wittenberg (1999), Strategy for a fire module in dynamic global vegetation models, *International Journal of Wildland Fire*, *9(1)*, 79-84.

French, N. H. F., E. S. Kasischke, B. J. Stocks, J. P. Mudd, D. L. Martell, and B. S. Lee (2000), Carbon release from fires in the North American boreal forest, in *Fire, Climate Change, and Carbon Cycling in the Boreal Forest*, Ecological Studies vol. 138, edited by E. S. Kasischke and B. J. Stocks, pp. 377-388, Springer-Verlag, New York.

Friedlingstein, P., J.-L. Dufresne, P. M. Cox and P. Rayner (2003), How positive is the feedback between climate change and the carbon cycle?, *Tellus, 55B*, 692-700.

Gillett, N. P., A. J. Weaver, F. W. Zwiers, and M. D. Flannigan (2004), Detecting the effect of climate change on Canadian forest fires, *Geophys. Res. Lett.*, *31*, L18211, doi:10.1029/2004GL020876

Global Soil Data Task Group (2000), Global Gridded Surfaces of Selected Soil Characteristics (International Geosphere-Biosphere Programme - Data and Information System), Oak Ridge National Laboratory Distributed Active Archive Center, Oak Ridge, Tennessee.

Harden, J. W., S. E. Trumbore, B. J. Stocks, A. Hirsch, S. T. Gower, K. P. O'Neill, and E. S. Kasischke (2000), The role of fire in the boreal carbon budget, *Global Change Biology, 6(Suppl. 1)*, 174-184.

Harden, J. W., J. C. Neff, D. V. Sandberg, M. R. Turetsky, R. Ottmar, G. Gleixner, T. L. Fries, and K. L. Manies (2004), Chemistry of burning the forest floor during the FROSTFIRE experimental burn, interior Alaska, 1999, *Global Biogeochem. Cycles, 18*, GB3014, doi:10.1029/2003GB002194.

Hicke, J. A., G. P. Asner, E. S. Kasischke, N. H. F. French, J. T. Randerson, G. J. Collatz, B. J. Stocks, C. J. Tucker, S. O. Los, and C. B. Field (2003), Postfire response of North American boreal forest net primary productivity analyzed with satellite observations, *Global Change Biology, 9*, 1145-1157

Hinzman, L. D., M. Fukuda, D. V. Sandberg, F. S. Chapin III, and D. Dash (2003), FROSTFIRE: an experimental approach to predicting the climate feedbacks from a changing boreal fire regime, *J. Geophys. Res., 108(D1)*, 8153, doi:10.1029/2001JD00415.

Hungate, B., J. S. Dukes, M. R. Shaw, Y. Luo, C. B. Field (2003), Nitrogen and climate, *Science, 302,* 1512-1513.

IPCC (2001), *Climate Change 2001: The Scientific Basis. Contribution of Working Group I to the Third Assessment Report of the Intergovernmental Panel on Climate Change.*, J.T. Houghton, Y. Ding, D. J. Griggs, M. Noguer, P. J. van der Linden, X. Dai, K. Maskell, and C. A. Johnson (eds), Intergovernmental Panel on Climate Change, Cambridge University Press, 572pp.

Johnson, E. A. (1992), *Fire and Vegetation Dynamics: Studies from the North American boreal forest*, 129 pp., Cambridge University Press, Cambridge.

Johnson, E. A. and D. R. Wowchuk (1993), Wildfires in the southern Canadian Rocky Mountains and their relationship to mid-tropospheric anomalies, *Can. J. For. Res., 23*, 1213-1222.

Johnstone, J.F. and F.S. Chapin III (2003), Non-equilibrium succession dynamics indicate continued northern migration of lodgepole pine, *Global Change Biology*, *9*, 1401-1409.

Johnstone, J. F. and F. S. Chapin III (2006), Effects of soil burn severity on post-fire tree recruitment in boreal forest, *Ecosystems*, *9*, 14-31.

Joos, F., I. C. Prentice, and J. House (2002), Growth enhancement to global atmospheric change as predicted by terrestrial ecosystem models: consistent with US forest inventory data, *Global Change Biology, 8,* 299-303.

Kasischke E., N. L. Christensen Jr., and B. J. Stocks (1995), Fire, global warming, and the carbon balance of boreal forests. *Ecol. Appl.*, *5*, 437-451.

Kasischke, E. S., D. Williams, and D. Barry (2002), Analysis of the patterns of large fires in the boreal forest region of Alaska, *International Journal of Wildland Fire*, *11*, 131-144.

Kasischke, E. S., E. J. Hyer, P. C. Novelli, L. P. Bruhwiler, N. H. F. French, A. I. Sukhinin, J. H. Hewson, and B. J. Stocks (2005), Influences of boreal fire emissions on Northern Hemisphere atmospheric carbon and carbon monoxide, *Global Biogeochem. Cycles*, *19*, GB1012, doi:10.1029/2004GB002300.

Kasischke, E. S. and M. R. Turetsky (2006), Recent changes in the fire regime across the North American boreal region – spatial and temporal patterns of burning across Canada and Alaska, *Geophysical Res. Lett.*, *33*, L09703, doi:10.1029/2006GL025677.

Keeling, C. D. and T. P. Whorf (2005), Atmospheric CO_2 records from sites in the SIO air sampling network, in *Trends: A Compendium of Data on Global Change*, Carbon Dioxide Information Analysis Center, Oak Ridge National Laboratory, U.S. Department of Energy, Oak Ridge, Tenn., U.S.A.

Kicklighter, D. W., M. Bruno, S. Dönges, G. Esser, M. Heimann, J. Helfrich, F. Ift, F. Joos, J. Kaduk, G. H. Kohlmaier, A. D. McGuire, J. M. Melillo, R. Meyer, B. Moore III, A. Nadler, I. C. Prentice, W. Sauf, A. L. Schloss, S. Sitch, U. Wittenberg, and G. Würth (1999), A first-order analysis of the potential role of CO_2 fertilization to affect the global carbon budget: a comparison of four terrestrial biosphere models, *Tellus*, *51B*, 343-366.

Kimball, J. S., M. Zhao, A. D. McGuire, F. A. Heinsch, J. Clein, M. Calef, W. M. Jolly, S. Kang, S. E. Euskirchen, K. C. McDonald, and S. W. Running (2007), Recent climate driven increases in vegetation productivity for the western Arctic: Evidence of an acceleration of the northern terrestrial carbon cycle, *Earth Interactions*, *11*, [available online at http://earthinteractions.org].

Körner, C., R. Asshoff, O. Bignucolo, S. Hättenschwiler, S. G. Keel, S. Peláez-Riedl, S. Pepin, R. T. W. Siegwolf, and G. Zotz (2005), Carbon flux and growth in mature deciduous forest trees exposed to elevated CO_2, *Science, 309*, 1360-1362.

Kurz, W. A. and M. J. Apps (1999), A 70-year retrospective analysis of carbon fluxes in the Canadian forest sector, *Ecol. Appl.*, *9(2)*, 526-547.

Logan, J. A., J. Regniere, and J. A. Powell (2003), Assessing the impacts of global warming on forest pest dynamics, *Front. Ecol. Environ.*, *1(3)*, 130-137.

Long, S. P., E. A. Ainsworth, A. D. B. Leakey, J. Nösberger, D. R. Ort. (2006), Food for thought: lower-than-expected crop yield stimulation with rising CO_2 concentrations, *Science, 312*, 1918-1921.

Luo, Y. Q., B. Su, W. S. Currie, J. S. Dukes, A. Finzi, U. Hartwig, B. Hungate, R. E. McMurtrie, R. Oren, W. J. Parton, W. E. Pataki, M. R. Shaw, D. R. Zak, and C. B. Field (2004), Progressive nitrogen limitation of ecosystem responses to rising atmospheric carbon dioxide, *BioScience, 54,* 731-739.

Luo, Y., C. B. Field, and R. B. Jackson (2006), Does nitrogen constrain carbon cycling, or does carbon input stimulate nitrogen cycling?, *Ecology*, *87*, 3-4.

McGuire, A. D., J. M. Melillo, L. A. Joyce, D. W. Kicklighter, A. L. Grace, B. Moore III, and C. J. Vorosmarty (1992), Interactions between carbon and nitrogen dynamics in estimating net primary productivity for potential vegetation in North America, *Global Biogeochem. Cycles*, *6*, 101-124.

McGuire, A. D., L. A. Joyce, D. W. Kicklighter, J. M. Melillo, G. Esser, and C. J. Vorosmarty (1993), Productivity response of climax temperate forests to elevated temperature and carbon dioxide: A North American comparison between two global models, *Climatic Change*, *24*, 287-310.

McGuire, A. D., J. M. Mellilo, D. W. Kicklighter, and L. A. Joyce (1995), Equilibrium responses of soil carbon to climate change: empirical and process-based estimates. *Journal of Biogeography*, *22*, 785-796.

McGuire, A. D., J. M. Melillo, D. W. Kicklighter, Y. Pan, X. Xiao, J. Helfrich, B. Moore III, C. J. Vorosmarty, and A. L. Schloss (1997), Equilibrium responses of global net primary production and carbon storage to doubled atmospheric carbon dioxide: Sensitivity to changes in vegetation nitrogen concentration, *Global Biogeochem. Cycles*, *11*, 173-189.

McGuire, A. D., J. Clein, J. M. Melillo, D. W. Kicklighter, R. A. Meier, C. J. Vorosmarty, and M. C. Serreze (2000a), Modeling carbon responses of tundra ecosystems to historical and projected climate: The sensitivity of pan-arctic carbon storage to temporal and spatial variation in climate, *Global Change Biology*, *6*, S141-S159.

McGuire, A. D., J. M. Melillo, J. T. Randerson, W. J. Parton, M. Heimann, R. A. Meier, J. S. Clein, D. W. Kicklighter, and W. Sauf (2000b), Modeling the effects of snowpack on heterotrophic respiration across northern temperate and high latitude regions: Comparison with measurements of atmospheric carbon dioxide in high latitudes, *Biogeochemistry*, *48*, 91-114.

McGuire, A. D., S. Sitch, J. S. Clein, R. Dargaville, G. Esser, J. Foley, M. Heimann, F. Joos, J. Kaplan, D. W. Kicklighter, R. A. Meier, J. M. Melillo, B. Moore III, I. C. Prentice, N. Ramankutty, T. Reichenau, A. Schloss, H. Tian, L. J. Williams, and U. Wittenberg (2001), Carbon balance of the terrestrial biosphere in the twentieth century: Analyses of CO_2, climate and land use effects with four process-based ecosystem models, *Global Biogeochem. Cycles, 15(1)*, 183-206.

McGuire, A. D., C. Wirth, M. Apps, J. Beringer, J. Clein, H. Epstein, D. W. Kicklighter, J. Bhatti, F. S. Chapin, III, B. de Groot, D. Efremov, W. Eugster, M. Fukuda, T. Gower, L. Hinzman, B. Huntley, G. J. Jia, E. Kasischke, J. Melillo, V. Romanovsky, A. Shvidenko, E. Vaganov, and D. Walker (2002), Environmental variation, vegetation distribution, carbon dynamics and water/energy exchange at high latitudes, *J. Veg. Sci., 13*, 301-314.

McGuire, A. D., M. Apps, F. S. Chapin III, R. Dargaville, M. D. Flannigan, E. S. Kasischke, D. Kicklighter, J. Kimball, W. Kurz, D. J. McRae, K. McDonald, J. Melillo, R. Myneni, B. J. Stocks, D. L. Verbyla, and Q. Zhuang (2004), Land cover disturbances and feedbacks to the climate system in Canada and Alaska, in *Land Change Science: Observing, Monitoring, and Understanding Trajectories of Change on the Earth's Surface*, edited by G. Gutman et al., pp. 139-161, Kluwer Academic Publishers, Dordrecht, Netherlands.

McGuire, A. D., and F. S. Chapin III (2006), Climate feedbacks in the Alaskan boreal forest, in *Alaska's Changing Boreal Forest*, edited by F. S. Chapin, III, M. Oswood, K. Van Cleve, L. A. Viereck, and D. L. Verbyla, pp. 309-322, Oxford University Press, New York.

McGuire, A. D., F. S. Chapin III, J. E. Walsh, and C. Wirth (2006), Integrated regional changes in arctic climate feedbacks: Implications for the global climate system, *Annual Review of Environment and Resources, 31,* 61-91.

McGuire, A.D., F.S. Chapin III, C. Wirth, M. Apps, J. Bhatti, T. Callaghan, T.R. Christensen, J.S. Clein, M. Fukuda, T. Maximov, A. Onuchin, A. Shvidenko, and E. Vaganov (2007), Responses of high latitude ecosystems to global change: Potential consequences for the climate system, in *Terrestrial Ecosystems in a Changing World.* Canadell, J.G., Pataki, D.E., and Pitelka, L.F. eds, pp. 297-310. The IGBP Series, Springer-Verlag, Berlin Heidelberg.

Melillo, J. M., A. D. McGuire, D. W. Kicklighter, B. Moore III, C. J. Vorosmarty, and A. L. Schloss (1993), Global climate change and terrestrial net primary production. *Nature*, *63*, 234-240.

Mitchell, T. D., and P. D. Jones (2005), An improved method of constructing a database of monthly climate observations and associated high-resolution grids, *International Journal of Climatology*, *25(6)*, 693-712.

Murphy, P. J., J. P. Mudd, B. J. Stocks, E. S. Kasischke, D. Barry, M. E. Alexander, and N. H. F. French (2000), Historical fire records in the North American boreal forest, in *Fire, Climate Change, and Carbon Cycling in the Boreal Forest*, Ecological Studies vol. 138, edited by E. S. Kasischke and B. J. Stocks, pp. 274-288, Springer-Verlag, New York.

Nakićenović, N. and R. Swart (eds.) (2000), Intergovernmental Panel on Climate Change, Special Report on Emissions Scenarios. Cambridge University Press, 599 pages.

National Geophysical Data Center (NGDC) (1994), TerrainBase v. 1.1, 5-minute digital terrain model data. Boulder, Colorado.

Nemani, R. R., C. D. Keeling, H. Hashimoto, W. M. Jolly, S. C. Piper, C. J. Tucker, R. B. Myneni, and S. W. Running (2003), Climate-driven increases in global terrestrial net primary production from 1982-1999, *Science*, *300*, 1560-1563.

Oren, R., D. S. Ellsworth, K. H. Johnsen, N. Phillips, B. E. Ewers, C. Maier, K. V. R. Schäfer, H. McCarthy, G. Hendrey, S. G. McNulty, and G. G. Katul (2001), Soil fertility limits carbon sequestration by forest ecosystems in a CO_2-enriched atmosphere, *Nature, 411,* 469-472.

Raich, J. W., E. B. Rastetter, J. M. Melillo, D. W. Kicklighter, P. A. Steudler, B. J. Peterson, A. L. Grace, B. Moore III, and C. J. Vörösmarty (1991), Potential net primary productivity in South America: application of a global model, *Ecol. Appl.*, *1*(4), 399-429.

Randerson, J. T., H. Liu, M. G. Flanner, S. D. Chambers, Y. Jin, P. G. Hess, G. Pfister, M. C. Mack, K. K. Treseder, L. R. Welp, F. S. Chapin, J. W. Harden, M. L. Goulden, E. Lyons, J. C. Neff, E. A. G. Schuur, and C. S. Zender (2006), The impact of boreal forest fire on climate warming, *Science, 314(5802)*, 1130-1132.

Reich, P. B. B. A. Hungate, and Y. Luo (2006), Carbon-nitrogen interactions in terrestrial ecosystems in reponse to rising atmospheric carbon dioxide, *Annual Review of Ecology, Evolution and Systematics, 37*, 611-636.

Scholze, M., W. Knorr, N. W. Arnell, and I. C. Prentice (2006), A climate-change risk analysis for world ecosystems, *PNAS, 103(35)*, 13116-13120.

Serreze, M. C., J. E. Walsh, F. S. Chapin III, T. Osterkamp, M. Dyurgerov, V. Romanovsky, W. C. Oechel, J. Morison, T. Zhang, and R. G. Barry (2000), Observational evidence of recent change in the northern high-latitude environment, *Climatic Change, 46*, 159-207.

Serreze, M.C. and J. A. Francis (2006), The Arctic amplification debate, *Climatic Change, 76,* 241-264.

Skinner, W. R., B. J. Stocks, D. L. Martell, B. Bonsal, and A. Shabbar (1999), The association between circulation anomalies in the mid-troposphere and area burned by wildland fire in Canada, *Theoretical and Applied Climatology, 63*, 89-105.

Skinner, W. R., M. D. Flannigan, B. J. Stocks, D. L. Martell, B. M. Wotton, J. B. Todd, J. A. Mason, K. A. Logan, and E. M. Bosch (2002), A 500 hPa synoptic wildland fire climatology for large Canadian forest fires, 1959-1996, *Theoretical and Applied Climatology, 71*, 157-169.

Soja, A. J., N. M. Tchebakova, N. H. French, M. D. Flannigan, H. H. Shugart, B. J. Stocks, A. I. Sukhinin, E. I. Parfenova, and T. Chapin (2006), Current evidence of climate-induced boreal forest change, *Global and Planetary Change*, doi:10.1016/j.gloplacha.2006.07.28

Stocks, B. J., M. A. Fosberg, T. J. Lynham, L. Mearns, B. M. Wotton, Q. Yang, J-Z. Jin, K. Lawrence, G. R. Hartley, J. A. Mason, and D. W. McKenney (1998), Climate change and forest fire potential in Russian and Canadian boreal forests, *Climatic Change*, *38*, 1-13.

Thompson, S. L., B. Govindasamy, A. Mirin, K. Caldeira, C. Delire, J. Milovich, M. Wickett and D. Erickson (2004), Quantifying the effects of CO_2-fertilized vegetation on future global climate and carbon dynamics, *Geophys. Res. Lett., 31*, L23211, doi: 10.1029/2004GL021239.

Tian, H., J. M. Melillo, D. W. Kicklighter, A. D. McGuire, and J. Helfrich (1999), The sensitivity of terrestrial carbon storage to historical climate variability and atmospheric CO_2 in the United States, *Tellus*, *51B*, 414-452.

Wirth. C., E. –D. Schulze, B. Lühker, S. Grigoriev, M. Siry, G. Hardes, W. Ziegler, M. Backor, G. Bauer, and N. N. Vygodskaya (2002), Fire and site type effects on the long-term carbon and nitrogen balance in pristine Siberian Scots pine forests, *Plant and Soil*, *242*, 41-63.

Wotton, B. M. and M. D. Flannigan (1993), Length of the fire season in a changing climate, *Forestry Chronicle*, *69*, 187-192.

Xiao, X., J. M. Melillo, D. W. Kicklighter, A. D. McGuire, R. G. Prinn, C. Wang, P. H. Stone and A. Sokolov (1998), Transient climate change and net ecosystem production of the terrestrial biosphere, *Global Biogeochemical Cycles, 12*, 345-360.

Zhuang, Q., V. E. Romanovsky, and A. D. McGuire (2001), Incorporation of a permafrost model into a large-scale ecosystem model: Evaluation of temporal and spatial scaling issues in simulating soil thermal dynamics, *J. Geophys. Res.*, *106*, 33649-33670.

Zhuang, Q., A. D. McGuire, J. Harden, K. P. O'Neill, V. E. Romanovsky, and J. Yarie. (2002), Modeling soil thermal and carbon dynamics of a fire chronosequence in interior Alaska. *J. Geophys. Res.*, *107*, 8147, doi:10.1029/2001JD001244.

Zhuang, Q., A. D. McGuire, J. M. Melillo, J. S. Clein, R. J. Dargaville, D. W. Kicklighter, R. B. Myneni, J. Dong, V. E. Romanovsky, J. Harden, J. E. Hobbie (2003), Carbon cycling in extratropical terrestrial ecosystems of the Northern Hemisphere during the 20th Century: A modeling analysis of the influences of soil thermal dynamics, *Tellus*, *55B*, 751-776.

Zhuang, Q., J. M. Melillo, B. S. Felzer, D. W. Kicklighter, A. D. McGuire, M. C. Sarofim, A. Sokolov, R. G. Prinn, P. A. Steudler, and S. Hu (2006), CO_2 and CH_4 exchanges between land ecosystems and the atmosphere in northern high latitudes over the 21st century, *Geophys. Res. Lett.*, *33*, L17403, doi:10.1029/2006GL026972.

Conclusion

Wildfire is a common occurrence in ecosystems of northern high latitudes and changes in the fire regime have consequences for carbon feedbacks to the climate system. In my dissertation research, I developed methods for incorporating fire into a temporally and spatially explicit biogeochemical modeling framework. In addition to the effects of fire on the carbon dynamics of the boreal region, this work highlights the importance of the relative roles of variable atmosphere CO_2 concentration and climate on short- and long-term carbon storage. The integration of fire into a biogeochemical modeling framework also allows for the coupling of estimates of future area burned by wildfire in response to climate change, which provides a basis for understanding the role of future fire in the carbon dynamics of the northern high latitudes.

The ability to project future spatial and temporal changes in carbon dynamics across the boreal forest is limited by the understanding of how the temporal and spatial aspects of fire influence historical carbon dynamics. I used the Terrestrial Ecosystem Model (TEM), a process-based biogeochemical model that simulates carbon and nitrogen pools and fluxes, in chapter one to understand the effects of historical fire on the carbon dynamics of the pan-boreal region. This study highlights the importance of accounting for the effects of stand-age distribution on carbon dynamics as well as the importance of fire severity, frequency, and size. Although the pan-boreal region responded as an overall carbon sink, this study highlights that fire plays an important role in source/sink relationships across the boreal forest and also suggests that the role of atmospheric CO_2 fertilization may be important to consider in addition to changes in climate and fire.

Fire is strongly linked to climate in the boreal forest. My research on this linkage in chapter two shows that the temporally and spatially explicit empirical relationships that relate area burned with air temperature and fuel moisture codes derived from the Canadian Fire Weather Index (CFWI) System explain on the order of 80% of the variation in annual area burned across the North American boreal region. The most frequently occurring predictor across Alaska and Canada was July temperature, but the fuel moisture codes and monthly severity rating of the CFWI system entered the models as the most important predictors of annual area burned. I extrapolated the fire models using output from the Canadian Climate Center CGCM2 global climate model to predict annual area burned through year 2100. Extrapolating the empirical models through the 21st Century shows that annual area burned will double by 2050 and that the increase by the end of the century will be 3.5-5.7 times the area burned in the late 20th Century. Although this study highlights the sensitivity of fire regime in boreal North America to future climate change, a major limitation is that the empirical models based on current conditions do not consider how changes in vegetation influence the relationships between climate and fire. Future research should focus on incorporating the effects of long-term successional vegetation changes on area burned to account more fully for interactions among fire, climate, and vegetation dynamics.

In chapter three of the dissertation, I used estimates of annual area burned simulated by the temporally and spatially explicit empirical models to drive TEM to simulate the effects of fire on the carbon dynamics of the North American boreal region. These estimates were downscaled using a simple rule-based method and individual fire

events were tracked across the study area to account for the legacy of multiple fires on the carbon dynamics of the North American boreal region. Relative to the last decade of the 20th Century, decadal total carbon emissions from fire increase on the order of 2.5 to 4.4 times by 2091-2100. Despite the increase in area burned for the 21st Century, the TEM simulations indicate that boreal North America is a carbon sink in response to CO_2 fertilization, climate variability, and fire, but an increase in fire results in a decrease in the sink strength.

While this study emphasizes the importance of fire on historical and future carbon dynamics across the boreal region, there are uncertainties in the effects of fire on carbon storage. These uncertainties are associated with sparse fire data for northern Eurasia, uncertainty in estimating carbon consumption, and difficulty in verifying assumptions about the representation of fires that occurred prior to the start of the historical fire record. Future studies should incorporate the role of dynamic vegetation to more accurately represent post-fire successional processes, incorporate fire severity parameters that change in time and space, and integrate the role of other disturbances and their interactions with future fire regime.

In summary, my dissertation research demonstrates that fire plays a major role in the carbon dynamics of the boreal region across multiple temporal and spatial scales throughout the 20th Century and 21st centuries. This study shows that it is important to account for the effects of stand-age and spatially explicit fire severity and fire frequency in estimating fire emissions and the carbon balance of the boreal region. While the response of the boreal forest to increases in fire results in an overall carbon sink, the

carbon sink is reduced during periods of large fires. Future area burned was incorporated into TEM to simulate the carbon dynamics of the North American boreal region for the 21st Century. These results indicate that despite the increase in future area burned and an increase in total carbon emitted at the time of fire, the North American boreal forest remains a net carbon sink throughout the 21st Century.